Hazard and Impact Synthesis and Attribution for Phase I use case

Deliverable 4.1

31st August 2025

Title	Hazard and Impact Synthesis and Attribution for Phase I use case
Lead Beneficiary	IRC RCCCCD (Red Cross Red Crescent Climate Centre)
Lead Author(s)	Jack, Christopher D (RCRCCC), Vogel, Martha (IRC RCRCCC), de Boer, Tesse (RCRCCC), Gale, Sarah (RCRCCC), Paprotny, Dominik (PIK), Muis, Sanne (DELTARES), Goulart, Henrique (DELTARES), Wilson, Emma (UKMO), Munday, Gregory (UKMO), Cotterill, Daniel (UKMO)
Contributors	Schultz Cornelia (RCRCCC), Doris Vertegaal (DELTARES), Anaïs Couasnon (DELTARES), Rachel Perks (UKMO), Anthi Manali (SEVEN), Maggie Kossida (SEVEN)
Deliverable number	4.1
Work Package	WP4: Developing actionable climate information for events
Submission date	29/08/2025

Dissemination Level

PU	Public — fully open (automatically posted online)	X
SEN	Sensitive — limited under the conditions of the Grant Agreement	
CI	EU classified —Restreint-UE/EU-Restricted, Confidentiel-UE/EU-Confidential, Secret-UE/EU-Secret under Decision 2015/444	

Version History

Date	Version	Contributors	Comments
06/06/2025	0.1	Tesse de Boer, Daniel Cotterill, Christopher D. Jack, Anais Couasnon, Henrique Goulart, Sanne Muis, Gregory Munday, Dominik Paprotny, Rachel Perks, Doris Vertegaal, Martha M. Vogel	First version for internal review
13/06/2025	0.2	Henrique Goulart, Sanne Muis, Gregory Munday, Dominik Paprotny, Roop Singh, Emma Wilson, Poppy Web	Internal review
29/08/2025	1.0	Anthi Manali, Maggie Kossida	Final review and first finished version

Citation

Jack, C., Vogel, M., de Boer, T., Gale, S., Paprotny, D., Muis, S., Goulart, H., Wilson, E., Munday, G., Cotterill, D. (2025): Hazard and Impact Synthesis and Attribution for Phase I use case. Horizon Europe project COMPASS. Deliverable D4.1.

Funded by the European Union

The COMPASS project has received funding from the European Union's HORIZON Research and Innovation Actions Programme under Grant Agreement No. 101135481

Disclaimer

Executive summary

This document provides an in-depth summary of the implementation, strengths, and challenges of the first phase of COMPASS Use Cases (UCs). The overarching goal of COMPASS is to develop a harmonized and flexible methodological framework for attributing climate and impact to complex extreme events, including compound, sequential, and cascading hazards such as storm surge and river flooding, or sequences of tropical cyclones. The UCs served as critical test beds for evaluating this framework, encompassing a diverse range of event types and geographical contexts. Two primary attribution analysis methods, probabilistic (risk-based) and storyline-based, were implemented, each offering distinct advantages in analysis and communicating results to stakeholders. This report details the observed hazards, impacts, modeling frameworks, and attribution results for each UC, concluding with a synthesis of key findings and avenues for future advancement through the phase to UCs.

In many of the use cases, climate change emerged as a significant driver of the observed and recorded impacts of the compounding hazards. At the same time, non-climate drivers including population and economic growth, the covid-19 pandemic, and chronic insecurity and poverty emerged as critical factors, highlighting the need to consider the wider complexity of extreme events and the holistic policy responses required to reduce the impacts of future extremes.

The UCs have demonstrated the value of a harmonized but flexible methodological framework, allowing implementation to adapt to local contexts and data availability, but still benefiting from considerable shared code, model components, and datasets. This success clearly suggests that the goal of operational attribution modeling is achievable. Moving forward several opportunities have emerged related to the further refinement and development of the COMPASS methodological framework including improved bias correction of climate datasets, improved inclusion of mitigation measures such as flood defenses in the relevant models, improved inclusion of quantitative vulnerability indicators, and further integration of quantitative and qualitative attribution approaches. With the initial methodological framework well established, an increased focus on stakeholder engagement and policy relevance is now possible.

Table of Contents

1. Introduction

The overarching goal of COMPASS is to develop a harmonised, yet flexible, methodological framework for climate and impact attribution of various complex extremes that includes compound, sequences, and cascading hazard events. This is an important step towards operationalizing event attribution, further supporting contextual understanding of the interplay between climate change and extreme event impacts, and supporting locally relevant responses.

The COMPASS Use Cases (UC) are central to the approach as they provide the development test beds through which the framework, including harmonized datasets, modeling workflows, and attribution experiments are evaluated in real world test cases. The first round of UCs was selected to span a range of event types as well as geographical contexts to ensure that the methodological framework was applicable across these different contexts. In support of the UCs, guidance on suitable datasets for exposure and vulnerability modeling was developed, including new economic and population exposure datasets, as detailed in D2.1 on the best available methods and datasets for impact attribution.

As the methodological framework and associated datasets were being developed in parallel with the first UCs, the UCs have followed the general principles of the framework, the actual implementation varied based on existing institutional modeling infrastructure and experience, and available local level exposure and impacts data. This has been valuable in exploring the advantages and disadvantages of different implementation approaches and is detailed in the associated D1.1 *Guidelines for compound extremes modeling in current and future climates.*

Two different attribution analysis methods have been implemented, probabilistic or risk based, and storyline-based methods. Each approach has advantages and disadvantages, particularly when communicating the results with stakeholders. While probabilistic approaches provide statistical estimates of the shifting probability of an event, or shifting intensity of events, as a result of climate change, storyline methods help to understand how a particular event may have unfolded without the influence of climate change and also allow consideration of other non-climate factors in contributing to or mitigating impacts.

The purpose of this report is to provide an in-depth summary of the implementation of each use case with a primary focus on the modeling framework implementation, strengths, and challenges emerging. While each UC description includes details of the actual event and reported impacts, these details are provided to help the reader interpret the modeling in context rather than to provide definitive event descriptions which already exist and are referenced. Strengths of the applied datasets and methods are identified while limitations and challenges are also noted in order to inform further advances in both datasets and modeling frameworks.

A concluding synthesis section provides an over-arching assessment of the implementation of the use cases and points towards possible avenues for advancement for the second set of use cases within COMPASS.

1.1. Overview of use cases

The use cases are summarized in the Table 1 below including the geography, types of hazards and compounding, and attribution method. For the classification of compounding events, we draw on the typology of Zscheischler et. al (2020)[1].

1 Zscheischler, J., Martius, O., Westra, S., Bevacqua, E., Raymond, C., Horton, R. M., ... & Vignotto, E. (2020). A typology of compound weather and climate events. *Nature reviews earth & environment*, *1*(7), 333-347.

Table 1 Summary of use cases including geography, types of hazards and compounding, and attribution method.

Name and date	Geography	Hazards	Compounding	Attribution method	Lead institution
UC1 – Xynthia 2010	France – west coast and inland	Wind, storm surge – coastal flooding	Multivariate/spatially	Storyline	PIK
UC2a – United Kingdom winter storms (2013/2014	United Kingdom, Somerset	Rainfall, wind, storm surge, flooding (fluvial, pluvial, coastal)	Multivariate, temporal	Probabilistic	Met Office
UC2b – United Kingdom drought heatwave (2022/2023)	United Kingdom	Drought, Heave	Multivariate, spatial	Probabilistic	Met Office
UC3a – East Africa Cyclones Idai and Kenneth (2019)	East Africa, Mozambique	Wind, storm surge, rainfall, flooding (fluvial, pluvial, coastal)	Multivariate, spatial	Storyline	Deltares
UC3b – East Africa Cyclone Freddy (2023)	East Africa	Wind, storm surge, rainfall, flooding (fluvial, pluvial, coastal)	Multivariate, spatial	Storyline	Deltares
UC4 – Tropical storms Eta and Iota (2020)	Caribbean, Honduras	Rainfall, flooding (fluvial, pluvial), COVID-19, Violence	Multivariate (non-climate) Temporal	Storyline (quantitative and qualitative)	Red Cross Red Crescent Climate Centre

2. Use Case 1: France

2.1. Summary of event

Extra-tropical cyclone 'Xynthia' was one of the most significant disasters to affect France in recent decades. The storm tore through the country in the early hours of 28th February 2010, causing 47 fatalities and some 2.5 billion euro in damages. Most of the fatalities and half of the economic damage resulted from storm-induced flooding on the western coast of France. Flooding directly affected some 10,000 people and the windstorm cut off power to one million people, and the whole event resulted in some 470,000 insurance claims of an average 3100 euro (Table 2).

The windstorm and its impacts were not unusual in France, especially when compared to the 1999 storms. However, the coastal flooding was unexpected, a combination of both the rare synchronicity of storm surge and spring high tide and many long-standing deficiencies in disaster management and planning. Since the event, many actions have been undertaken to reduce exposure and vulnerability through improved flood protection (including temporary barriers), spatial planning, new emergency-response organizations and building adaptation requirements.

2.2. Geographical context

Several European countries were impacted, but most were concentrated in France, including 47 out of 59 fatalities. The map (Figure 1) presents the departments where fatalities had occurred, and the 25 departments with the highest insured economic losses (72% of the total). 41 fatalities and 54% of damages were concentrated in two departments, Charente-Maritime and Vendée (marked with blue hatching on map). Most fatalities and highest economic loss occurred in La Faute-sur-Mer municipality in Vendée (Figure 2).

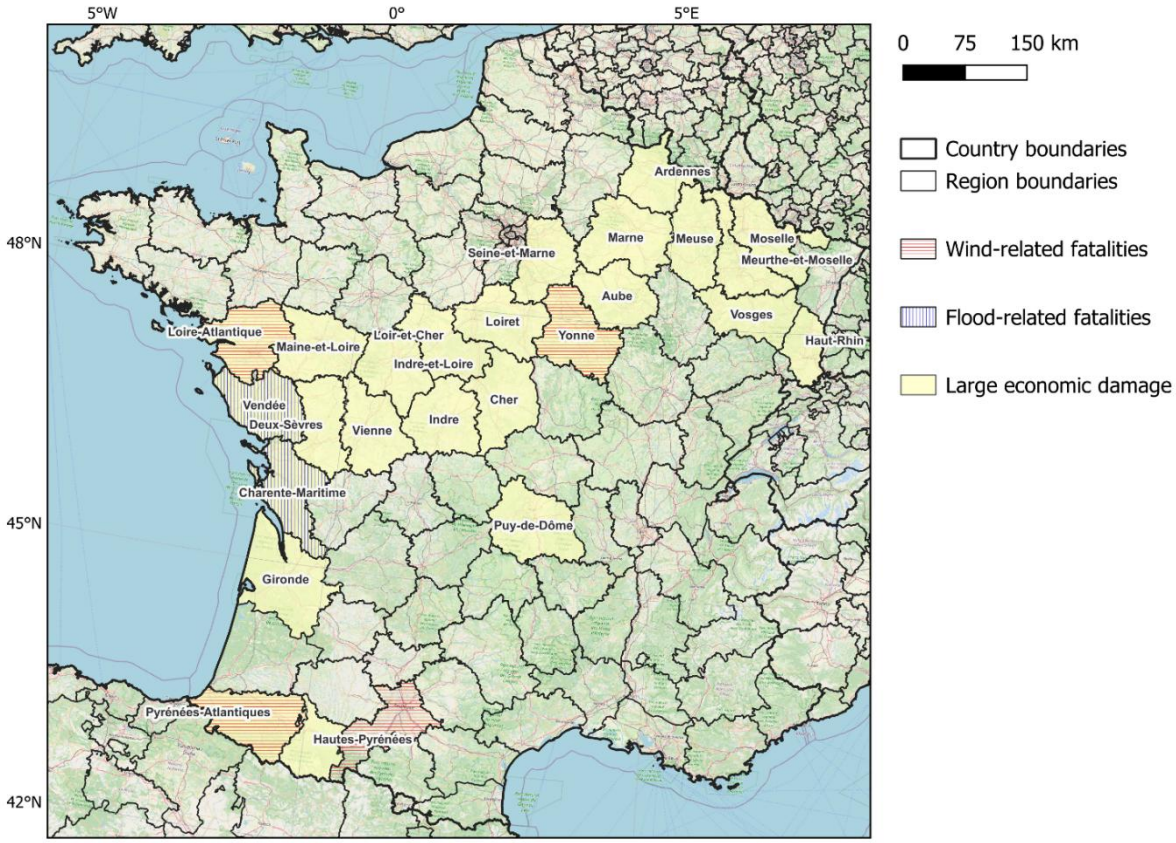

Figure 1 Main regions affected by extra-tropical cyclone Xynthia in 2010. Background map: OpenStreetMap

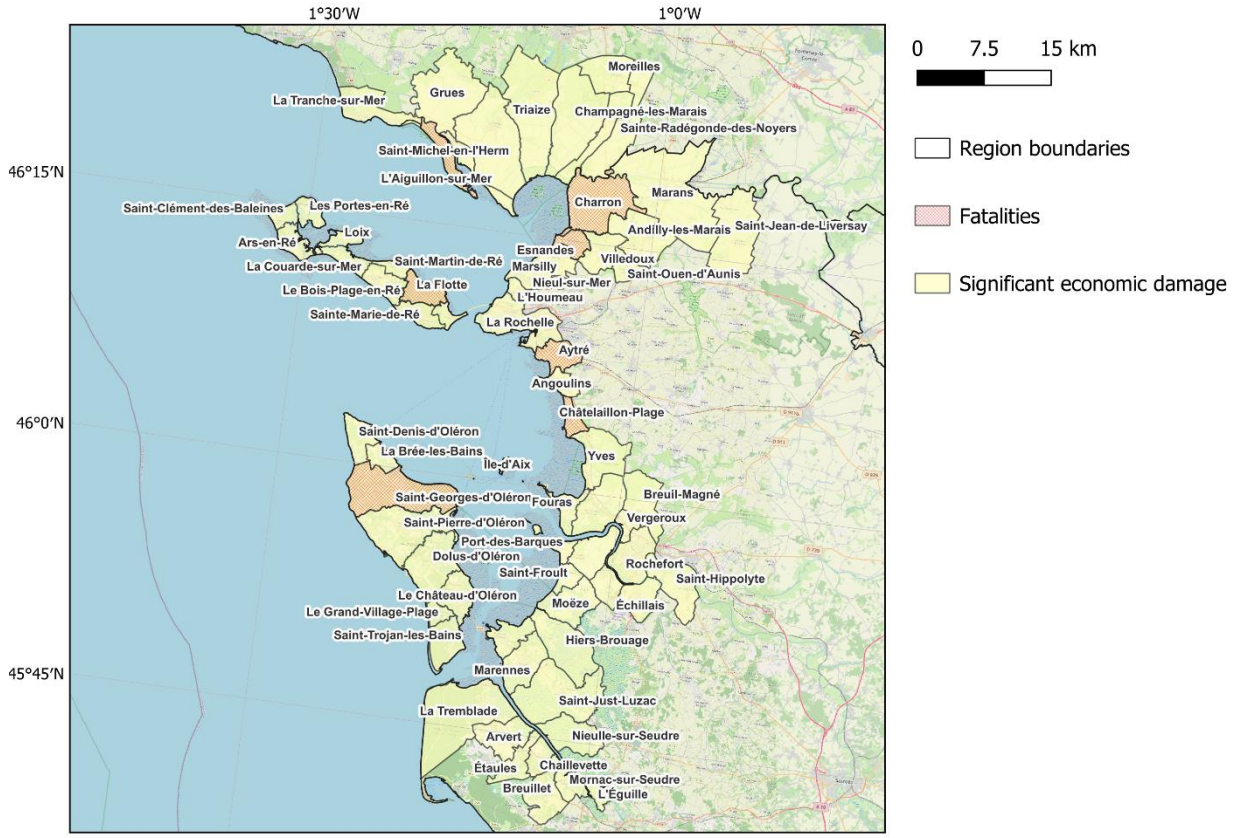

Figure 2 Principal municipalities that were affected in the Charente-Maritime and Vendée departments. Background map: OpenStreetMap

2.3. Observed hazards

2.3.1. Type of hazards

Windstorm (high wind speeds).

Coastal flooding (resulting from storm surge induced by high wind speeds and low atmospheric pressure, combined with high spring tide).

2.3.2. Form of compounding

Spatially and temporarily compounding, as both wind and flooding were caused by the same event.

2.3.3. Driving dynamics

Extra-tropical cyclone 'Xynthia' was an unusual event among winter storms that affect Europe annually. Despite being weaker than some other storms (particularly compared with 1999 storms), it was particularly damaging due to the coastal flooding component. The storm developed around 30◦N, which is more southerly than typical winter storms. It developed during the record-breaking negative values of the North Atlantic Oscillation (NAO) index. It followed a very unusual trajectory from the Canary Islands through the Iberian Peninsula into France. The storm was also particularly fast-moving, covering 1400 km in 24 hours while it moved across Spain and France and then Germany and Benelux countries[2].

2 Kolen, B., Slomp, R., Van Balen, W., Terpstra, T., Bottema, M., & Nieuwenhuis, S. (2010). *Learning from French experiences with storm Xynthia; damages after a flood*. HKV.

Still, the important driver of coastal flooding was the synchronicity with a spring high tide, as the wind-driven surge was lower than in the 1999 storm. This allowed the water level to reach unprecedented heights[3].

2.3.4. Intensity/Extremity/Magnitude

The wind gusts during the storm reached up to 238 km/h at Pic du Midi in the Pyrenees. At the coastline, wind gusts were up to 160 km/h in Ile-de-Ré (island in the Bay of Biscay) and up to 130 km/h in coastal towns on the mainland. Inland, speeds of 160 km/h were also reached in the Deux-Sèvres department. The sea level reached a record-breaking 4.51 m in La Pallice (harbour of La Rochelle)[4], though only 1.58 m was the actual surge (estimated to be less than in 1924, 1940, 1941 and 1999 events).

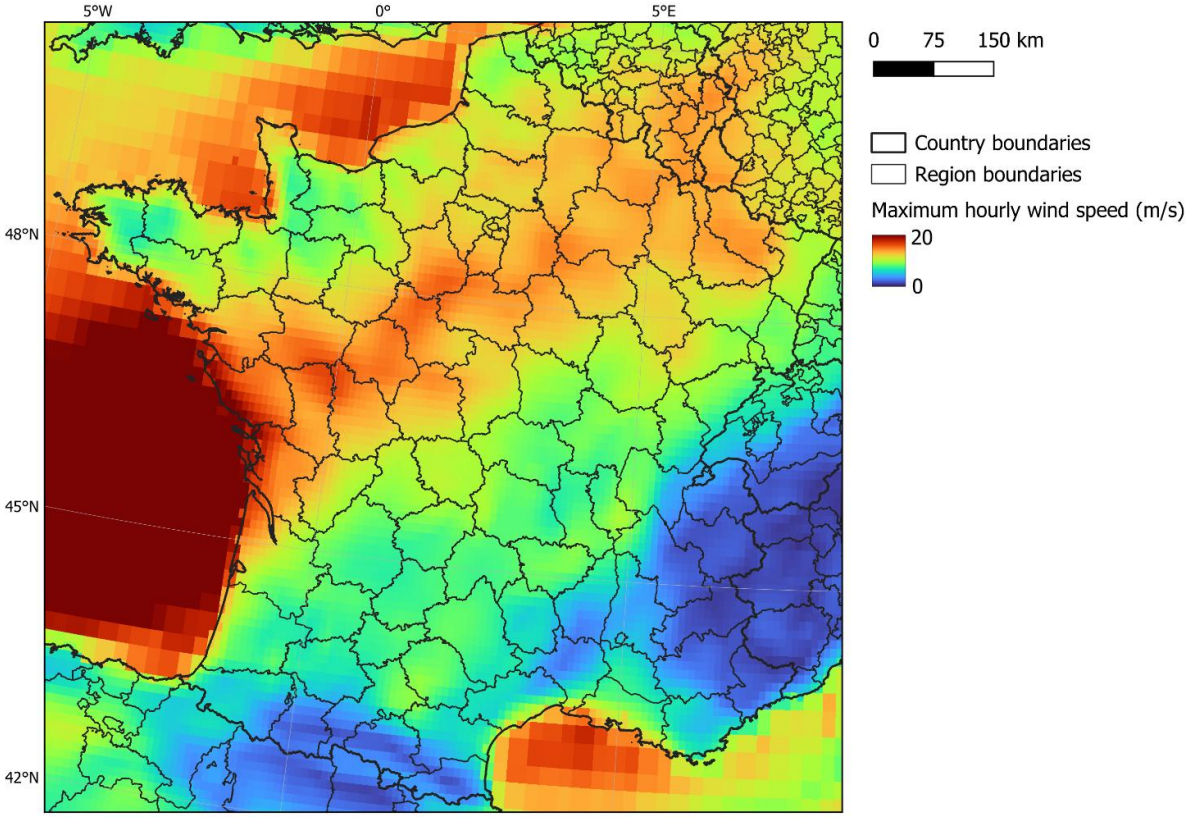

Figure 3 Maximum wind speed during Xynthia storm according to ERA5/ERA5-Land reanalysis.

3 Liberato, M. L. R., Pinto, J. G., Trigo, R. M., Ludwig, P., Ordóñez, P., Yuen, D., & Trigo, I. F. (2013). Explosive development of winter storm Xynthia over the subtropical North Atlantic Ocean. *Natural Hazards and Earth System Sciences*, *13*(9), 2239-2251.

4 Breilh, J. F., Bertin, X., Chaumillon, É., Giloy, N., & Sauzeau, T. (2014). How frequent is storm-induced flooding in the central part of the Bay of Biscay?. *Global and Planetary change*, *122*, 161-175.

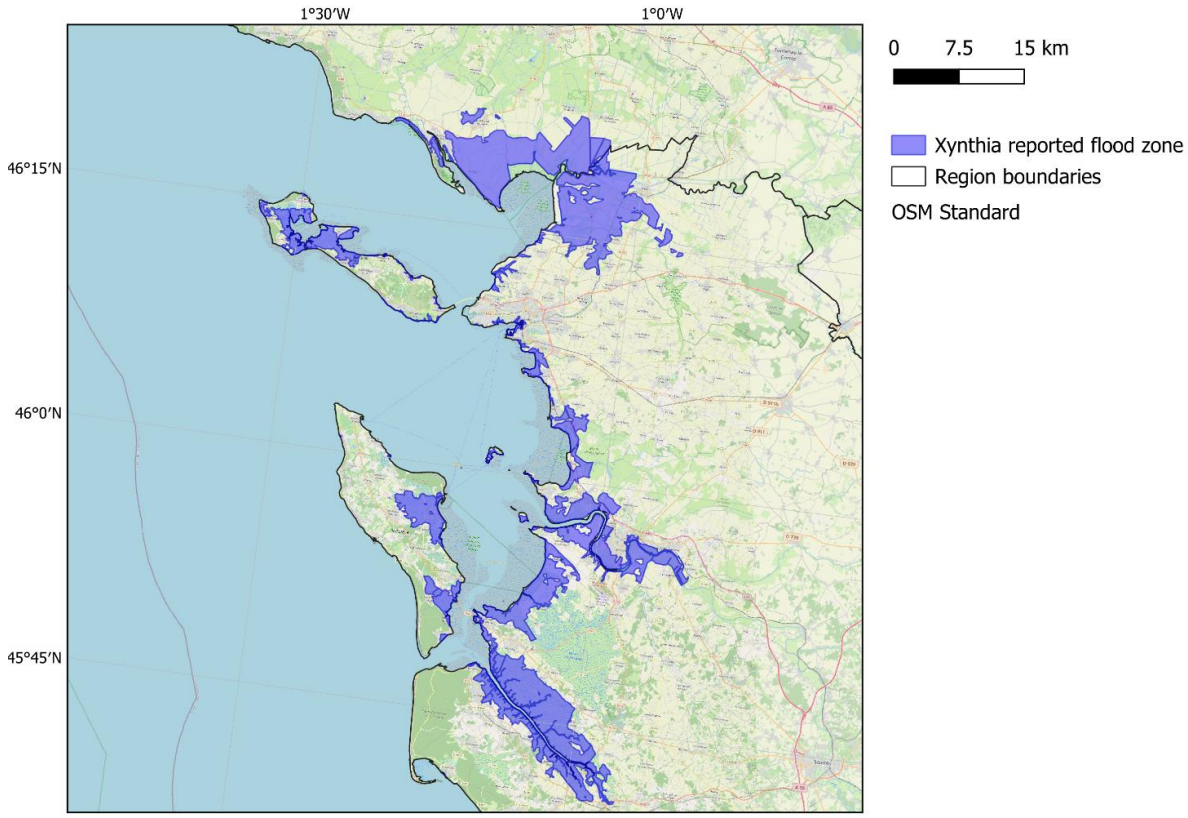

Figure 4 Reported flood extents resulting from the Xynthia storm. Flood data courtesy of Xavier Bertin (CNRS/La Rochelle University). Background map: OpenStreetMap

The storm was first detected as a depression in the Atlantic Ocean on 25th February 2010. On the 26th, the Canary Islands were impacted. On the 27th the storm moved through the Iberian Peninsula into the Bay of Biscay. The highest red warning for four departments of France were issued on the 27th at 16.00 pm. The storm made landfall in France on the 28th around 2.00 am. By 6.00 am, it has moved to Paris and continued into Belgium, the Netherlands and Germany. It had finally dissipated over the Baltic Sea before midnight on 2nd March.

2.4. Observed impacts

2.4.1. Quantitative impacts

Xynthia caused extensive losses to people and the national economy, as summarized in Table 2. The most detailed data is available for fatalities and insured economic losses (damage to houses, cars, businesses and agriculture). The six fatalities from the windstorm were highly scattered all over France, but flood fatalities were highly concentrated. 29 out of 41 fatalities occurred in a single municipality (La Faute-sur-Mer), of which 28 occurred in an area of just 0.3 km^2 (compared to 560 km^2 flooded area and 12 km^2 of the whole municipality). Similarly, though the 25 departments with the highest losses were responsible for 72% of insured windstorm losses, 89% of flood losses were recorded in the top two departments (formally 'natural disaster' loss, which could include some rainfall-related damage).

Table 2 Principal impacts of extra-tropical cyclone Xynthia in 2010.

Impact	Magnitude/scale	Source
Area inundated	560 km^2 (agricultural land)	Kolen et al. (2013)[5]
Fatalities	41 (flood) 6 (windstorm)	Vinet et al. (2011) based on official data[6]
People affected directly by flooding	10,000	Rough estimate[7] (HANZE)
Persons affected by loss of electricity	958,000	Wikipedia, citing national power distributor ERDF[8]
Economic loss	2.5 billion euro (flood + windstorm)	Typically quoted estimate of total direct loss[9]
Insurance claims	470,000 (35,000 flood / 435,000 windstorm) Value of claims: 1.48 billion euro (flood 745 million / windstorm 735 million)	Estimate based on data from insurance companies representing 89% of French market, compiled by their association FFSA-GEMA (2011)[10]

Table 3 Details of insured losses from FFSA-GEMA (2011). Insurance data formally refer to flooding as 'natural disaster'.

Category	Source	Households	Cars	Farms	Businesses	Total
Insurance claims (number)	Flooding	19,000	10,500	1700	3800	35,000
	Windstorm	339,500	22,500	33,500	39,500	435,000
	Total	358,500	33,000	35,200	43,300	470,000
Insured loss (million euro)	Flooding	450	60	26	209	745
	Windstorm	430	35	112	158	735
	Total	880	95	138	367	1480

5 Kolen, B., Slomp, R. and Jonkman, S.N. (2013). Impacts of storm Xynthia. J. Flood Risk Manage, 6: 261-278.

6 Vinet, F., Lumbroso, D., Defossez, S. et al. (2012). A comparative analysis of the loss of life during two recent floods in France: the sea surge caused by the storm Xynthia and the flash flood. *Var. Nat Hazards* 61, 1179–1201.

7 Hanze (n.d.) Coastal flood in France, 2010. *Natural Hazards.* https://naturalhazards.eu/details,15586

8 Tempête Xynthia (2012). *Wikipedia*. https://fr.wikipedia.org/wiki/Temp%C3%AAte_Xynthia

9 Kolen, B., Slomp, R. and Jonkman, S.N. (2013), Impacts of storm Xynthia. J. *Flood Risk Manage*, 6: 261-278.

10 FFSA-GEMA (2011). La tempête Xynthia du 28 février 2010: Synthèse.
https://www.argusdelassurance.com/mediatheque/6/7/9/000008976.pdf

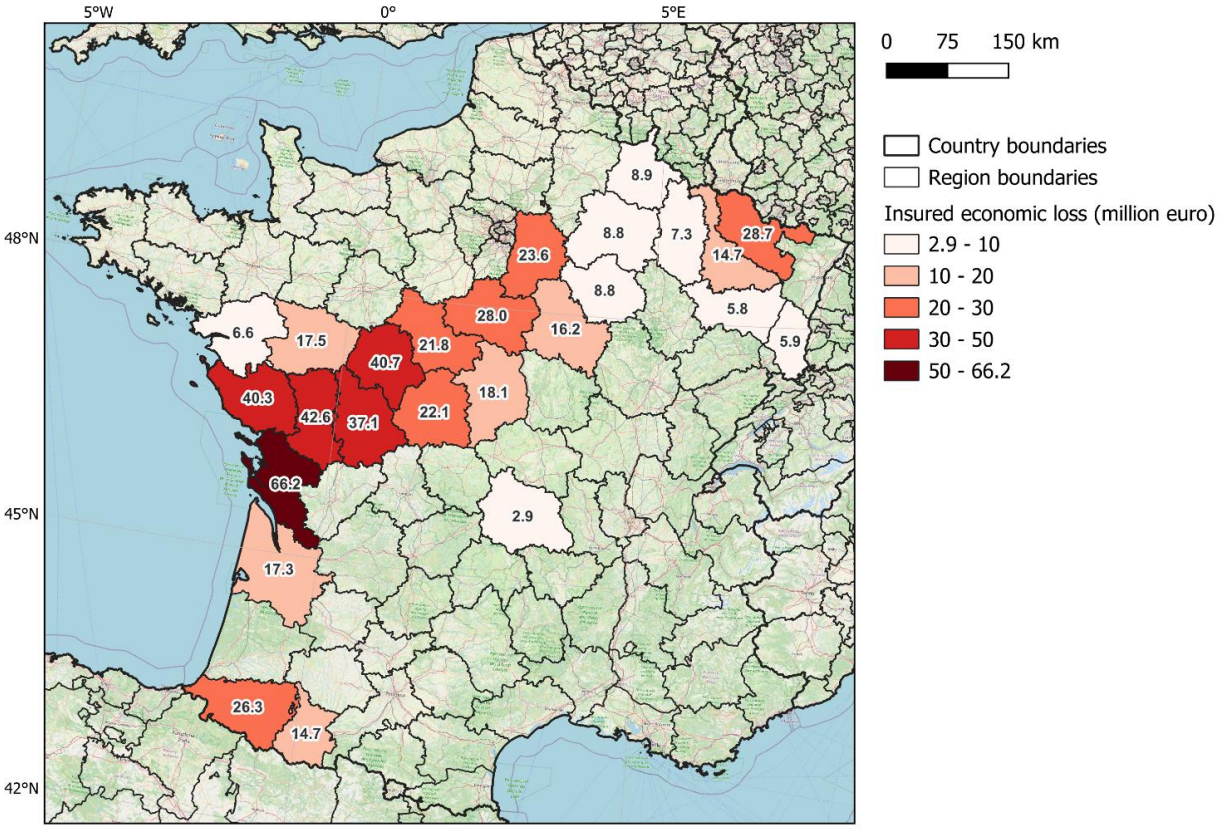

Figure 5 Distribution of insured economic loss from wind damage during Xynthia (only 25 departments with highest losses).

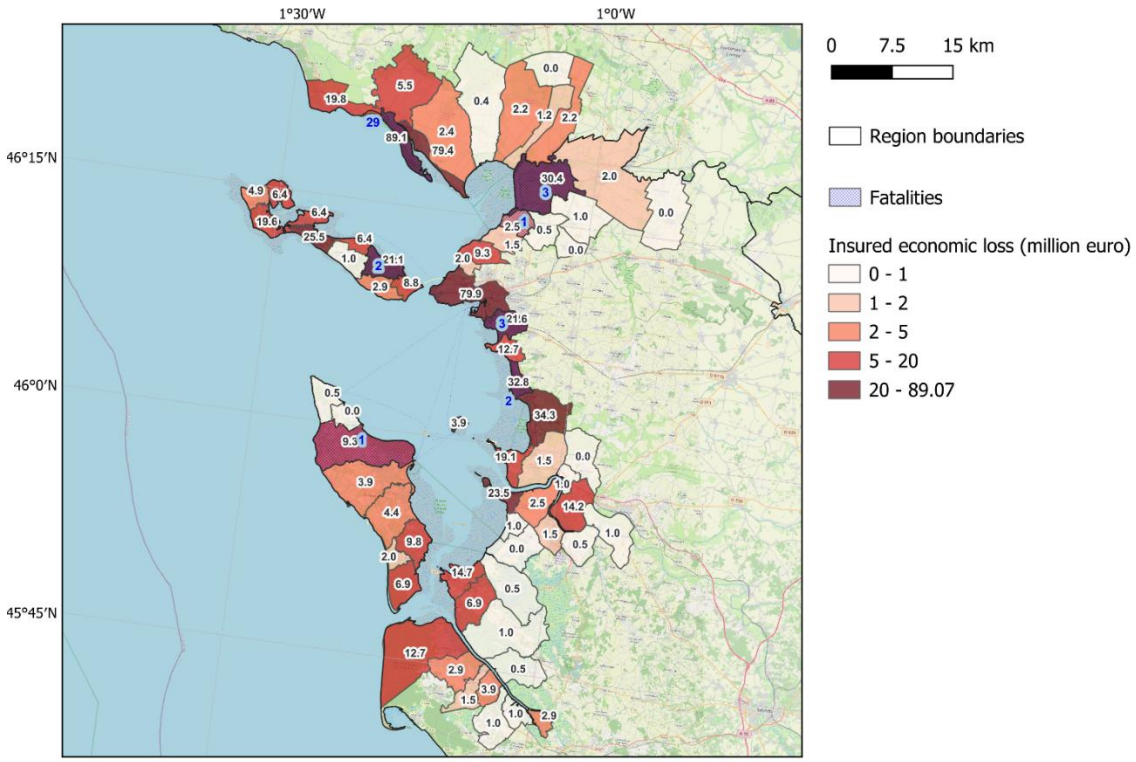

Figure 6 Distribution of insured economic loss from 'natural disaster' (flooding) in the Charente-Maritime and Vendée departments during Xynthia (black numbers) and fatalities (blue numbers).

2.4.2. Qualitative impacts and responses

Relatively little is mentioned in context of the windstorm, as it was not particularly impactful (compared to particularly 1999) and remains overshadowed by the unprecedented magnitude of coastal impacts. Post-flood analyses list several reasons for the scale of impacts (Kolen et al. 2013, Enet 2021)[11]:

- **Early warning:** the windstorm was correctly forecast well in advance, but storm surge warning was not precise and actionable.
- **Disaster management:** upon warning, no action was taken by local authorities, who considered windstorm the larger risk, rendering evacuation not feasible (except campsites, due to windstorm rather than flooding). However, local authorities had no possibility of knowing the possible severity of flooding.
- **Flood prevention:** many dikes, seawalls and beaches were badly maintained, partially due to unclear titles or private ownership. Some dikes were also still unrepaired after the 1999 storm surge, except Gironde department which was most affected in the previous event. Long-term investments in coastal protection have also protected most of the town of Châtelaillon-Plage.
- **Spatial planning:** the coastal zone experiences decades of rapid growth in housing stock (see below). In addition, many houses were built in violation of a 1995 spatial planning law, which aimed at stopping construction in areas at risk of flooding, but local authorities still often authorized housebuilding even in the most flood-prone areas.
- **Architectural style:** between 1960s and 1980s, houses were built typically with the bedroom on the first (upper) floor, reducing vulnerability especially in terms of mortality. However, newer houses were built with only a ground floor to imitate the more traditional style of the 1950s and earlier houses.
- **Societal factors:** ground-floor-only houses were preferred by older people, who had lower chances of escaping floodwaters, further exacerbated by possible exit through windows often being blocked by electric shutters in conditions of power failure due to windstorm. Consequently, the median age of Xynthia fatalities was 75, while there were no fatalities between the ages of 15 and 42 (Vinet et al. 2011).
- **Timing:** the flood occurred in wintertime, when few seasonal homes were occupied, which reduced the number of fatalities, though it didn't decrease economic losses. However, the occupancy wasn't at its lowest possible due to winter school holidays, and 14 out of 41 fatalities were non-residents. All five children who died in the flood were on holidays (Vinet et al. 2011).

Population and housing data for the most affected La Faute-sur-Mer municipality from national statistics institute INSEE reveals the specifics of risk and its dynamics typical in the region, but particularly acute in this location (Figure 7). Firstly, it is noticeable that seasonal housing far exceeds permanent housing. Further, this ratio increased from 4:1 in 1968 to almost 7:1 before the flood, and the overall number of houses increased nearly 4-fold. At the same time, the population had only increased 70% in the same timeframe. After the flood, exposure reduction was implemented in the two affected departments of Charente-Maritime and Vendée by (mostly) voluntary purchase and demolition of 1162 houses in the highest-risk zones. This was paid by the national government to the amount of nearly 318 million euro[12]. In La Faute-sur-Mer, the reduction in the number of seasonal houses by 2016 was 36%, permanent houses by 28% and population by 34%. However, since then the population and housing have started to increase in numbers again.

11 *supra* note 1.

12 Enet P. (2021). National Strategic Plan for Coastal Protection Considering the Effects of Climate Change. Output 4.1.2: Description of EU case studies in France. *Spanish Ministry for the Ecological Transition and the Demographic Challenge (MITECO)*. [not available online, shared by author]

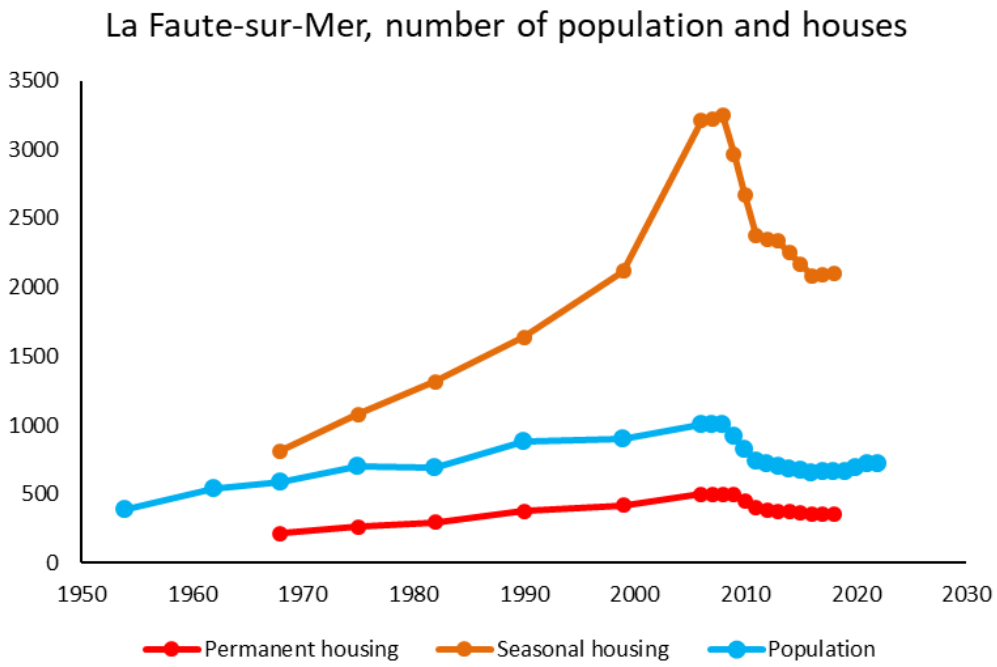

Figure 7 Resident population (1954-2022) and number of houses (1968-2018) in the most affected municipality, La Faute-sur-Mer (census data from INSEE). No housing data after 2018 is available due to the merger of the municipality with L' Aiguillon-sur-Mer.

One exception to seasonal housing being generally unoccupied due to winter can be noted. Many mobile homes in the area were inhabited by students who couldn't afford to rent flats in La Rochelle. The mobile park in Aytre was completely flooded, but the young people were able to escape to the roofs and survive. This is in contrast to older inhabitants of permanent houses that came under water, especially in La Faute-sur-Mer. However, six fatalities of the windstorm include two inside a camper that was washed away by waves from a pier.

2.5. Modeling framework

2.5.1. Hazard modeling

For extreme sea levels, a Delft3D-based simulation of storm surges along European coasts[13] was carried out, driven by ERA5 reanalysis data. Hourly storm surge heights were combined with data on tidal elevations from the FES2014 model[14], significant wave height (converted to wave run-up) from ERA5, mean dynamic topography of the ocean[15], glacial isostatic adjustment from the ICE-6G_C model[16] and long-term sea level rise, to estimate the total water level. Long-term sea level rise after 1950 is represented by annual sea level data for 1950-1999

13 Paprotny D., Morales Nápoles O., Nikulin G. (2016). Extreme sea levels under present and future climate: a pan-European database. *E3S Web of Conferences* 7, 02001, https://doi.org/10.1051/e3sconf/20160702001.

14 F. H. Lyard, D. J. Allain, M. Cancet, L. Carrère, N. Picot, (2021). FES2014 global ocean tide atlas: design and performance. *Ocean Sci.* 17, 615–649.

15 Mulet, S., Rio, M.-H., Etienne, H., Artana, C., Cancet, M., Dibarboure, G., Feng, H., Husson, R., Picot, N., Provost, C., and Strub, P. T. (2021). The new CNES-CLS18 global mean dynamic topography, *Ocean Sci.*, 17, 789–808, https://doi.org/10.5194/os-17-789-2021

16 D. F. Argus, W. R. Peltier, R. Drummond, R., A. W. Moore, (2014). The Antarctica component of postglacial rebound model ICE-6G_C (VM5a) based upon GPS positioning, exposure age dating of ice thicknesses, and relative sea level histories. *Geophys. J. Int*. 198, 537-563

W. R. Peltier, D. F. Argus, R. Drummond, (2015). Space geodesy constrains ice-age terminal deglaciation: The global ICE-6G_C (VM5a) model. J. *Geophys. Res. Solid Earth* 120, 450-487.

from a high-resolution reconstruction[17] and for 2000-2020 from satellite altimetry[18]. Based on those water levels, flood hazard maps were computed in Paprotny et al. (2024)[19] according to the methodology of Vousdoukas et al. (2016)[20] to derive footprints and water depths and combined with sea levels as in the riverine flood events.

The counterfactual coastal flood was computed by modifying three components of extreme sea levels, then recalculating inundation zones and impacts. Hourly storm surge height and significant wave height were calculated for 1950 using tsEVA approach (implemented as Matlab toolbox)[21]. The applied tsEVA method decouples the detection of non-stationary patterns from the fitting of the extreme value distribution with a generalized Pareto distribution (GPD). Firstly, a time series of storm surges and wave heights is created, using values above the 99th percentile (in hourly resolution) and a minimum distance between peaks of 3 days (actual distance is determined by continuous exceedance of height threshold). Then, using a moving 30-year time window (typical timeframe for climate analyses) the long-term changes in mean and standard deviation over time were detected. This enables transforming a non-stationary time series into a stationary one, on which the GPD distribution can be applied. After the extreme value analysis, the result is reverse transformed into a non-stationary GPD distribution. The scale and location parameters of the resulting distribution are time-varying (both long-term and seasonally), but it is still assumed that the shape parameter doesn't change over time. Additionally, long-term sea level rise after 1950 added to factual sea level was subtracted in the counterfactual.

Uncertainty of factual and counterfactual extreme sea level is assumed to be the result of the uncertainty of the non-stationary GPD fitting. The analysis is simplified as follows to make it computationally feasible at European scale. The standard error in trends of average and standard deviation of storm surge and wave heights is the basis of standard error in the GPD parameters in the tsEVA approach. For every extreme storm event, the relative difference in discharge due to error of fit was calculated and an average difference was computed for each NUTS3 region. We assume that the uncertainty in extreme sea level can be represented by a normal distribution with a location parameter of zero. The scale parameter of the distribution is assumed to be equal to the mean absolute error in sea level due to uncertainty of the non-stationary GPD fitting. Then, a transformation factor of sea level uncertainty into impact uncertainty was estimated per NUTS3 region using available flood hazard maps and exposure maps for 2020. Impact magnitude at different discharge values (corresponding to different return periods of hazard maps) was calculated with the vulnerability model from Paprotny et al. 2025a[22]. The results were converted into a linear function between extreme sea level deviation and impact magnitude change. In this way, the uncertainty distribution of discharge could be sampled and then converted into a percent deviation

17 S. Treu, S. Muis, S. Dangendorf, T. Wahl, J. Oelsmann, S. Heinicke, K. Frieler, M. Mengel, (2024). Reconstruction of hourly coastal water levels and counterfactuals without sea level rise for impact attribution. *Earth Syst. Sci. Data* 16, 1121–1136.

18 M.-I. Pujol, Y. Faugère, G. Taburet, S. Dupuy, C. Pelloquin, M. Ablain, N. Picot, (2016). DUACS DT2014: the new multi-mission altimeter data set reprocessed over 20 years. *Ocean Sci.* 12, 1067–1090.

G. Taburet, A. Sanchez-Roman, M. Ballarotta, M.-I. Pujol, J.-F. Legeais, F. Fournier, Y. Faugere, G. Dibarboure, (2019). DUACS DT2018: 25 years of reprocessed sea level altimetry products. *Ocean Sci.* 15, 1207–1224.

19 Paprotny, D., Rhein, B., Vousdoukas, M. I., Terefenko, P., Dottori, F., Treu, S., Śledziowski, J., Feyen, L., and Kreibich, H., (2024). Merging modelled and reported flood impacts in Europe in a combined flood event catalogue for 1950–2020, Hydrol. *Earth Syst. Sci.*, 28, 3983–4010, https://doi.org/10.5194/hess-28-3983-2024.

20 M. I. Vousdoukas, E. Voukouvalas, L. Mentaschi, F. Dottori, A. Giardino, D. Bouziotas, A. Bianchi, P. Salamon, L. Feyen, (2016). Developments in large-scale coastal flood hazard mapping. *Nat. Hazards Earth Syst. Sci.* 16, 1841–1853.

21 L. Mentaschi, M. Vousdoukas, E. Voukouvalas, L. Sartini, L. Feyen, G. Besio, L. Alfieri, (2016). The transformed-stationary approach: a generic and simplified methodology for non-stationary extreme value analysis. *Hydrol. Earth Syst. Sci.* 20, 3527–3547.

22 *supra* note 21.

of flood impacts from mean prediction of impacts made by the combining hazard, exposure and vulnerability models under any scenario[23].

Windstorm wind speeds were taken from ERA5-Land, filled over coastal areas with ERA5. The tsEVA approach was used to derive the 1950 counterfactual wind speeds the same way as storm surge and wave counterfactuals, described above. Alternative estimates were taken from HadGEM3-A simulations (Ciavarella et al. 2018) with historical and natural forcing, by computing extreme value statistics over 15 ensemble members for 2006-2013. This gave 120 years of data, which were fitted (using SciPy) to stationary Generalized Extreme Value distribution with a block maxima approach and bootstrapped with 1000 samples to derive uncertainty of the fit.

2.5.2. Impact modeling

Exposure mapping

Attribution of exposure covers two connected aspects: raw exposure growth in a broader area (related to demographic and economic developments far beyond the scale of the case study) and change in exposure distribution within the affected area (related rather to local-scale circumstances). The two hazards had similar approaches, though different data sources, as summarized in Table 4.

Table 4 Summary of exposure approaches.

Aspect	Coastal flood exposure	Windstorm exposure
Data source	HANZE-Exposure (Paprotny and Mengel 2023)[24]	Global exposure model[25]
Baseline for counterfactual	1950	1850, 1950
Exposure growth	NUTS3 (department)-level change in population, gross domestic product (GDP) per capita and fixed asset value relative to GDP	Country-level (France) change in population, gross domestic product (GDP) per capita and fixed asset value relative to GDP
Exposure distribution	Change in spatial distribution (100 m grid) of population and fixed asset value, considering change in sectoral distribution of assets (affecting vulnerability estimates)	Change in spatial distribution (0.1 degree, ~10 km) of total fixed asset value

Vulnerability modelling

Flood vulnerability and flood protection, factual and counterfactual, were computed with the approach of[26]. Briefly, it utilizes a set of multivariate vine-copula models that were trained on empirical data on flood occurrence and flood impacts for 1950-2020 among European countries. Each model contains a set of hydrological and socio-economic predictors of flood occurrence (separately for coastal and riverine floods) or flood vulnerability (separately for fatalities, persons affected and economic loss). This enables predicting flood

23 Paprotny D., Tilloy A., Treu S., Buch A., Vousdoukas M. I., Feyen L., Kreibich H., Merz B., Frieler K., Mengel M. (2025). Attribution of flood impacts shows strong benefits of adaptation in Europe since 1950. *Science Advances* 11:eadt7068, https://doi.org/10.1126/sciadv.adt7068

24 Paprotny D., Mengel M. (2023). Population, land use and economic exposure estimates for Europe at 100 m resolution from 1870 to 2020. *Scientific Data* 10:372, https://doi.org/10.1038/s41597-023-02282-0

25 Paprotny, D. (2025): Exposure datasets at multiple scales. Horizon Europe project COMPASS. Deliverable D3.1.

26 *Supra* note 21.

protection and vulnerability for any given year (in this case factual – 2010, and counterfactual – 1950) at the resolution of NUTS3 regions. At the grid-cell level, flood vulnerability is calculated with depth-damage functions, and the vulnerability estimates at regional level serve as modifiers of the static predictions of the damage curves. In case of fatalities, depth-damage function of Boyd et al. (2010)[27] and in Jonkman et al. (2008)[28] is used, for economic loss curves for six classes of economic assets from Huizinga et al. (2017), while persons affected were assumed to be all population with the flood zone (defined by water depths above 10 cm).

Windstorm damage (economic loss) was computed using a damage function of Klawa and Ulbrich[29]. This approach was found to work better for Xynthia than other pan-European wind damage modelling approaches listed by Gliksman et al. (2023)[30]. The damage function is as follows:

$$D(v) = \left(\frac{v_{\max}}{v_{98}} - 1\right)^3$$

where D is the damaged fraction in %, vmax is the maximum wind speed and v98 is the 98th percentile of daily maximum wind speed. The function assumes, based on historical experience, that no damage is possible where the wind speed did not exceed the local 98th percentile. Therefore, damages for Xynthia were only computed for grid cells exceeding the threshold (under any given climate scenario), which was computed using counterfactual wind extremes from ERA5 using the tsEVA approach. No counterfactual vulnerability was considered here due to a lack of adequate methods.

The damaged fraction per grid cell is multiplied by exposure (factual or counterfactual) and aggregated per department (NUTS3 region). The factual estimate of impact per department was compared with insurance data. The ratio between modelled factual estimate and insured loss per department was applied to counterfactual scenarios to provide a more accurate total windstorm damage estimate for the event. As specific impact data is available only for 25 departments with the highest loss, all other departments were lumped together into a single impact region, which was computed by subtracting loss for the 25 departments from total loss from Xynthia.

2.6. Attribution modeling framework

Losses from the extra-tropical cyclone Xynthia are considered here separately for those caused by floods and those caused by high wind speeds. This due to different mechanisms of loss, requiring very different modelling approaches, and scale of impacts (windstorm affected a large part of France, but coastal flooding only a small part of the coastal zone). An approach was devised that is applicable at European scale to increase transferability, but which can be validated with reported loss data from specific events. In case of windstorms, only economic loss was attributed due to lack of methods for modelling other impacts.

---

27 Boyd, E., Levitan, M., and van Heerden, (2010). I.: Improvements in Flood Fatality Estimation Techniques Based on Flood Depths, in: *Wind Storm and Storm Surge Mitigation,* edited by: Uddin, N., American Society of Civil Engineers, Reston, Virginia, USA, 126–139, https://doi.org/10.1061/9780784410813.ch11

28 Jonkman, S. N., Vrijling, J. K., and Vrouwenvelder, (2008). A. C. W. M.: Methods for the estimation of loss of life due to floods: a literature review and a proposal for a new method, *Nat. Hazards,* 46, 353–389, https://doi.org/10.1007/s11069-008-9227-5.

29 Klawa, M. and Ulbrich, U. (2003). A model for the estimation of storm losses and the identification of severe winter storms in *Germany, Nat. Hazards Earth Syst. Sci.*, 3, 725–732, https://doi.org/10.5194/nhess-3-725-2003.

30 Gliksman, D., Averbeck, P., Becker, N., Gardiner, B., Goldberg, V., Grieger, J., Handorf, D., Haustein, K., Karwat, A., Knutzen, F., Lentink, H. S., Lorenz, R., Niermann, D., Pinto, J. G., Queck, R., Ziemann, A., and Franzke, C. L. E.: Review article: A European perspective on wind and storm damage – from the meteorological background to index-based approaches to assess impacts, Nat. Hazards Earth Syst. Sci., 23, 2171–2201, https://doi.org/10.5194/nhess-23-2171-2023.

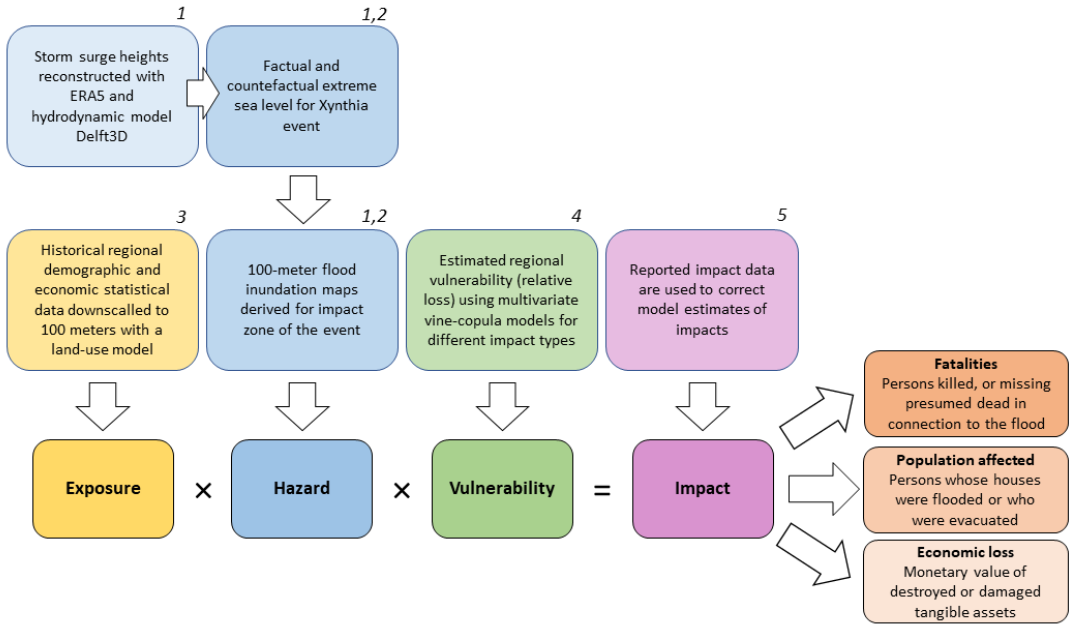

Figure 8 Flood attribution framework. Numbers refer to papers describing the detailed methodology, (1) Paprotny et al. (2024a)[31], (2) Paprotny et al. (2025b)[32], (3) Paprotny and Mengel (2023)[33], (4) Paprotny et al. (2025a)[34], (5) Paprotny et al. (2024b)[35].

31 Paprotny D., Rhein B., Vousdoukas M.I., Terefenko P., Dottori F., Śledziowski J., Treu S., Feyen L., Kreibich H. (2024a). Merging modelled and reported flood impacts in Europe in a combined flood event catalogue for 1950-2020. *Hydrology and Earth System Sciences* 28:3983–4010, https://doi.org/10.5194/hess-28-3983-2024

32 Paprotny D., Tilloy A., Treu S., Buch A., Vousdoukas M.I., Feyen L., Kreibich H., Merz B., Frieler K., Mengel M. (2025b). Attribution of flood impacts shows strong benefits of adaptation in Europe since 1950. *Science Advances* 11:7068, https://doi.org/10.1126/sciadv.adt7068

33 Paprotny D., Mengel M. (2023). Population, land use and economic exposure estimates for Europe at 100 m resolution from 1870 to 2020. *Scientific Data* 10:372, https://doi.org/10.1038/s41597-023-02282-0

34 Paprotny D., 't Hart C.M.P., Morales-Nápoles O. (2025a). Evolution of flood protection levels and flood vulnerability in Europe since 1950 estimated with vine-copula models. *Natural Hazards* 121:6155–6184, https://doi.org/10.1007/s11069-024-07039-5

35 Paprotny D., Terefenko P., Śledziowski J. (2024b). HANZE v2.1: an improved database of flood impacts in Europe from 1870 to 2020. *Earth System Science Data* 16:5145–5170, https://doi.org/10.5194/essd-16-5145-2024.

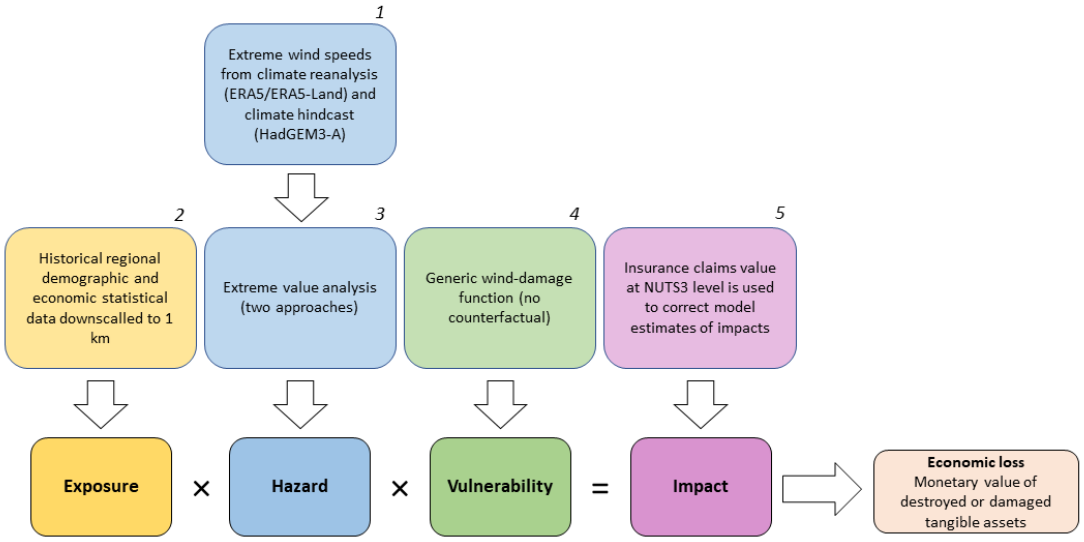

Figure 9 Windstorm attribution framework. Numbers refer to sources describing the detailed methodology: (1) ERA5: Hersbach et al. (2020)[36], ERA5-Land: Muñoz-Sabater et al. (2021)[37], HadGEM3-A: Ciavarella et al. (2018), (2) see Deliverable D3.1, (3) non-stationary EVA: Mentaschi et al. (2016)[38], (4) Klawa and Ulbrich (2003)39, (5) FFSA/GEMA (2011)[40].

2.6.1. Event definition

The coastal flood event is defined by maximum water extent and depth, while windstorm is defined by maximum wind speed.

2.6.2. Factual and counterfactual simulations

For coastal flooding, hazard, exposure and vulnerability counterfactuals refer to the 1950 baseline for three types of impacts (see Table 5). For windstorm economic impacts, two baselines are analysed, 1950 and preindustrial (defined as 1850 for exposure). Vulnerability counterfactuals were not considered for the windstorm due to the lack of applicable methods.

36 Hersbach, H., Bell, B., Berrisford, P., Hirahara, S., Horányi, A., Muñoz-Sabater, J., Nicolas, J., Peubey, C., Radu, R., Schepers, D., Simmons, A., Soci, C., Abdalla, S., Abellan, X., Balsamo, G., Bechtold, P., Biavati, G., Bidlot, J., Bonavita, M., De Chiara, G., Dahlgren, P., Dee, D., Diamantakis, M., Dragani, R., Flemming, J., Forbes, R., Fuentes, M., Geer, A., Haimberger, L., Healy, S., Hogan, R. J., Hólm, E., Janisková, M., Keeley, S., Laloyaux, P., Lopez, P., Lupu, C., Radnoti, G., de Rosnay, P., Rozum, I., Vamborg, F., Villaume, S., and Thépaut, J.-N. (2020). The ERA5 global reanalysis, *Q. J. Roy. Meteor. Soc.*, 146, 1999–2049, https://doi.org/10.1002/qj.3803.

37 Muñoz-Sabater, J., Dutra, E., Agustí-Panareda, A., Albergel, C., Arduini, G., Balsamo, G., Boussetta, S., Choulga, M., Harrigan, S., Hersbach, H., Martens, B., Miralles, D. G., Piles, M., Rodríguez-Fernández, N. J., Zsoter, E., Buontempo, C., and Thépaut, J.-N. (2021). ERA5-Land: a state-of-the-art global reanalysis dataset for land applications, *Earth Syst. Sci. Data*, 13, 4349–4383, https://doi.org/10.5194/essd-13-4349-2021.

38 *supra* note 20.

39 *supra* note 28.

40 *supra* note 9.

Table 5 Summary of counterfactual scenarios.

Hazard	Coastal flood			Windstorm	
Climate counterfactual approach	Non-stationary EVA for storm surge and wave height; sea level rise removal (1950 baseline)			Non-stationary EVA (1950 baseline)	Climate modelling (preindustrial baseline)
Exposure counterfactual	1950 baseline				1850 baseline
Vulnerability counterfactual	Flood protection level, relative loss (1950 baseline)			not considered	
Impacts	Fatalities;	Population affected	Economic loss		

2.7. Results

2.7.1. Factual hazards and impacts

Modelled impacts were compared with reported losses in Table 6. The modelled flood extent is generally larger than observed during the event (Figure 10), as many low-lying, but uninhabited areas were subject to high sea levels for shorter time than predicted in the model. Consequently, seawater didn't extend that far inland during the actual event. As those were mostly natural or agricultural land, this has limited relevance for estimating exposure to the event.

Overall, predicted flood losses were much lower than reported after applying the region-specific vulnerability adjustment. This indicates that the vulnerability is underestimated, which could be explained by very local factors set out in section 2.4.2, especially construction characteristics, societal factors or timing of the event, and particularly in context of fatalities, which are most underestimated here. Still, all components of the model (hazard, exposure, vulnerability) are subject to cascading uncertainties. By contrast, economic losses from the windstorm are considerably overestimated by the generic pan-European damage function. This suggests that France, possibly due to better adaptation resulting from high frequency of damaging windstorms, has lower vulnerability. Windstorm fatalities were not modelled due to lack of methods and the very incidental circumstances of the six deaths during the event.

Table 6 Comparison of reported and modelled flood losses.

Impact	Reported loss	Modelled loss (generic damage function)	Modelled loss (with local vulnerability estimate)	Difference modelled/ reported loss
Coastal flood				
Area inundated (km^2)	560	1138	*n.a.*	2.03
Fatalities	41	952	5	0.12
Persons affected	10,000	50,750	4053	0.41
Economic loss (million euro, 2020 prices)	1387	3750	219	0.16
Windstorm				
Fatalities	6	*n.a.*	*n.a.*	*n.a.*
Economic loss (million euro, 2010 prices)	735	6753	*n.a.*	9.2

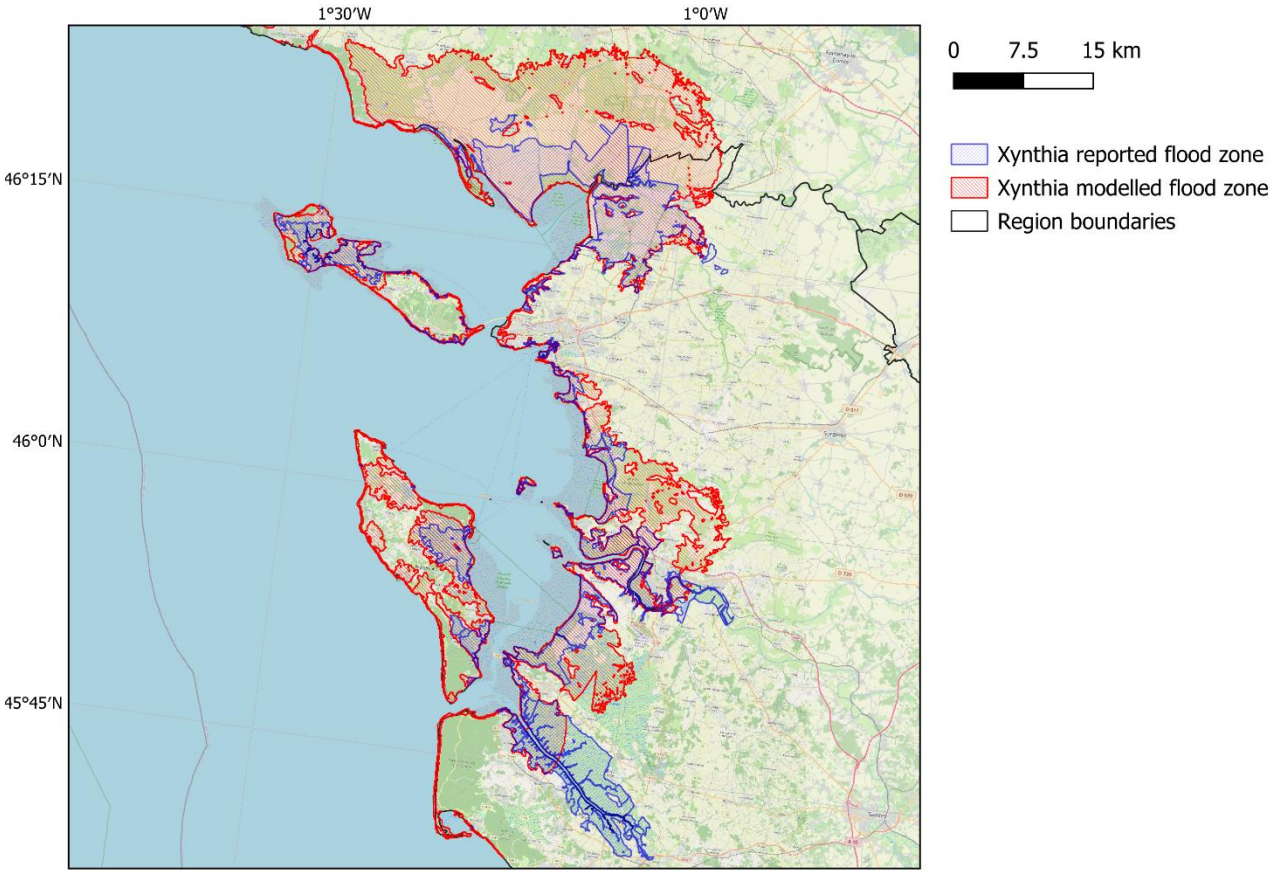

Figure 10 Modelled vs reported maximum extent of the Xynthia coastal flood.

Modelled losses were also compared with insured losses at the level of administrative divisions. The coefficient of determination between modelled and reported flood losses per municipality was 0.47, while the indicator for wind losses per department (NUTS3 region) was 0.31. This shows that the modelling chain resulted in a model that is able to capture at least some of the spatial variation of observed losses considering detailed hazard and exposure, but only generalized vulnerability modelling.

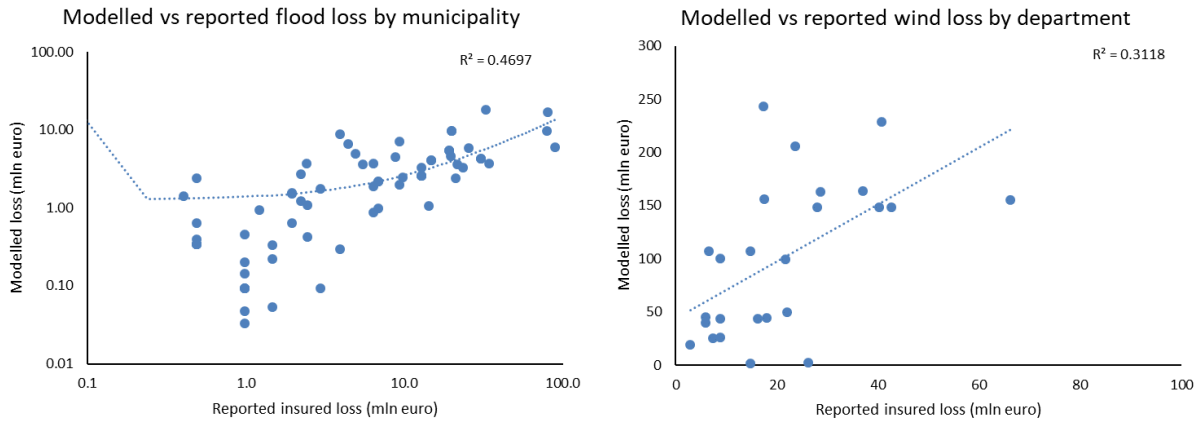

Figure 11 Modelled vs reported insured losses: coastal flooding by municipality (left) and windstorm by department (right).

2.7.2. Attribution results

Climate change is shown to have increased the impacts of both coastal flooding and windstorm. As the coastal flood levels were influenced especially by well-quantified sea level rise since 1950, the confidence of this finding is very high (90% confidence interval is +10% to +14%). For the windstorm, the uncertainty using the hadGEM-

3A approach is high, as the 90% confidence interval spans from –71% to +44% influence of climate change relative to preindustrial levels (for the tsEVA approach, the uncertainty was not quantified). The statistical approach with a 1950 baseline both indicates a greater influence of long-term changes in climate (22% versus 7%), but with considerable spatial differences (Figures 12-13). This indicates the strong influence of the choice of method and baseline in attributing climate impacts.

Table 7 Change in impacts due to individual drivers (% change relative to counterfactual).

Hazard		**Coastal flood**			**Windstorm**	
Baseline		1950				Preindustrial
Impact		Fatalities	Population affected	Economic loss		
Driver						
Climate change		11	10	12	22	7
Exposure growth	Population	45	48	49	51	74
	GDP per capita	x	x	393	336	1314
	Fixed assets to GDP	x	x	16	9	-39
Exposure spatial distribution*		1		-13	-2	-25
Flood protection		-1		-2	x	x
Vulnerability		-65		-66	..	..

x - driver not applicable

.. - no data

* for floods, includes effect of changing shares of different economic assets, each with different vulnerability

Windstorm losses are heavily driven by GDP growth, with much lower contribution of population growth or increase in relative asset value. Spatial distribution of assets in context of the Xynthia windstorm changed very little since 1950 but has noticeably moved from towards lower-impact zones since 1850.

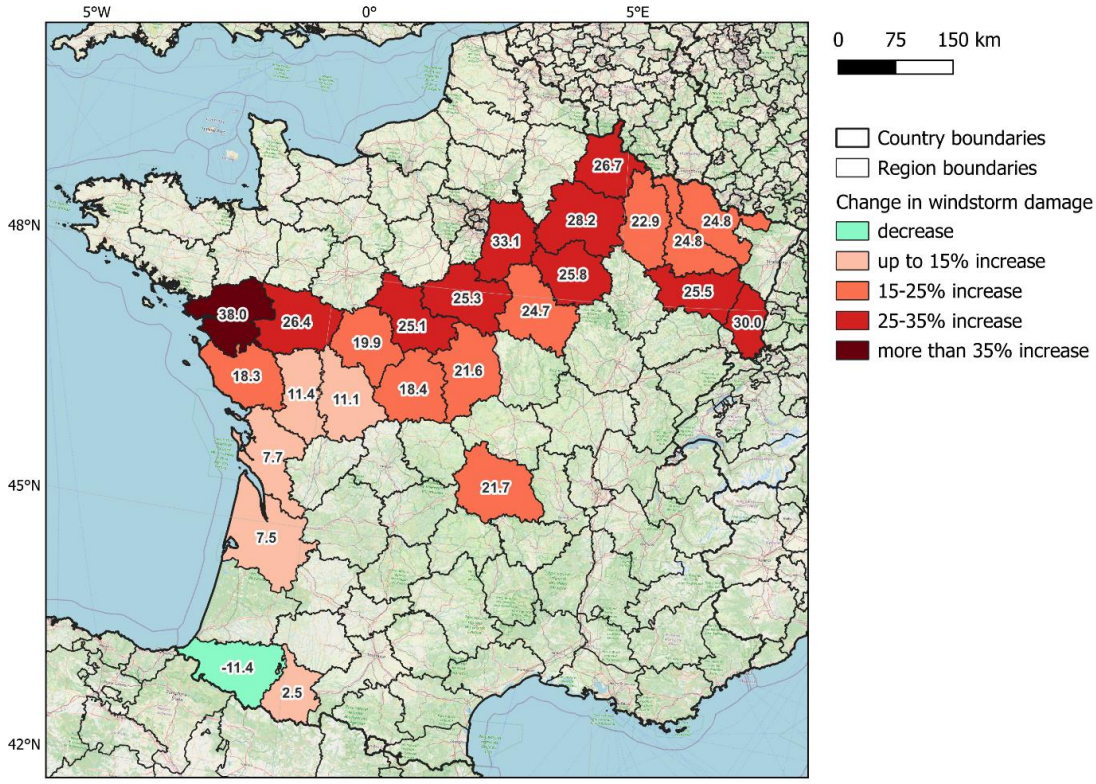

Figure 12 Change in windstorm damage due to observed long-term changes in climate since 1950 using the transformed-stationary EVA approach.

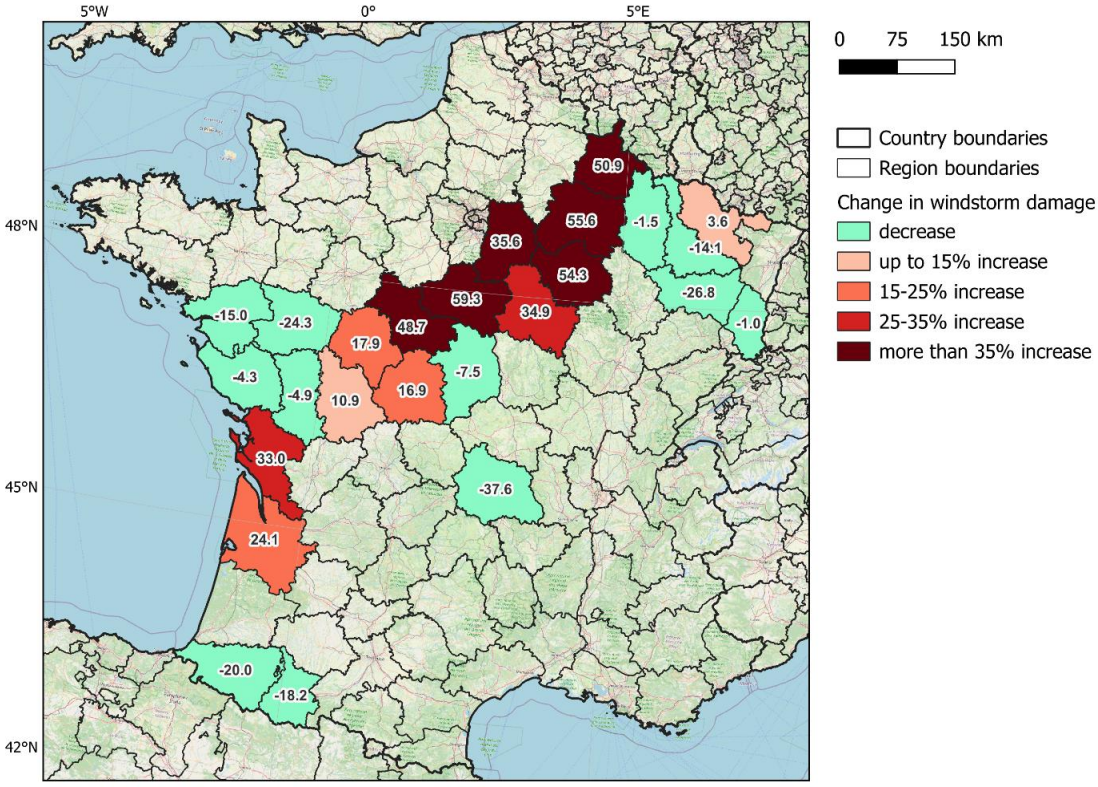

Figure 13 Change in windstorm damage due to anthropogenic climate forcing relative to natural forcing using the hadGEM-3A dataset.

The attribution of flood impacts was more comprehensive in terms of the number of impacts and drivers used. Relative to the 1950 baseline, climate change contributed to a 10-12% increase in impacts across all three types

of impacts. Economic loss was substantially increased by economic growth (633%, Figure 14), but population growth contributed much less (45-48%). Spatial distribution of population and assets, as well as change in economic structure, is estimated to contribute little to the losses. Similarly, changes in flood protection levels are estimated to have very limited influence on the magnitude of losses.

Most importantly, changes in vulnerability are estimated to have compensated substantially for increases due to climate change and exposure growth (56-66% decrease). However, the uncertainty in estimating past vulnerability is high, similarly to the protection levels. Therefore, confidence in this finding is low, especially in context of the model underestimating factual flood impacts in the first place.

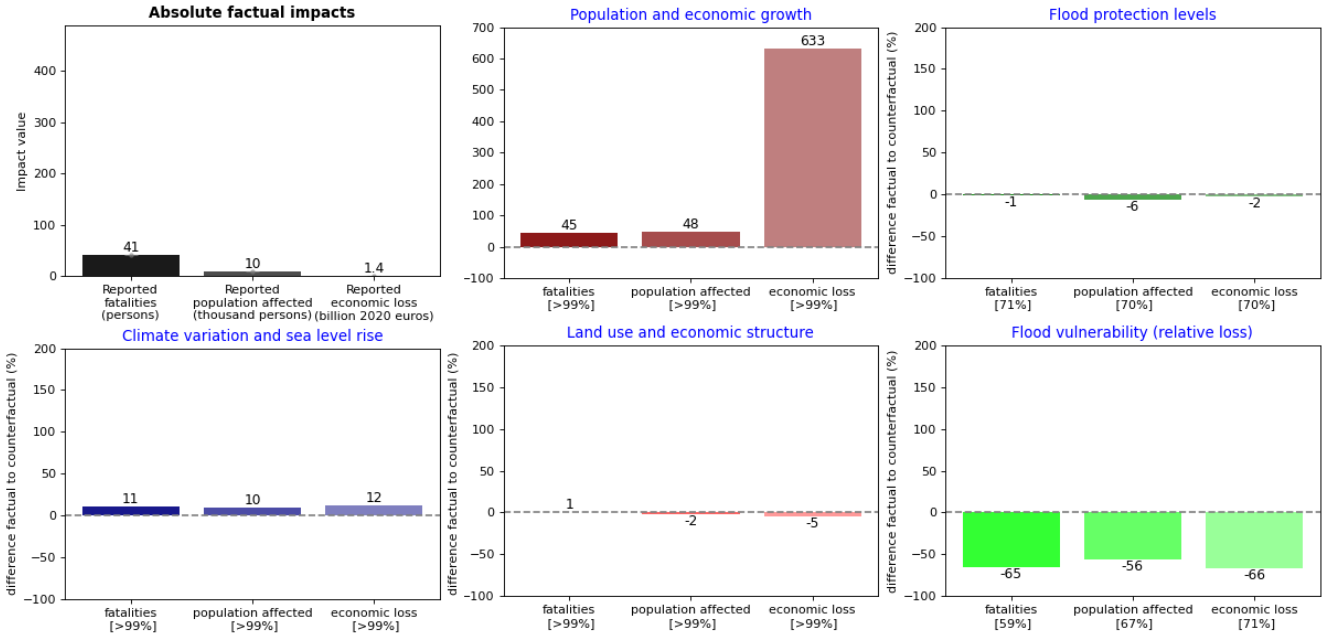

Figure 14 Attribution of flood impacts (% change relative to 1950 counterfactual). The percentages below graphs indicate the confidence that factual is different from counterfactual.

2.7.3. Stakeholder and policy relevance

In the two affected regions, extensive seawall and dike renovations as well as smaller technical adaptation measures have been carried out since the flood and will continue to be implemented at least until 2030, at a cost of some 1.5 billion euro (Enet 2021)[41]. Within the 'agglomeration communality of La Rochelle' (which combines the city with several smaller municipalities) several adaptation measures are currently implemented. According to the civil protection office of the agglomeration (personal communication), they include:

- Prefectural flood maps and flood prevention plans
- Use of Xynthia flood level as baseline for planning plus 20 and 60 cm sea level rise
- Requirement of floor levels in new or extended buildings to be above potential flood levels
- Supporting adaptation of existing buildings in the *Xynthia + 20 cm* zone
- Reducing new construction in the *Xynthia + 60 cm* zone
- Early warning procedures plus a voluntary response force
- An 800-meter temporary barrier to protect La Rochelle harbour (deployment time: 7 hours with 28 persons)

41 *supra* note 11.

Attribution analysis indicates a contribution of climate change to windstorm losses, though with considerable uncertainty. This indicates the need to frequently reevaluate the minimum standards for buildings – European construction regulations state that they are required to withstand wind with a return period of 1 in 50 years.

Figure 15 Trees painted blue to signify Xynthia water level and 20 cm sea level rise. This part of La Rochelle was actually flooded to that level in 2010. (Photos DP)

Figure 16 Public evacuation centre in La Rochelle and Xynthia flood marker. (Photos DP)

Figure 17 Movable flood barriers in La Rochelle harbour (left) and Châtelaillon-Plage (right). (Photos DP)

3. Use Case 2a: United Kingdom winter storms 2013/2014

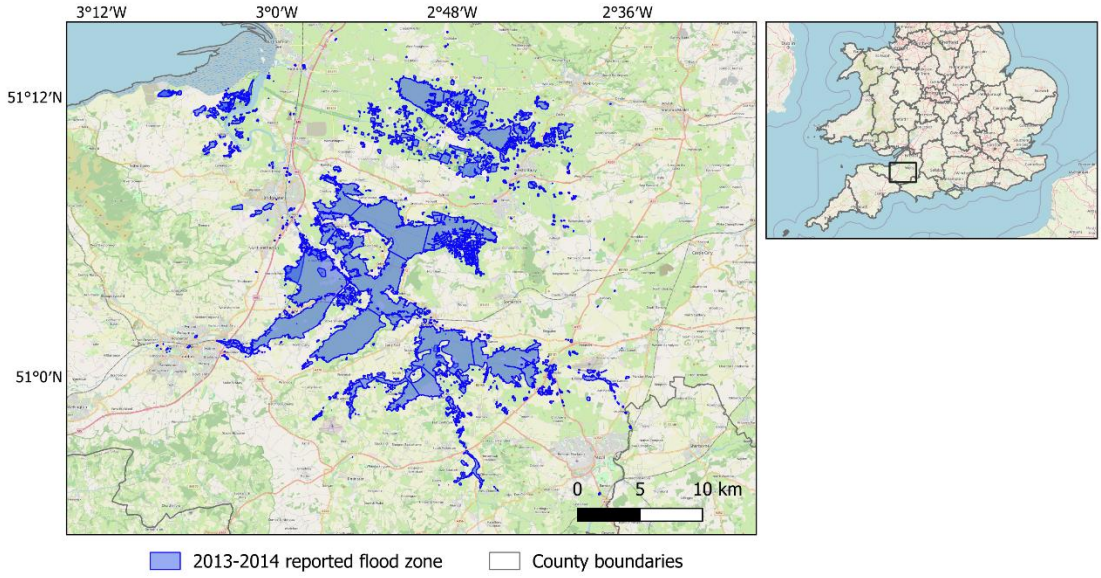

Figure 18 Observed flood extent over the entire Somerset Region from December 2013 to March 2014.

3.1. Summary of event

From December 2013 to March 2014 a sequence of powerful Atlantic low-pressure systems hit the UK over a three-month period. The storms yielded widespread impacts over the UK, mainly in the form of flooding and coastal damage leading to extensive power outages impacting hundreds of thousands of homes. Sustained heavy rain, high spring tides and strong winds exacerbated these impacts and fueled conditions for coastal flooding. Furthermore, the successive storms brought record levels of rainfall onto already saturated ground, adding pluvial and fluvial flooding as key hazards of concern. The economic cost of these impacts over England and Wales from December 2013 to March 2014 came to approximately £1.3 billion, with England absorbing 91% of the damages[42].

The Somerset Levels and Moors accounted for around 30% of flooded agricultural land nationwide, with more than 100 pumps deployed to reduce the impact of the floods. The UK's Environment Agency (EA) provided over 150,000 sandbags, helping to limit the £5.7 million in flood damages to the region[43]. The average economic cost of damages per property in the Somerset region was about £52,000 – over twice the national average. According to the EA, 870 Devon and Somerset Fire and Rescue Service members were deployed to aid with the Somerset floods, totaling 4,985 hours of assistance[1]. In addition to the economic costs, 957 emergency service personnel were deployed during the event and there were significant social impacts ranging from depression and anxiety in flooded and cut-off communities.

Following the 2013-2014 Somerset floods several adaptation strategies were implemented including: raising road levels, setting up control structures to avoid road flooding, and dredging of the Parrett and Tone rivers. There were repairs to flood banks, new flood alleviation schemes were built as well as improvements to existing schemes. The EA are now working on the Bridgewater Tidal Barrier, which will prevent high water levels from

[42] Environment Agency, 2016. https://rpaltd.co.uk/uploads/report_files/the-costs-and-impacts-of-the-winter-2013-to-2014-floods-report.pdf

[43] Morris, J, 2014. Assessing the impacts of floods 2012-2014 on agricultural land in Currymoor and adjoining drainage districts, Somerset Levels and Moors. Report to Somerset Drainage Boards Consortium.

travelling inland in order to protect around 11,300 homes and 1,500 businesses from tidal flooding in Somerset[44].

3.2. Geographical context

England, Wales, Scotland and Northern Ireland. We focus on the Somerset region.

3.3. Observed hazards

3.3.1. Type of hazards

Intense rainfall, storm surges, fluvial flooding, pluvial flooding, coastal flooding, groundwater flooding, coastal erosion.

3.3.2. Form of compounding

Multivariate and temporal.

3.3.3. Driving dynamics

A series of powerful Atlantic low-pressure systems with multiple contributing drivers:

a. A strong positive North Atlantic Oscillation (NAO) index was present at the time, which in the winter is associated with above average precipitation[7].
b. Heavy rainfall in the tropical pacific strengthened the Atlantic jet stream through well-understood teleconnections, resulting in enhanced storm development conditions[7].
c. Westerly wind adjustment in the upper troposphere in the East Pacific allowed for additional atmospheric disturbances to enter the Atlantic jet stream's origin[7].
d. Teleconnection from the Quasi-Biennial Oscillation (QBO) in a strong westerly phase over the tropics may have increased the pressure gradient in the Atlantic and contributed to heavy rainfall and stormy conditions[45].

3.3.4. Intensity

Over the winter, the UK rainfall total was 545 mm – 1.65 times the 1981-2010 average. Winds gusted above 70kn over exposed coastlines, with gusts over 100kn recorded on some of Scotland's mountain summits and some areas in the Somerset region experienced gusts of 62kn or higher. The combination of particularly long-period ocean swell, strong winds and high spring tides led exceptionally large waves, with dangerous and damaging coastal conditions in southwest England and South Wales (Kendon and McCarthy, 2015)[46]. In February 2014, a record-breaking 25m wave height was record off the south coast of Ireland (Met Eireann, 2014)[47]. In Somerset, the winter rainfall total was 536.6mm – a record which is still held to this day.

[44] Environment Agency, 2023. Somerset Levels and Moors: reducing the risk of flooding. https://www.gov.uk/government/publications/somerset-levels-and-moors-reducing-the-risk-of-flooding/somerset-levels-and-moors-reducing-the-risk-of-flooding

[45] Huntingford, C. et al., (2014). Potential influences on the United Kingdom's floods of winter 2013/14. *Nature Climate Change*

[46] Kendon, M. and McCarthy, M. (2015), The UK's wet and stormy winter of 2013/2014. Weather, 70: 40-47. https://doi.org/10.1002/wea.2465

[47] Met Éireann: Major Weather Events, available at: http://www.met.ie/climate-ireland/major-events.asp.

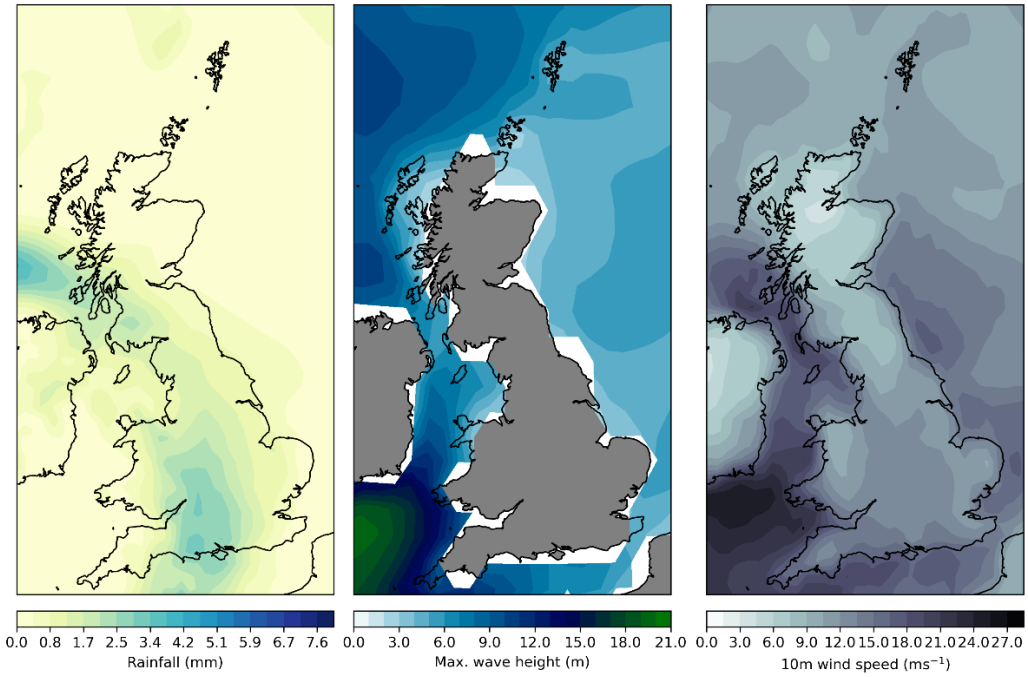

Figure 19 UK instantaneous rainfall, maximum wave height and 10m wind speed from ERA5 for 1pm 12th February 2014, close to when a record-breaking wave was recorded off the coast of southern Ireland.

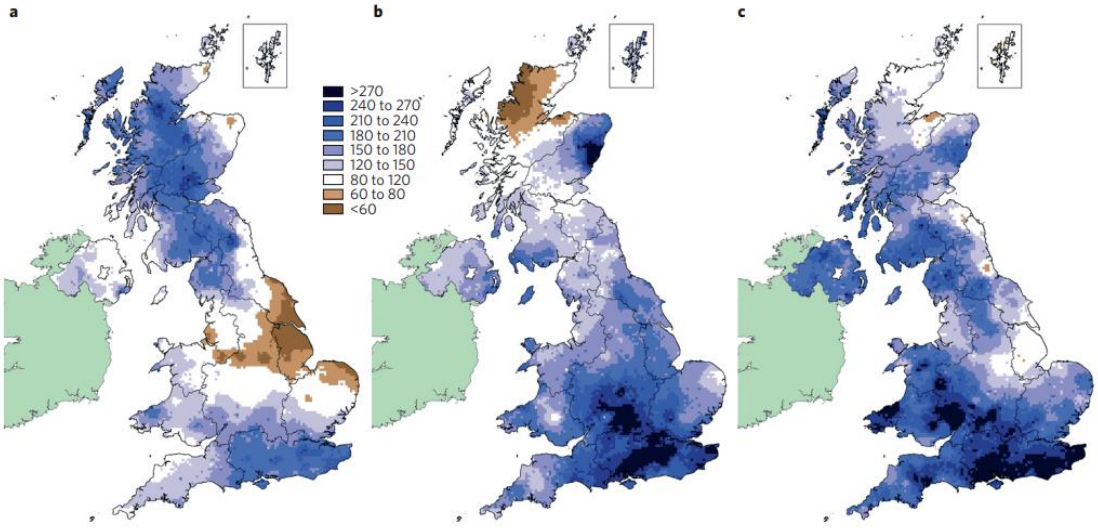

Figure 20 UK rainfall anomaly for (a) December 2013, (b) January 2014, (c) February 2014, taken from Huntingford et al. (2013).

3.4. Observed impacts

3.4.1. Quantitative impacts

The impacts listed below are for the Somerset region.

Table 8 Key impact data and statistics.

Impact	Magnitude/scale	Source
Residential property	• 165 residential properties flooded internally (16.0m ±4.0m)	SRA (2015)[48]
Emergency responses	• 957 emergency service personnel deployed • Floodwater pumping with 128 pumps operating at peak • Costs of services totaled £16.8m ±2.5m	EA (2016)
Transport	• 81 road closures (£12.0m ±3.0m) • The Muchelney community was cut off by flood waters for over 2 months • The major railway line between Bridgewater and Taunton was closed for weeks (£17.0m ±4.3m)	SRA (2015)
Agricultural	• 12,800 Ha of pasture was flooded • 1,100 Ha of arable land was flooded • Costs totaled £5.5m ±1.4m	SRA (2015)
Local businesses	• ~50% of businesses were either directly or indirectly impacted by flooding • ~85% of businesses were impacted by road closures • ~12 farmsteads were significantly flooded • Business premises were damaged by floodwaters • Costs to businesses totaled £3.3m ±0.8m	SRA (2015)
Social impacts	• 'Devastating' impact on mental health, depression and anxiety in flooded and cut-off communities • Significant delays, disruption and diversions were caused over 3 months • Social impact costs totalled £3.2m ±1.6m	SRA (2015)
Tourism	• Lost tourism days due to the flooding in Somerset as high as 698,091, equating to economic losses up to £51.4m	SRA (2015)

[48]Somerset Rivers Authority, (2015). Somerset Economic Impact Assessment of the winter 2013/14. https://www.somersetriversauthority.org.uk/wp-content/uploads/2018/06/22-July-2015-ITEM-8-Economic-Impact-Assessment-full-report.pdf

3.5. Modeling framework

3.5.1. Hazard modeling

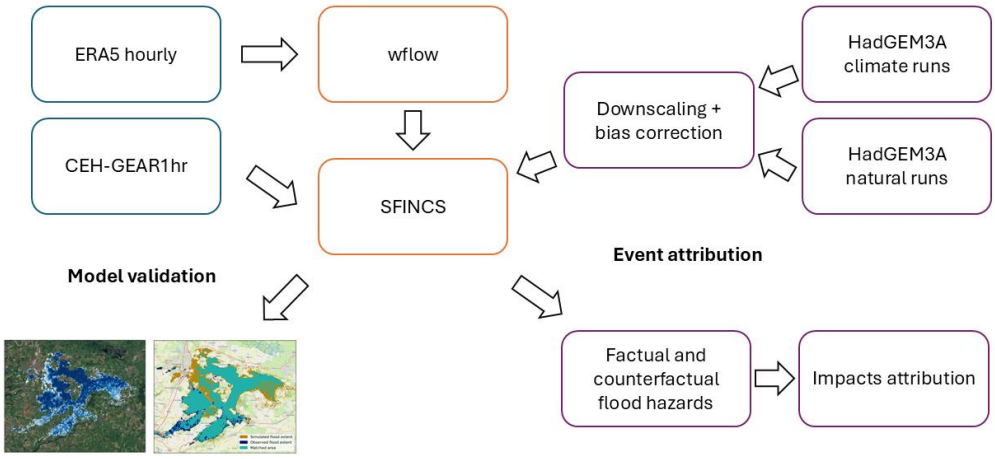

Figure 21 Flowchart of hazard and attribution modelling framework. Where CEH-GEAR1hr represents the precipitation dataset, wflow is the hydrological model, SFINCS is the compound flood model.

To simulate flood extent over the Somerset Levels under the observed atmospheric conditions we used the SFINCS[49] reduced-complexity compound flood events model at a 90m^2 resolution, driven with the CEH-GEAR 1hr precipitation dataset over the event period, with a warmup simulation forced by ERA5 for the preceding year providing antecedent conditions for the event period of interest. The CEH-GEAR 1hr dataset contains gridded precipitation interpolated from a network of in-situ hourly and daily rain gauge data. ERA5 was used to provide antecedent conditions because the wflow model requires auxiliary meteorological variables such as temperature and evapotranspiration – these are also used by wflow during the event period. No coastal or river defenses were explicitly included in the model, though they could be included in future analyses. The model performs well compared to observations of flood extent in certain areas in Somerset, especially in one of the most impacted regions between Bridgwater, Langport and Glastonbury. In other areas it performs less well, such around the river Parret's river mouth. We were unable to include explicit coastal and river defenses during the event simulation and estimate that the inclusion of these structures as well as increasing the resolution of the model would have significantly improved the representation of flooding in these areas. As a result, we selected one of the better-represented regions with respect to observed flood extent to focus our analysis and improve the reliability of our attribution results. The chosen area was impacted mostly by pluvial and groundwater flooding as opposed to fluvial and coastal flood types which are impacted more by waterside structures. The smaller chosen area does however narrow the focus of our attribution to a relatively small area, increasing our exposure to large spatial variability in meteorological and climatological conditions – in other words, it may be more difficult to detect a climate signal in the noise.

[49] SFINCS: Super-Fast Inundation of CoastS model. https://doi.org/10.5281/zenodo.10118583

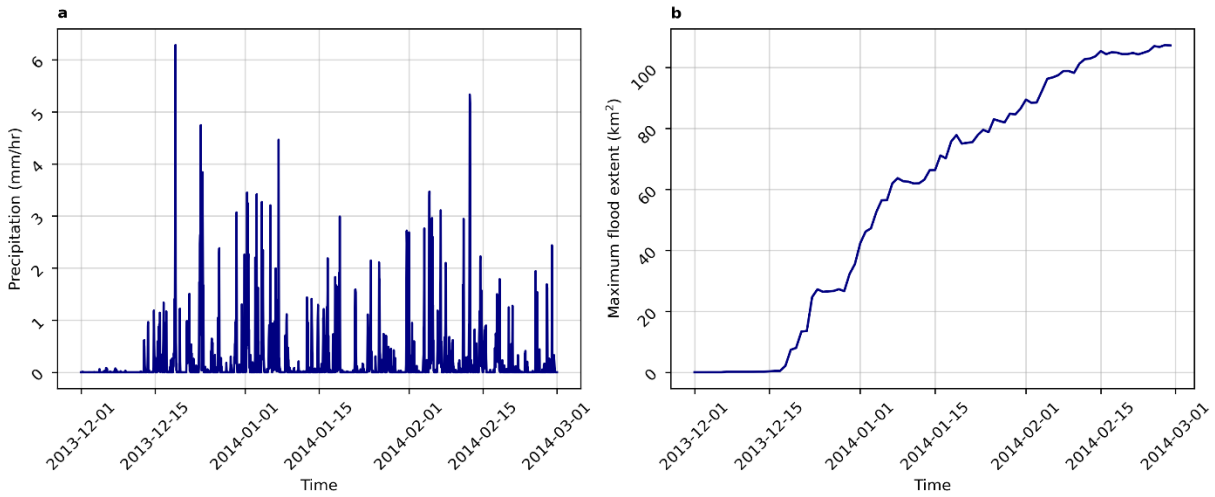

Figure 22 Observed rainfall from CEH-GEAR 1hr (a) and corresponding simulated flood extent (b) in the Somerset sub-region from December 2013 to March 2014.

Figure 22a illustrates the observed rainfall over the Somerset region during the winter of 2013/14. Most of the rain falls towards the beginning of the period and is generally consistent thereafter, if trending slightly downward. This trend is replicated in the simulated observed flood extent (Figure 22b), which grows quickly through the end of December 2013 and reaches its peak towards the end of February 2014. This matches observations of flooding during this time – the worst flooding occurred between mid-January and the end of February, although impacts were felt for long afterwards as critical infrastructure and transport networks were damaged.

3.5.2. Impact modeling

Exposure modelling

We used the HANZE v2.0 exposure dataset[50] to calculate population exposure change due to both climate change and economic/population growth.

Vulnerability modelling

The Huizinga et al. (2017) damage function dataset[51] land cover types don't match well against spatial land-cover datasets for our chosen sub-region and may not fit this use-case very well because much of the impacts were infrastructure and transportation-based.

3.6. Attribution modeling framework

Figure 23 illustrates the modelling framework we used to attribute a climate signal (if any) to our observed compound flood event. We attempt to make an attribution statement at each step, from the meteorological conditions which led to the event, to the extent of flood hazard, to socioeconomic impacts.

[50] Paprotny, D. (2023). Pan-European exposure maps and uncertainty estimates from HANZE v2.0 model, 1870-2020 [Data set]. In Scientific Data (v2.0.3, Vol. 10, Number 372). Zenodo. https://doi.org/10.5281/zenodo.7885990

[51] Huizinga, J., De Moel, H. and Szewczyk, W., Global flood depth-damage functions: Methodology and the database with guidelines, EUR 28552 EN, Publications Office of the European Union, Luxembourg, 2017, ISBN 978-92-79-67781-6, doi:10.2760/16510, JRC105688.

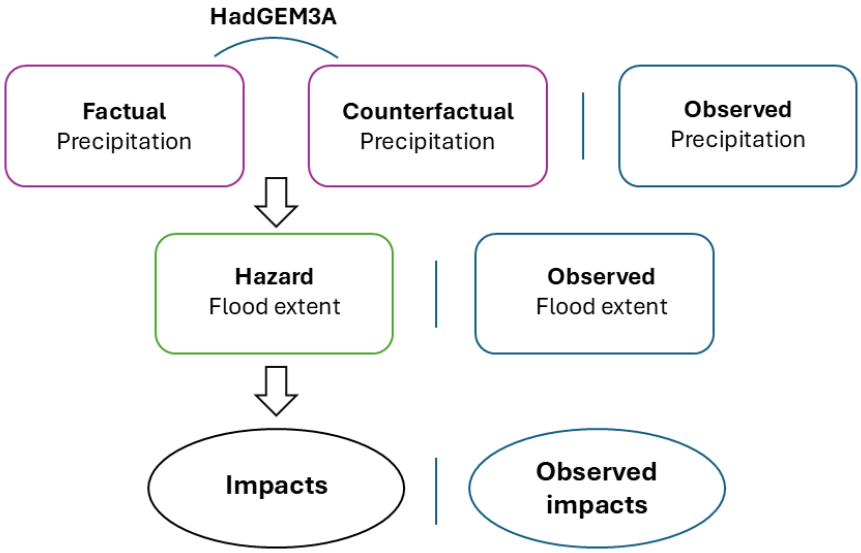

Figure 23 Attribution modelling flowchart, indicating each attribution step from the driving meteorological hazard down to the impacts.

3.6.1. Event definition

The sequential storms over the UK during the winter of 2013-14 caused many compound impacts that differed in nature for different parts of the UK. In this case we focus on the Somerset Levels where there was very heavy flooding in the Parrett and Tone catchments. To capture the temporally compounding aspect of the sequential storms, we examine flood extent over the worst hit catchments in the Somerset Levels.

To capture the impacts, we use the flood modelling workflow for this location (Figure 23), comparing season-long (DJF) precipitation simulations in the current and counterfactual climates. Season long simulations are used to include the temporally compounding nature of the event, with the large number of sequential storms present in 2013/14. We also attempt to partially capture the spatially compounding nature of the flooding in the Somerset Levels (both high tides and extreme seasonal rainfall) with the high tides stopping the large volume of flood water over the Somerset Levels from escaping to sea. One way we aim to address this is by including a counterfactual sea-level for the region in the flood modelling chain.

3.6.2. Factual and counterfactual simulations

The main dataset we use for the climate attribution is the HadGEM3-A large-ensemble attribution runs (Ciavarella et al., 2018) containing members in both factual and counterfactual climates. These attribution runs each contain 15 members between 1960-2013, 105 members between 2014-2015 and 525 members, between 2016-2025. These runs are conditioned on monthly sea surface temperatures (SSTs) and sea ice concentrations (SICs) for the year in question using the HadISST1 dataset. In the counterfactual runs the estimated contribution to these from anthropogenic climate change since the pre-industrial pattern are subtracted from the SST patterns and SICs in the current climate. The global dataset contains 3-hourly temporal resolution precipitation and temperature, with the spatial resolution approximately 60km for the UK. The event in question occurred in 2013-14, therefore we create 20 year-long time slices for each of the 15 original ensemble members between 2005-2024 for both factual and counterfactual ensembles for the attribution analysis, randomly sampling the larger ensembles for the more recent years. This leaves 300 winters to simulate through the flood modelling chain in both factual and counterfactual climates.

We validate the HadGEM3-A model runs for winter precipitation over the somerset levels by comparing the factual runs (ALL forcings) between 1961-2010, to the HadUK-gridded observations at the same spatial resolution (Hollis et al., 2019) over the same period. We use this dataset instead of CEH-GEAR 1-hourly (used as

input to the flood model) for the validation, as it contains a longer time series. Validation plot (Figure 24a) shows strong agreement between the attribution runs and observations for total winter precipitation over the somerset levels, especially for wet extremes. Figure 24b also shows agreement in the sign of the overall trend in DJF rainfall over the region, with a slight increase in winter precipitation. There is a stronger signal in the observations, however the model trend is well within the 95% confidence intervals of the observed trend.

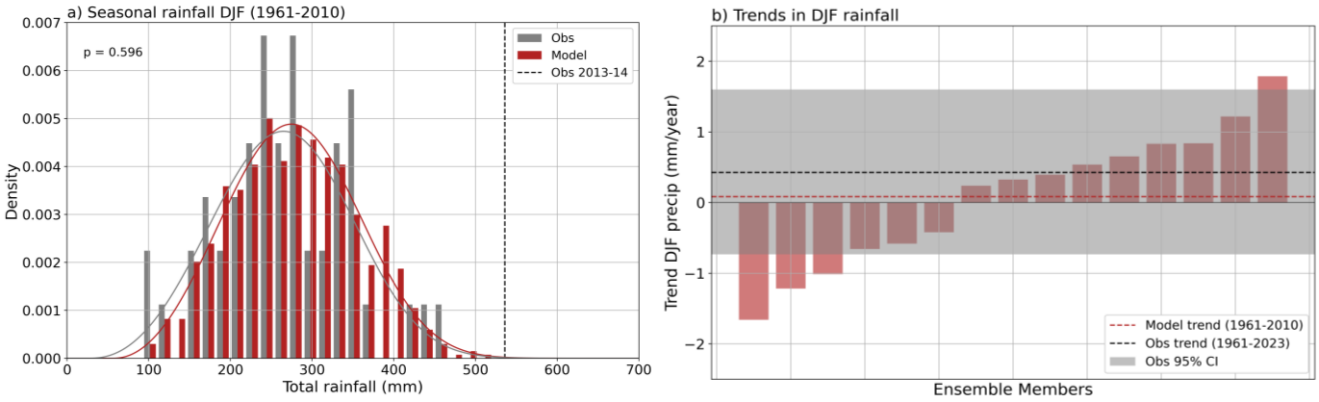

Figure 24 Validation plot comparing total winter precipitation over the somerset levels (small domain) in the HadUK-gridded 60km observations (Hollis et al., 2019) and HadGEM3-A attribution runs. a) histogram of total winter precipitation between 1961-2010 for the observations and 15 ensemble members, fitted to Weibull minimum distribution, with the winter of 2013-14 event represented by the black dotted line. b) shows the trend in winter precipitation for the 15 ensemble members (red bars) with the overall model trend and observed model trend. The 95% confidence intervals on the observed trend were calculated by bootstrapping the observational timeseries with replacement.

Although there was good agreement between the model and observed data at the same spatial resolution (60km), when testing the high-resolution observations (12km) vs the model data (60km) while regridding to the Somerset levels domain, we found 19.7% more rainfall in the model runs than the observations at this higher resolution. This showed that the coarse resolution of the climate model runs would deposit too much rainfall over the local region as it cannot resolve finer-grained rainfall variability over the area. Therefore, a local resolution-related 'bias correction' is needed for the climate model runs to account for the fact that in reality, spatial variability in rainfall is much higher than was modelled, and is influential on the flooding in the chosen Somerset sub-region. To do this, we simply multiplied the climate model precipitation for the region by 0.84 to align the distributions to the HadUK gridded observations over the 1961-2010 historical period. While this produced more realistic rainfall distribution magnitudes, more sophisticated methods could be incorporated into future work, such as spatial downscaling of climate model output over the target region.

3.7. Results

3.7.1. Factual hazards and impacts

We first examine total winter precipitation in the factual climate runs to the counterfactual runs over the area most impacted by the floods. The hazard analysis shows the total winter rainfall seen in 2013-14 over somerset in the current climate has an approximate return period of 64 000 years, compared to a pre-industrial climate (return period: approximately 1 million years). This climate signal contains very large uncertainty intervals, and the 2013-14 DJF precipitation totals are very far in the tail of the distribution to make any strong attribution statements on the hazard for this specific location. The comparative ALL and NAT distributions suggest there could be a shift in variability with the driest winters becoming drier and the wettest winters becoming wetter.

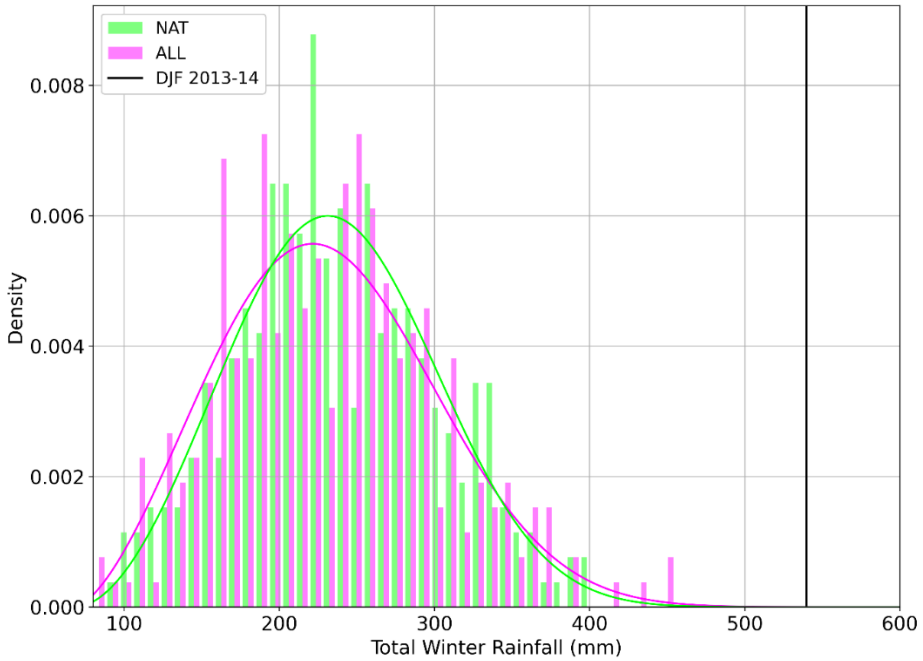

Figure 25 Histogram showing the distribution of total winter precipitation over the somerset levels region in both the 300 factual (ALL) and 300 counterfactual (NAT) bias corrected HadGEM3-A attribution simulations that drive the flood model (15 ensemble members between 2005-2024). Weibull minimum distributions are fitted to each experiment, with the black line representing the observed event in 2013-2014 based on the CEH-GEAR 1-hourly observations dataset.

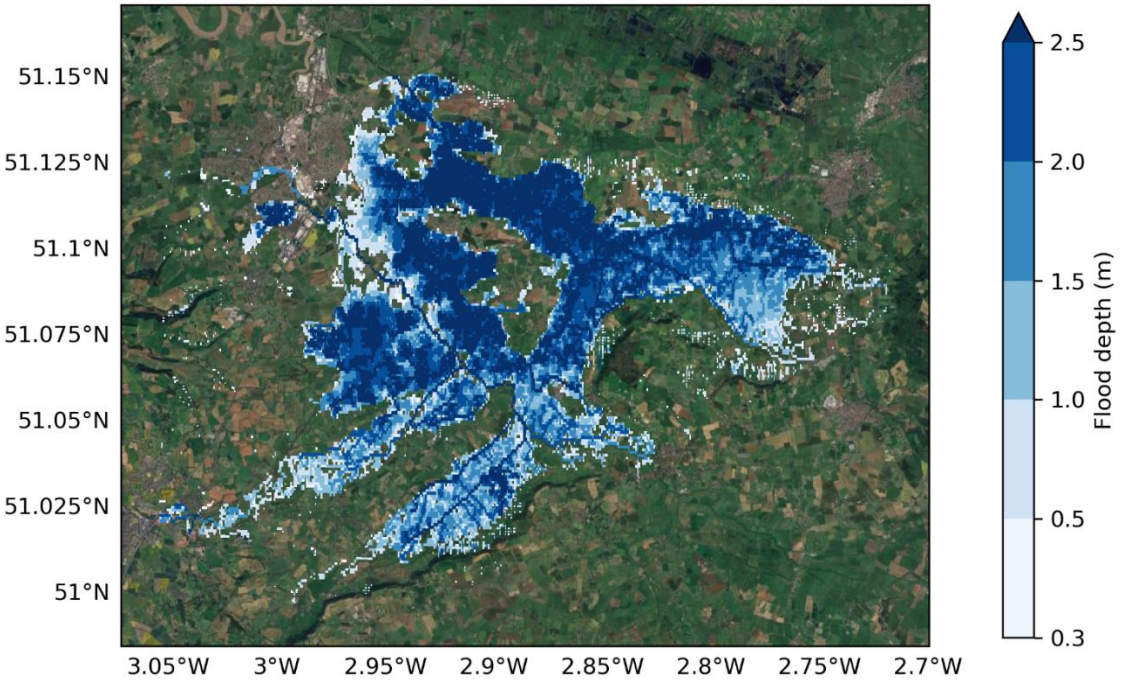

Figure 26 Simulated flood extent and depths under observed atmospheric forcing conditions for the selected region.

A smaller area over the Somerset Levels region was selected for the attribution of flood extent both because it experienced some of the more severe flood impacts during the winter of 2013/2014, and simulated flooding in

the area validates well against observed flood extent[52]. A nearby area to the north-east also experienced severe impacts but is excluded from the analysis due to poor model performance against observations. Figure X overlays the simulated flood extent from observed forcing (using the CEH-GEAR1hr[53] dataset). We calculate a critical success index (CSI) of 0.64 for this validation simulation, where only flood depths above 0.30m are considered. This threshold was chosen following the EA's methodology in designating national Flood Risk Areas.

In Figure 27 we can see SFINCS floods correctly over almost all of the observed flooded area in the sub-region, however floods too much towards the north-west, especially in more urban areas of Bridgwater, and surrounding villages. As a result, we expect to generally overestimate the number of people exposed to flooding in the selected area. Most of the flooded area in both the model and observations is over agricultural land and known flood-risk areas.

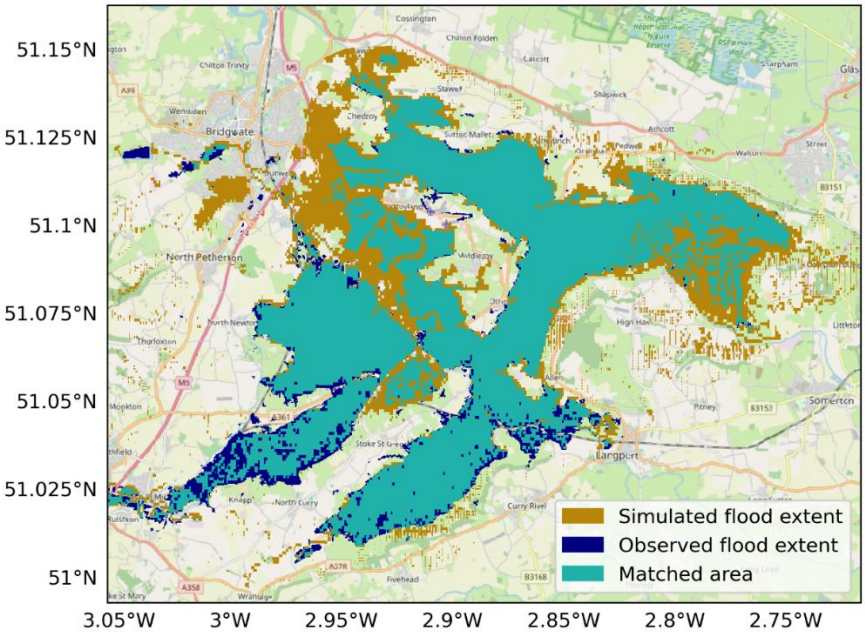

Figure 27 Validation map of simulated flood extent under observed atmospheric forcing overlayed with the actual observed flood extent for the winter 2013/2014 event(s).

3.7.2. Attribution results

We find only a small attributable climate signal for flood extent in our selected area. Figure 28 demonstrates this, where Weibull distributions fit to the data differ only slightly between the climate and natural forcing-drive simulations. A total of 600 simulations (300 anthropogenic, 300 pre-industrial forcing) were run to build these distributions, and the final flood extent is the maximum observed extent over a 3-month winter period. Figures shown in square brackets are the 95% confidence interval.

We calculate the return period of the (simulated) observed flood event as 206.43 [98.75-610.97] years under factual forcing conditions, and 248.90 [117.18-750.79] years under natural forcing. This indicates an event like that observed over the winter of 2013/2014 is about 1.21 [0.33-4.45] times more likely under climate change than under pre-industrial climate conditions, a result that is not statistically significant. A flood event in the selected area with the same factual return period but under natural forcings would be slightly less severe:

[52] Environment Agency (2025). Recorded Flood Outlines. https://www.data.gov.uk/dataset/16e32c53-35a6-4d54-a111-ca09031eaaaf/recorded-flood-outlines1

[53] Lewis, E. et al., (2022). Gridded estimates of hourly areal rainfall for Great Britain 1990-2016 [CEH-GEAR1hr] v2. *NERC EDS Environmental Information Data Centre*. https://doi.org/10.5285/fc9423d6-3d54-467f-bb2b-fc7357a3941f

113.40km^2 [110.66-116.12] instead of 114.02km^2 [111.23-116.81] as shown in Figure 28b and again, not statistically significant.

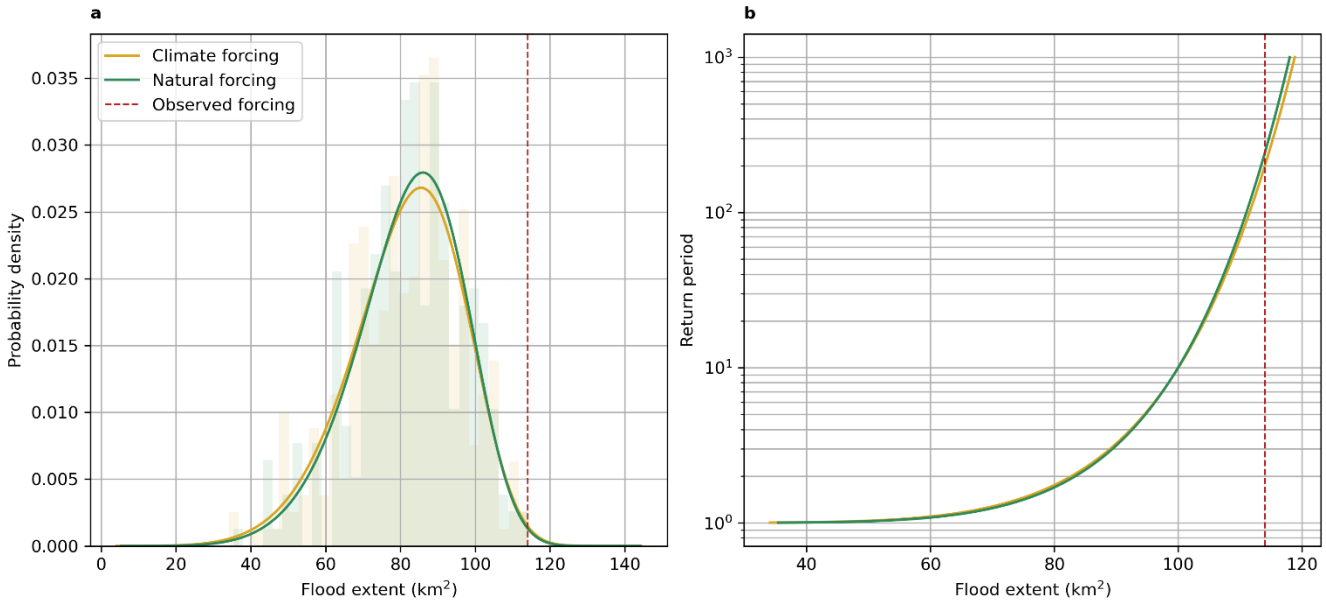

Figure 28 Probability distribution functions (PDFs) (a) and return period curves (b) related to flood extent for the climate and natural forcing-driven flood simulations. The simulated flood extent of the observed compound winter 2013/2014 events is shown by the dashed red line on each panel.

The not significant differences in the natural vs. factual flood extents may be the result of a few factors. Even though the cumulative rainfall in the region over each of the winters has quite a different spread (see Figure 29) between the factual and counterfactual, this does not necessarily lead to a corresponding difference in SFINCS. River flows at the beginning of the simulations are derived from a common ERA5 forcing which may lead to overly full rivers to start with; additional rainfall may make less of a difference when it comes to fluvial flooding in this case. Secondly, the timing of the rainfall could make a significant difference – heavy rainfall over a short period may lead to large, transient flood extents, obfuscating a potentially dry seasonal average. Further, the chosen resolution and characteristics of the model itself may make it generally less sensitive to change in rainfall over this region. Figure 29 shows the range of cumulative rainfall and flood timings and magnitudes over the climate and natural forcing simulations compared to the simulated observed forcing. Many simulations experience large accumulated rainfall (and hence flooding) towards the beginning of the period, and tail off towards the end, as opposed to in the observed forcing which sees a sharp and then relatively constant increase from mid-December to mid-February, tailing off with lower rainfall toward the end of the event period. Effectively, the factual and counterfactual simulations accumulate rainfall at a slower rate than during the observed event. The orange (climate-driven) simulations in Figure 29a, b correspond with that of Figure 29a, where the climate forcing distribution is wider at the tails of the distribution compared to the natural forcing and so we see climate-driven simulations with both the highest and lowest rates of accumulation and flooding.

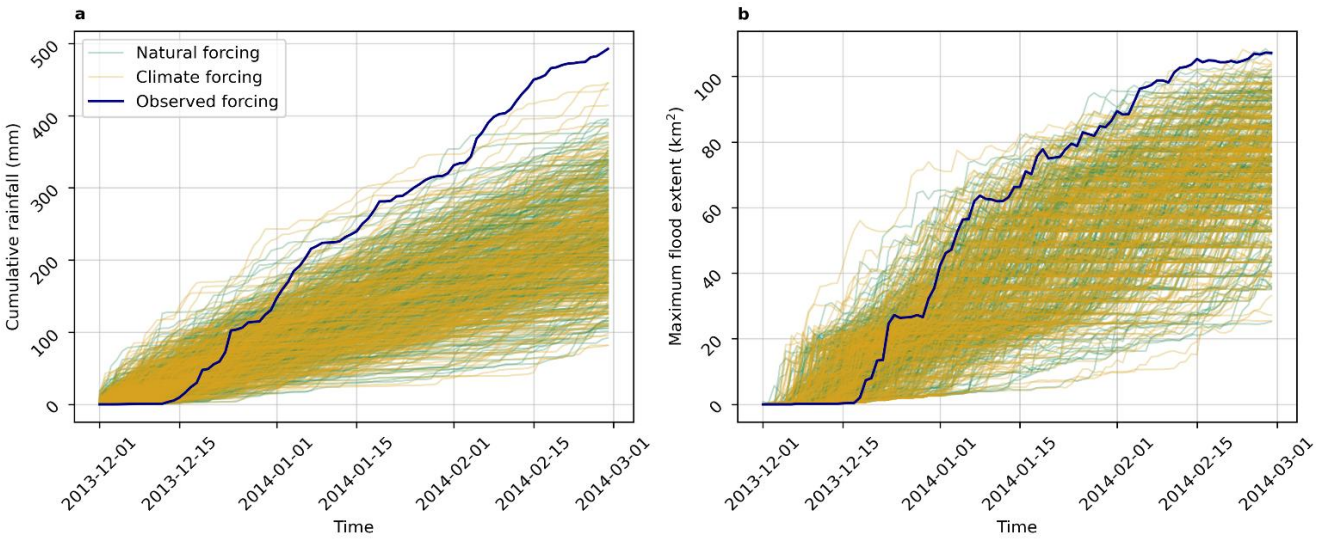

Figure 29 Cumulative rainfall (a) and spatially averaged maximum daily flood extent (b) for the Somerset sub-region over the three-month study period.

To test the effects of rainfall timing over the 3-month period, we re-calculated the attribution metrics using the average daily-maximum flood extent, instead of the maximum overall extent. The climate signal here is larger, with a likelihood of seeing the observed event or more intense increasing to 1.67 [0.38-7.81] times more likely. The return periods also change and increase, with that of the observed event under climate change increasing to 246.51 [111.00-808.23] years, and 412.44 [170.73-1585.05] years under pre-industrial climate conditions. It's worth noting here that because the observed event falls out on the upper tail of the forcing distribution, the results from the bootstrapped sampling technique are quite sensitive to slightly different underlying distributions: hence the large 95% confidence intervals associated with these estimates. These numbers are smaller than the confidence intervals of the precipitation forcing that drives them, compared to the observed event pricipitation, pointing to the relative insensitivity of SFINCS to differences in rainfall over our sub-region. Using this method of selecting the flood extent, the observed-forcing simulation validates slightly better against observations of flood extent – with a CSI of 0.66.

Since this methodology doesn't match that used to create the observed recorded flood outline dataset, and different to that used as standard in similar literature, we do not include these as main findings in this use-case; instead they are a useful indicator of the sensitivity of these results to methodology, and the sensitivity to the chosen factual and counterfactual distributions used to compare the observed event against.

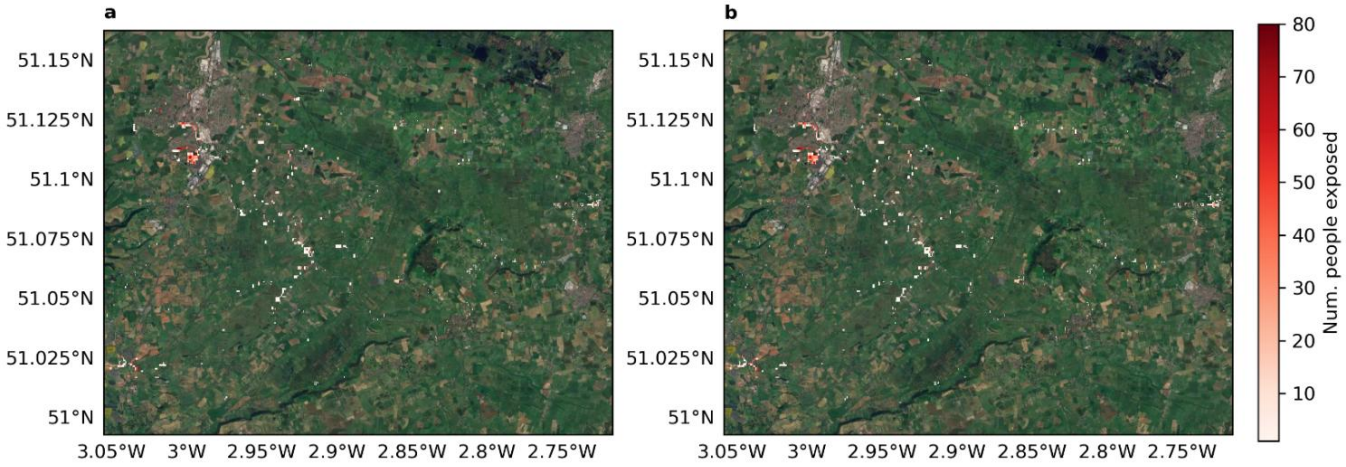

Figure 30 Maps of population exposed to flooding in the selected region under (a) factual climate conditions and (b) counterfactual climate conditions.

The difference in population under factual and counterfactual climate conditions is insignificant and is visually almost impossible to distinguish between Fig. 30a and Fig. 30b. The area is a known flood risk, so very few people have houses on the plains hardest hit by the flood event – however there are many farms and roads which were submerged completely for a prolonged period during the event. Population directly exposed to the impacts of the flooding, in this case, is not the best measure of attributed exposure; further analysis could include people indirectly impacted by having vital transport networks cut-off and areas of farmland exposed under factual/counterfactual climate forcings.

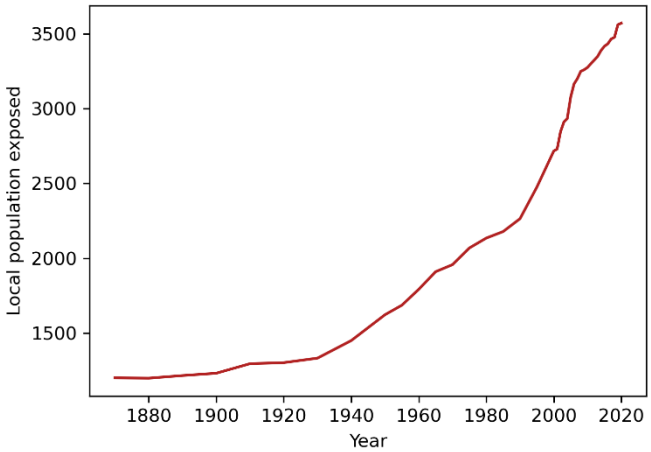

Figure 31 illustrates the increase in population exposure to flood events like those of winter 2013/2014 from 1870 to 2020. Most of the increase in exposure in this region has come from increasing population and population density, rather than from a change in magnitude of impact due to climate change. As previously mentioned, this particular area is quite sparsely populated with the hardest-hitting impacts on agriculture, businesses and transport networks rather than residential homes.

Figure 31 Timeseries of population exposed to the simulated observed flood event over the last 150 years.

3.7.3. Summary of attribution results

We attribute the likelihood of the magnitude of the observed flood extent in the chosen region to be 1.21 [0.33-4.45] times more likely due climate change. The return period of such a flood event is approximately 42.47 years shorter than it would be without anthropogenic warming, turning a 1-in-249 year event into a 1-in-206 year event. The signal due to climate change in the flood extent is relatively small and with large uncertainty bounds, which can be attributed to the rainfall forcing which the SFINCS model was driven with. The major difference between the factual and counterfactual rainfall distributions in this region is seen in the tails, and this difference propagates through to the simulated flood extent where the same result appears.

Multiple other attribution studies examined the wet and stormy UK winter more generally with inconclusive results. Christidis and Stott 2015[54], found there was no detectable climate signal in total winter rainfall such as that in 2013/14, with it only being detectable at shorter timescales (i.e. 10 days or less). The record number of storms in the UK winter of 2013/14 could also not be attributed to anthropogenic induced warming of the tropical west pacific (Wild et al., 2015)[55]. However, another study finds a climate signal in the number of days in January with westerly flows, conducive to more extreme precipitation over southern England (Schaller et al., 2016)[56]. This study also carried out impact attribution on the Thames catchment for the winter of 2013-14 using peak river flow events and flood risk mapping, to show that there was a small increase in the number of properties impacted due to climate change, however this change had large uncertainties and was not significant. These results are consistent with the output of this study for flood extent over the somerset levels. In terms of the compounding aspect of multiple successive storms, storms in general over the UK are becoming wetter, but there is no clear change in the number of stormy days (Kew et al., 2024)[57].

Future steps for this attribution work will be to include sea-level change as a boundary condition to the flood model framework in order to appropriately assess coastal flooding, as well as to include flood defenses in the model which may require increasing the resolution of the flood model to resolve small but potentially important defenses. Additionally, to avoid having to account for the difference in resolution between the observations and counterfactual simulations by applying a simplistic correction to the model output, we could use higher resolution counterfactual data which accounts for spatial variability in rainfall over our subregion. This could be achieved by either applying more effective and complex spatial downscaling methods or using a different set of attribution simulations with higher model resolution.

3.7.4. Stakeholder and policy relevance

After the floods of winter 2013/2014, the Somerset Rivers Authority (SRA) was formed to work with partners and stakeholders to reduce flood impacts risk in the Somerset county. A 20-year action plan was put forward, introducing more than £20 million of funding to repair damaged local infrastructure and manage future flood risk for the area – supported by the Somerset County Council. More than £45 million has been put forward for these efforts over the last 10 years[58], and a further 10-year 2024-34 strategy[59] is currently under implementation to further reduce flood risk and impacts in the county under a changing climate.

Since 2014, work has been carried out adding and improving culverts, drains, flood relief channels, raised roads, control structures and flood banks, as well as carrying out dredging of the Parrett and Tone rivers. The Bridgwater Tidal Barrier – a £249 million projection - is currently under construction and due to be completed in 2027, which will aim to protect over 11,300 homes and 1,500 business from flooding.

Climate adaptation plans for towns in Somerset have recently been funded by the SRA, which are still in their developmental stages, with solutions across environmental domains being implemented both at a community and local government level. For example, Glastonbury Town Council has worked with the Somerset Wildlife Trust

---

[54] Christidis N. & Stott P. (2015). Extreme Rainfall in the United Kingdom During Winter 2013/14: The Role of Atmospheric Circulation and Climate Change. *Bull. Amer. Met. Soc.* **96**: S46–S50.

[55] Wild, S. et al., (2015). 'Was the Extreme Storm Season in Winter 2013/14 Over the North Atlantic and the United Kingdom Triggered by Changes in the West Pacific Warm Pool?' *Bull. Amer. Met. Soc* **96**(12), S29–S34.

[56] Schaller, N et al., (2016). Human influence on climate in the 2014 southern England winter floods and their impacts. *Nature Clim Change* **6**, 627–634. https://doi.org/10.1038/nclimate2927

[57] Kew, S.F. et al., (2024). Autumn and Winter storms over UK and Ireland are becoming wetter due to climate change. DOI: 10.25561/111577

[58] Somerset Rivers Authority Annual Report 2024-25 (2025). https://www.somersetriversauthority.org.uk/flood-risk-work/sra-annual-report-2024-25/

[59] Somerset Rivers Authority (2024). Somerset Rivers Authority (SRA) Strategy 2024-34. https://www.somersetriversauthority.org.uk/about-somerset-rivers-authority/sra-strategy-2024-34/

to produce a plan[60] which identifies key priorities in building resilience to the impacts of climate change; including planting more trees in urban and suburban environments, adapting to flooding in residential, industrial, and public spaces, and installing green roofs on schools, public buildings, and infrastructure.

[60] Somerset Wildlife Trust & Glastonbury Town Council (2024). https://www.somersetwildlife.org/act-adapt-glastonbury

4. Use Case 2b: United Kingdom Drought Heatwave 2022

4.1. Summary of event

The UK summer of 2022 was characterised by extremely hot and dry conditions leading to severe drought and five heatwave periods[61]. Between 18th to 19th July, an unprecedented extreme heatwave affected the UK, setting new maximum temperature records across the UK and Ireland with temperatures of 40 °C recorded for the first-time[62].

The drought-heatwave had wide-reaching impacts across the UK. Between 10th to 25th July, 2,227 excess deaths were recorded, with the greatest number on 19th July[63+64]. National infrastructure experienced severe disruption with cancellations to trains and flights, road closures, power cuts and temporary water use bans. Wildfires broke out across the UK with multiple fire services declaring major incidents. The agricultural sector also suffered a reduction in crop and livestock production alongside marked increases in energy consumption.

The event caused the Met Office to issue its first red warning for extreme heat and a Level 4 alert was issued by the UK Health Security[62]. Following the event, the Adverse Weather and Health Plan was launched in April 2023 alongside a new impact-based Weather-Health Alerting System. Both were designed to improve guidance on heatwaves and support stakeholders in preparing and responding to adverse weather[65].

4.2. Geographical context

The July drought-heatwave affected much of the UK, but its impacts were most severe in central and southern England. These regions recorded the highest temperatures during the heatwave and lowest rainfall amounts in July, resulting in the greatest number of excess deaths and wildfires[66], as well as notable disruption to infrastructure and agriculture.

We focus on these regions during our case study but draw particular attention to the impact on transport infrastructure. The extreme temperatures resulted in roads and airport runways melting and railways buckling, which caused widespread disruption across the transport network[67] (Figure 32).

[61] Howarth, C., Mcloughlin, N., Armstrong, A., Murtagh, E., Mehryar, S., Beswick, A., Ward, B., Ravishankar, S., Stuart-Watt, A., Pearson, N., & Kyriacou, G. (2024). Turning up the heat Learning from the summer 2022 heatwaves in England to inform UK policy on extreme heat Evidence report. www.lse.ac.uk/granthaminstitute

[62] Kendon, M., McCarthy, M., Jevrejeva, S., Matthews, A., Williams, J., Sparks, T., & West, F. (2023). State of the UK Climate 2022. International Journal of Climatology, 43(S1), 1–82. https://doi.org/10.1002/joc.8167

[63] Office for National Statistics. (2022). Excess mortality during heat-periods 1 June to 31 August 2022.

[64] UK Health Security Agency. (2025, April). Heat mortality monitoring report: 2022. Https://Www.Gov.Uk/Government/Publications/Heat-Mortality-Monitoring-Reports/Heat-Mortality-Monitoring-Report-2022.

[65] UK Health Security Agency. (2024). Adverse Weather and Health Plan Annual Report. https://www.gov.uk/government/publications/adverse-weather-and-health-plan

[66] Burton, C., Ciavarella, A., Kelley, D. I., Hartley, A. J., McCarthy, M., New, S., Betts, R. A., & Robertson, E. (2025). Very high fire danger in UK in 2022 at least 6 times more likely due to human-caused climate change. Environmental Research Letters , 20(4). https://doi.org/10.1088/1748-9326/adb764

[67] The Guardian (2022). Heatwave 'melts runway' at Luton airport and hundreds of trains cancelled. https://www.theguardian.com/uk-news/2022/jul/18/uk-transport-operators-say-worst-heatwave-problems-yet-to-come

In our study, we have chosen to investigate the temporary closure of Luton airport, located in Bedfordshire, on 18th July when part of its runway melted in the extreme heat[67]. Little research exists surrounding the impact of climate change on airports, so we aim to increase awareness to improve long-term resilience.

4.3. Observed hazards

4.3.1. Type of hazards

Extreme temperatures, heatwave, drought, wildfires.

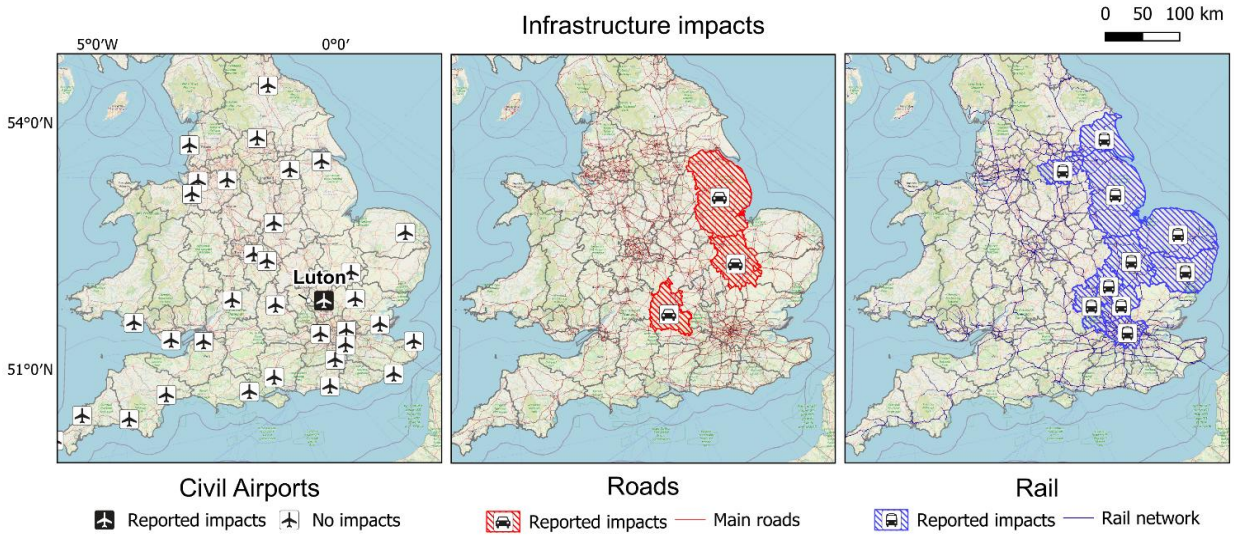

Figure 32 Transport impacts of the 2022 drought-heatwave event, synthesised from literature. Background map: OS StreetMap.

4.3.2. Form of compounding

Multi-variate (heatwave and drought) and preconditioned (low soil moisture from preceding winter/spring).

4.3.3. Driving dynamics

During the July drought-heatwave event, a stationary high pressure over continental Europe caused a persistent southerly flow over the UK, which drew in very hot, dry air from northern Africa. Mass subsidence led to the development of a heat-dome, which trapped warm air at the surface and encouraged the buildup of extreme heat[62].

The July drought-heatwave event had several drivers:

- **Strong La Nina and expansion of Indo-Pacific Warm Pool:** Higher-than-normal sea surface temperatures in the tropical Pacific coincided with an extension of the warmer-than-average Indo-Pacific Warm Pool towards Japan. This generated heavy rainfall in the West Pacific Ocean and caused large-scale Rossby waves to develop along the jet stream, allowing for surface high-pressure development[68].
- **A positive Summer North Atlantic Oscillation (SNAO):** A positive SNAO (+0.6) shifted the North Atlantic storm track northwards, reducing rainfall and increasing temperatures across the UK[62].
- **Increased Gulf Stream sea surface temperature (SST) anomalies:** Unusually high SSTs in the Gulf Stream extended into the central North Atlantic, likely enhancing atmospheric instability and reinforcing the stationary Rossby wave and surface high over Western Europe[69].

[68] Slingo, J., Paul Davies, Jason Lowe, & Michael Eastman. (2023). EHTF Weather and Climate Change Report: March 2023.
[69] Kim, J. H., Nam, S. H., Kim, M. K., Serrano-Notivoli, R., & Tejedor, E. (2024). The 2022 record-high heat waves over southwestern Europe and their underlying mechanism. Weather and Climate Extremes, 46. https://doi.org/10.1016/j.wace.2024.100729

- **Reduced soil moisture combined with increased sunshine amounts:** Increased sunshine in winter/spring months led to higher surface evaporation and evapotranspiration rates, in turn reducing soil moisture levels. Depleted soil moisture in summer results in less evaporative cooling, causing higher air temperatures[68].
- **Increased regional sea surface temperatures (SST):** Record-breaking SSTs exceeding 20°C were recorded across the south and east of England in summer 2022[70]. This may have increased air temperatures through the advection of warm air from the sea.

4.3.4. Intensity

The drought-heatwave event was momentous for the UK. A new maximum temperature record of 40.3°C was set at Coningsby, Lincolnshire on 19th July, exceeding the previous record by 1.6 °C. In the months prior, much of the UK experienced a notably dry and sunny period, particularly in eastern and southern England. Only 62% of average rainfall was recorded from January to August, equating to a deficit of 183 mm (compared to the 1991-2020 baseline). Sunshine totals were also above average, with southern and eastern England seeing their sunniest January on record and March seeing 152% of the UK average[62].

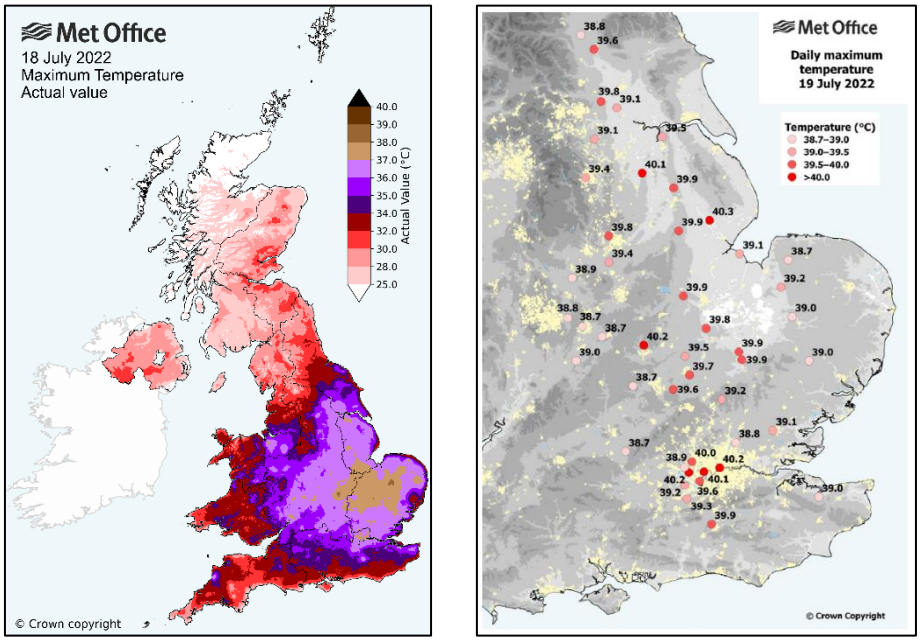

Figure 33 Maximum temperatures recorded on 18th July (a) and 19th July (b) 2022. Figure 33b shows the 46 climate stations across England that equaled or exceeded the previous UK record of 38.7 °C. Figure 33b is provided by Kendon et al. (2023)[62].

[70] CEFAS. (2023). 2022 WaveNet data shows record breaking UK sea temperatures. Https://Www.Cefas.Co.Uk/News-and-Resources/News/2022-Wavenet-Data-Shows-Record-Breaking-Uk-Sea-Temperatures/.

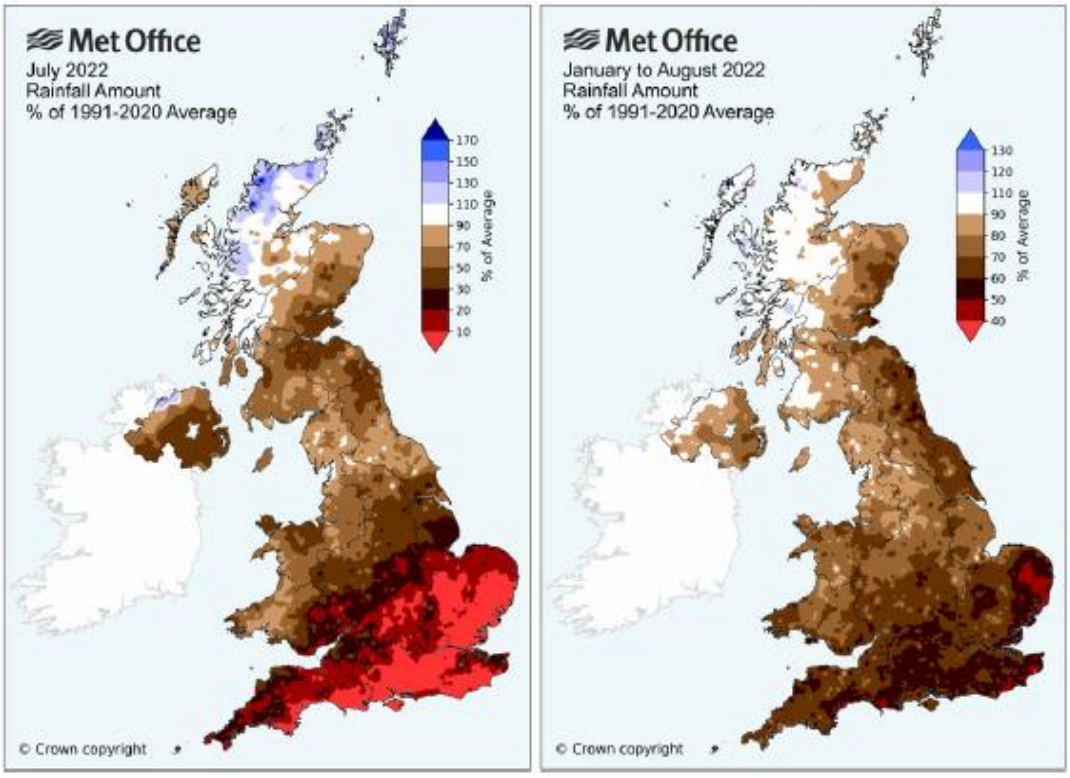

Figure 34 UK rainfall (a) July and (b) January-August 2022 anomalies relative to 1991-2020 average. Figure provided by Kendon et al. (2023)[62].

For Luton Airport, 10 days exceeded the county's heatwave threshold of 28 °C[71] during summer 2022. On the day of the runway melting (18th July), a new surface temperature record of 56.9°C was recorded, alongside an air temperature of 35.9°C. A day later, a new maximum air temperature of 38.6°C was set[72].

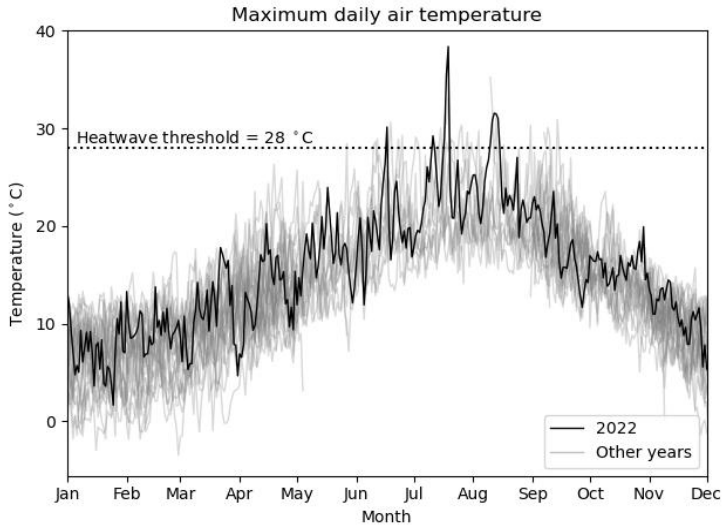

Figure 35 Timeseries of Luton Airport maximum daily air temperature for 2022 (black line), overlaid on annual cycles from 2001 to 2024 (grey lines). 10 days in the summer exceeded the county's heatwave threshold of 28 °C.

[71] Mccarthy, M., Armstrong, L., & Armstrong, N. (2019). A new heatwave definition for the UK (Vol. 74, Issue 11).
[72] Vaisala RoadDSS. Accessed 15/05/2025. https://rds.vaisala.com/

4.4. Observed impacts

4.4.1. Quantitative impacts

The July drought-heatwave event had significant impacts across a variety of UK sectors, particularly in central and southern England. These impacts are detailed in the Table 9 below.

The temporary closure of Luton airport led to 13 flights being diverted to other London airports and the cancellation of 100 flights, split between arrivals and departures. This caused significant disruption to both passengers and terminal staff[73].

Table 9 Table of key impact data and statistics.

Impact	Magnitude/scale	Source
Fatalities	2,227 excess deaths due to heat between 10-25th July	ONS, UKHSA (2022)[63] [64]
	13 deaths due to open water swimming (between 8th-19th July)	BBC News (2022)[74]
Emergency services	500% increase in fire 999 calls during heatwave peak (13,500 on 19th July)	NFCC (2024)[75]
	14 fire and rescue services declared major incidents as they tackled 983 wildfires in summer 2022 (84 on 19th July)	NFCC (2024)[75]
	A fifth of UK hospitals had to cancel operations between 16-19th July due to unsafe theatre environments and staff shortages due to the extreme heat	Guardian (2023)[76]
	RSPCA received 7,186 calls on 18th July due to wildlife casualties	Weston (2022)[77]
Infrastructure	6 water companies issued Temporary User Bans affecting at least 19 million people	Barker et al (2024)[78]
	An extra 300 million liters of water a day was being used during the peak of the heatwave	BBC News (2022)[79]
	41 properties destroyed in London due to wildfires	Hartley (2024)[80]
	8000 properties in Yorkshire, Lincolnshire and the Northeast experienced power cuts	BBC News (2022)[81]

[73] London Luton Airport Operations Limited. (2024). LONDON LUTON AIRPORT OPERATIONS LIMITED Climate Change Adaptation Report (CCAR) 2024 Revision.
[74] BBC News. (2022d). The hidden dangers of summertime swims. Https://Www.Bbc.Co.Uk/News/Uk-England-62207996#:~:Text=Since%20the%202022%20heatwave%20started,Water%20in%20Hampton%2C%20west%20London.
[75] National Fire Chiefs Council (NFCC). (2024). Wildfires position statement. Https://Nfcc.Org.Uk/Our-Services/Position-Statements/Wildfires-Position-Statement/.
[76] The Guardian. (2023). Peak of 2022 heatwave forced fifth of UK hospitals to cancel operations – research. Https://Www.Theguardian.Com/Society/2023/Mar/23/Heatwave-2022-Uk-Hospitals-Cancelled-Operations-Research.
[77] Phoebe Weston. (2022). Falling birds and dehydrated hedgehogs: heatwave takes its toll on UK wildlife. Https://Www.Theguardian.Com/Environment/2022/Jul/25/Falling-Birds-and-Dehydrated-Hedgehogs-Heatwave-Takes-Its-Toll-on-Wildlife-Aoe.
[78] Barker, L. J., Hannaford, J., Magee, E., Turner, S., Sefton, C., Parry, S., Evans, J., Szczykulska, M., & Haxton, T. (2024). An appraisal of the severity of the 2022 drought and its impacts. Weather, 79(7), 208–219. https://doi.org/10.1002/wea.4531
[79] BBC News. (2022). Water firms see "extraordinary" demand in heatwave. Https://Www.Bbc.Co.Uk/News/Uk-England-Bristol-62180060#:~:Text=Water%20use%20in%20the%20Thames,Water%20a%20day%2C%20it%20said.
[80] Emma Hartley. (2024). Scientists look into London's 2022 "firewaves." Https://Www.Bbc.Co.Uk/News/Articles/C8rxgmmg4g7o#:~:Text=According%20to%20London%20Mayor%20Sadiq,Properties%20were%20destroyed%20by%20fire.
[81] BBC News. (2022). UK heatwave: Thousands suffer power cuts after equipment overheats. Https://Www.Bbc.Co.Uk/News/Uk-England-South-Yorkshire-62222195#:~:Text=UK%20heatwave%3A%20Thousands%20suffer%20power%20cuts%20after%20equipment%20overheats,-

	More than 50 schools were closed in southeast England	ITV News (2022)[82]
Transport	Passenger train numbers were 40% lower between 18-19th July compared to the previous week	BBC News (2022)[83]
	A 'Do not travel' warning was issued by Network Rail	Transport Focus (2022)[84]
	16.3% and 21% reduction in planned trains on 18th and 19th July	(ORR, 2022)[85]
	Closure of East Coast Main Line on 19th July and partial closure on 20th due to overhead cable fire	ITV News (2022)[86]
	Roads in Cambridgeshire, Oxfordshire and Lincolnshire were closed	BBC News (2022)[87]
	Luton Airport and RAF Brize Norton temporarily closed due to melting runway, delaying and diverting flights	(Reuters, 2022)[88]
Agriculture	9.2% reduction in chicken meat production	Davie et al. (2023)[89]
	18,500 chickens died in transport due to heat stress (July-August)	
	8% higher wheat yields than 2017-2021 average	
	Reduced milk yield in dairy cows	Clarke and Michael (2022)[90]
Environment	Wildfires destroyed habitats of nesting birds, reptiles and amphibians	Weston (2022)[77]
	Marked decline in insect populations e.g. dragonflies, butterflies	

4.4.2. Qualitative impacts and responses

Qualitative impacts

During the drought-heatwave event, frontline workers were put under severe pressure and resources were extremely stretched. For example, many fire responders felt there was a lack of preparedness for the event and raised the need for better communication, education and public engagement to reduce preventable impacts, such as wildfires[61]. For many social care workers, the event led to increased workload as extra care was required

[82] ITV News. (2022). School closures: Students in South East sent home due to extreme heat. Https://Www.Itv.Com/News/Meridian/2022-07-18/Has-Your-School-in-the-South-East-Closed-Due-to-the-Hot-Weather.
[83] BBC News. (2022) A day of train chaos https://www.bbc.co.uk/news/live/uk-62184978
[84] Transport Focus. (2022). Extreme-heat-July-22-report_passenger report.
[85] Office of Rail and Road. (2022). Passenger rail performance July to September 2022.
[86] ITV News. (2022b). Train delays after fire melts signalling equipment and burns level crossing on East Coast Main Line. Https://Www.Itv.Com/News/Anglia/2022-07-20/Train-Delays-after-Fire-Melts-Signalling-Equipment-and-Burns-Level-Crossing.
[87] BBC News. (2022). Oxfordshire road melts in extreme heat. Https://Www.Bbc.Co.Uk/News/Av/Uk-England-Oxfordshire-62243643.
[88] Reuters. (2022). Flights briefly disrupted at UK's Luton airport as heat damages runway. Https://Www.Reuters.Com/World/Uk/Uks-Luton-Airport-Suspends-Flights-Due-Runway-Defect-2022-07-18/#:~:Text=The%20airport%20said%20its%20runway,A%20small%20section%20to%20lift%22.
[89] Davie, J. C. S., Falloon, P. D., Pain, D. L. A., Sharp, T. J., Housden, M., Warne, T. C., Loosley, T., Grant, E., Swan, J., Spincer, J. D. G., Crocker, T., Cottrell, A., Pope, E. C. D., & Griffiths, S. (2023). 2022 UK heatwave impacts on agrifood: implications for a climate-resilient food system. Frontiers in Environmental Science, 11. https://doi.org/10.3389/fenvs.2023.1282284
[90] Philip Clarke, & Michael Priestley. (2022). Philip Clarke and Michael Priestley 13 July 2022 More in Feed and nutritionLivestockWeather Hot, dry weather puts pressure on UK livestock farmers. Https://Www.Fwi.Co.Uk/News/Weather/Hot-Dry-Weather-Puts-Pressure-on-Uk-Livestock-Farmers.

for vulnerable patients. This was balanced alongside staff shortages resulting from school closures and transport disruption. Some workers were not able to take breaks, leading to fatigue, stress and anxiety[91].

In the transport sector, passengers faced significant disruption from train delays and cancellations, due to risks associated with power supply for critical operations. Many reported feelings of frustration and discomfort as they dealt with overcrowded trains, miscommunication from rail companies and poorly ventilated services. Those who could not work from home, such as healthcare workers or those needing to travel for medical reasons, were most significantly affected and had to find alternative transportation or cancel their plans altogether[84].

For agriculture, impacts on farmers extended over a much longer period due to the prolonged drought from late spring to mid-autumn. Increased frequency of such events has led to greater uncertainty around farmers' livelihoods. From a recent 2024 survey, 95% of UK farmers under 40 believe the impacts of climate change have been detrimental to their mental health. Stress, anxiety and depression are strongly linked to crop and livestock failures, market instability and rising costs[92].

Response

In response to the changing climate, steps have been taken to better the UK's climate resilience. Guidance to deal with extreme temperatures was updated and improved in the release of the third National Adaptation Programme (NAP3) and through the introduction of the Adverse Weather and Health Plan (AWHP) in 2023 [93]. The AWHP included a new Weather-Health Alerting system which forewarns of periods of high temperatures or cold weather with potential impact to public health. Since its inception, it has been used on numerous occasions to raise public awareness of extreme heat events, most recently in July and August 2025[94]. Although there has been advancement in climate policy, a 2025 government report found current guidance for extreme temperatures is mainly focused on the impact of heat on the health sector and fails to address concerns in transport, education and agriculture[95]. As such, there is room for improvement. Progress on implementing adaptation outcomes remains inadequate and significant work is needed to achieve UK climate resilience across all sectors.

4.5. Modeling framework

4.5.1. Hazard modeling

For hazard modeling, we use a linear regression modeling framework, as shown in Figure 36.

[91] UKHSA. (2024). Research exploring the experience of social care practitioners in relation to extreme temperatures. Https://Www.Gov.Uk/Government/Publications/Hot-Weather-and-Health-Exploring-Extreme-Heat-in-Adult-Social-Care/Research-Exploring-the-Experience-of-Social-Care-Practitioners-in-Relation-to-Extreme-Temperatures#references.

[92] The Newsroom. (2024). Poor mental health is ranked as farming industry's biggest hidden problem. Https://Www.Farminglife.Com/News/Environment/Poor-Mental-Health-Is-Ranked-as-Farming-Industrys-Biggest-Hidden-Problem-4514044.

[93] UK Health Security Agency. (2025). Adverse Weather and Health Plan annual report 2023 to 2024 [PDF]. GOV.UK. AWHP Annual Report 2023 to 2024

[94] The Guardian (2025) UK weather: heat health warnings issued across England. Accessed 11/08/25. https://www.theguardian.com/uk-news/2025/aug/11/uk-weather-heat-health-warning-england

[95] Climate Change Committee. (2025). Progress in adapting to climate change – 2025 report to Parliament.

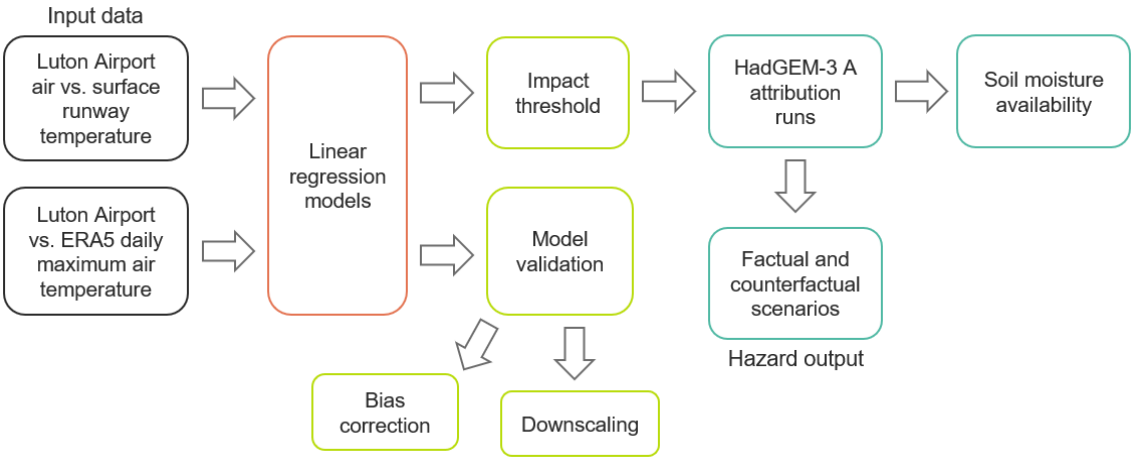

Figure 36 Flowchart of modelling framework.

This case study uses sub-hourly air and surface runway temperature data at 10-minute resolution from Luton Airport, provided by Vaisala, which extends from 2001 to 2025. We use linear regression to determine the relationship between air and runway temperature to find an impact threshold for our attribution study. Our linear regression model revealed extreme runway surface temperatures (> 45°C) are best represented by the average 6-hourly air temperature preceding the maximum surface temperature event (Figure 37). This metric and timestep were subsequently used during our model validation, as discussed below.

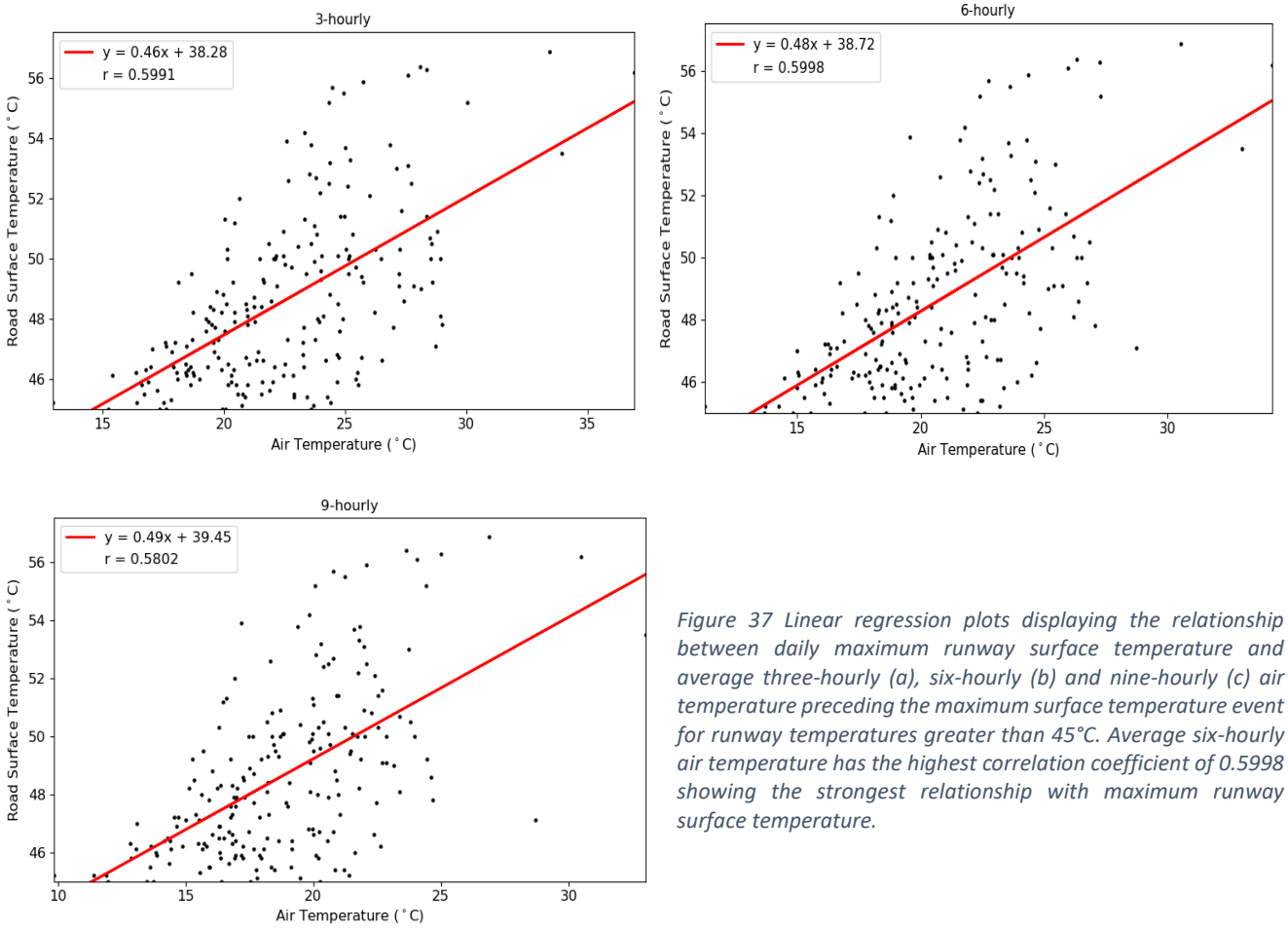

Figure 37 Linear regression plots displaying the relationship between daily maximum runway surface temperature and average three-hourly (a), six-hourly (b) and nine-hourly (c) air temperature preceding the maximum surface temperature event for runway temperatures greater than 45°C. Average six-hourly air temperature has the highest correlation coefficient of 0.5998 showing the strongest relationship with maximum runway surface temperature.

It is assumed that runway temperature directly links to impact. Since Luton Airport runway has only melted once, we use the average 6-hour air temperature preceding the maximum surface temperature event on 18th July 2022 (which was 56.9°C) to determine our impact threshold. We use the 6-hourly timeframe (0730-1330) during our attribution analysis as a way of keeping the time-of-day constant to account for the diurnal cycle of solar intensity.

Using linear regression, we also explore the relationship between Luton Airport local observations and ERA5-land hourly data, which was gridded to the resolution of the climate model runs for spatial downscaling. This was carried out for the summer months (June, July, August (JJA)) between 2001 and 2024 and explored for air temperatures above 28°C (the heatwave threshold for Luton as derived by Mccarthy et al. (2019))[96]. We use this relationship to find the equivalent impact threshold in the ERA5 dataset (29.5°C), which is taken forward into our attribution work. Below this temperature, it is assumed the runway would not melt and hence, no impacts would be observed.

4.5.2. Impact modeling

Exposure modelling

Luton Airport has seen rapid expansion over the last 40 years. For exposure, we consider the change in usage of Luton airport between 1980 to 2022 by using flight and passenger data from the UK Civil Aviation Authority and Luton Airport's historical records. This allows us to estimate how such changes in usage and hence exposure to impacts has changed since 1980 compared to the current day.

	1980	2022
Data source	UK Civil Aviation authority[97]	London Luton Airport[98]
Total passengers	2,088,000	13,136,542
Total flights	57680	111,477
Passengers per day (July)	7271	45872
Flights per day (July)	200	388

Table 10 Exposures indicators. Passengers and flights per day are estimated for July 1980 by using the same percentage of flights that occurred in July 2022 when compared to the whole of 2022.

Vulnerability modelling

We qualitatively assess the vulnerability of Luton Airport to extreme temperatures with support from existing literature. Our assessment focuses on both the physical infrastructure of the airport and its dependence on external networks.

4.6. Attribution modeling framework

Figure 38 summaries our attribution modelling framework. To explore the influence of anthropogenic climate change, we simulate factual and counterfactual scenarios of the 2022 drought-heatwave event. The factual scenario is representative of the current climate, whereas the counterfactual represents a scenario where the

[96] Mccarthy, M., Armstrong, L., & Armstrong, N. (2019). A new heatwave definition for the UK (Vol. 74, Issue 11).
[97] UK Civil Aviation Authority https://www.caa.co.uk/data-and-analysis/uk-aviation-market/airports/uk-airport-data/uk-airport-data-1990-2014/
[98] London Luton Airport https://www.london-luton.co.uk/corporate/lla-publications/statistics

event occurred under pre-industrial climate conditions. This investigation is combined with an assessment of exposure and vulnerability to determine the overall impact of the 2022 drought-heatwave event.

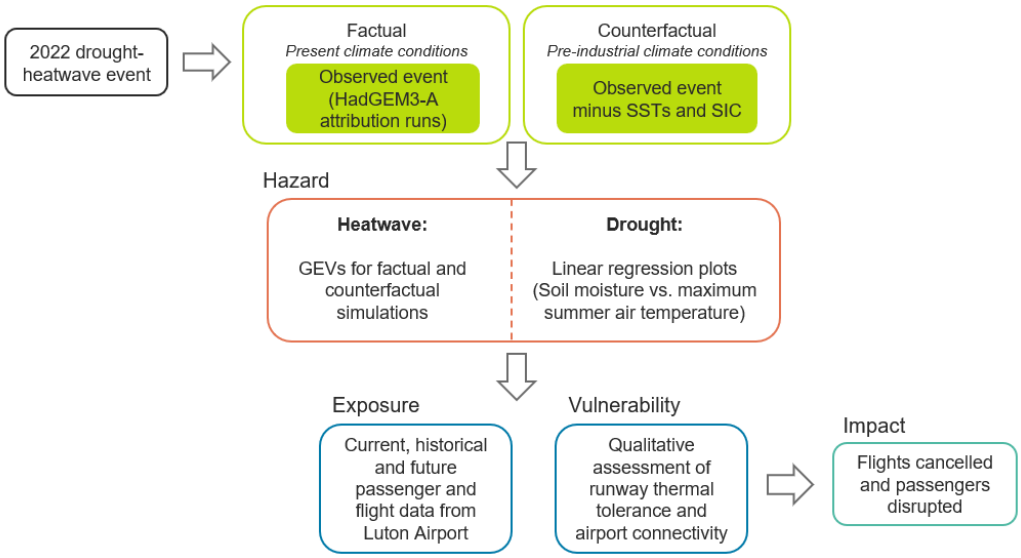

Figure 38 Flowchart of the attribution modeling framework.

4.6.1. Event definition

To represent the event of the runway melting (runway surface temperature reaching temperatures of 56.9°C), we use 6-hour annual air maximum temperature between 0730-1330 for the location. The 6-hour temperature impact metric correlates best with runway maximum temperatures, as shown in the hazard modelling section. We fix the time of day to account for the diurnal cycle of solar intensity.

4.6.2. Factual and counterfactual simulations

The main dataset we use for the climate attribution is the HadGEM3-A large-ensemble attribution runs containing members in both factual and counterfactual climates[99]. These attribution runs contain 525 ensemble members in both factual and counterfactual climates for the year 2022, conditioned on the sea surface temperatures (SSTs) and sea ice fields (SICs) for that year. In the counterfactual runs the estimated contribution to these from anthropogenic climate change since the pre-industrial pattern are subtracted from the SST patterns and SICs in the current climate. This attribution approach using large ensembles conditioned on SST patterns for the year of the event has been used in multiple studies[100,101+102]. The global dataset contains 3-hourly temporal resolution precipitation and temperature, with the spatial resolution approximately 60km for the UK.

Validation of the HadGEM3-A attribution runs with the ERA5-land reanalysis re-gridded to the same resolution as the attribution runs is shown in Figure 39, for the grid box covering Luton Airport[103]. Figure 39a and 39c show that for 6-hour annual maximum air temperature in JJA (Rx6hr) the HadGEM3-A model runs show good

[99] Ciavarella, A., Christidis, N., Andrews, M., et al. (2018). Upgrade of the HadGEM3-A based attribution system to high resolution and a new validation framework for probabilistic event attribution. Weather Clim. Extrem., 20, pp. 9-32, https://doi.org/10.1016/j.wace.2018.03.003.

[100] Cotterill, D. F., Mitchell, D., Stott, P. A., & Bates, P. (2024). Using UNSEEN approach to attribute regional UK winter rainfall extremes. International Journal of Climatology, 44(7), 2406–2424. https://doi.org/10.1002/joc.8460

[101] Dalagnol, R., Gramcianinov, C. B., Crespo, N. M., et al. (2022). Extreme rainfall and its impacts in the Brazilian Minas Gerais state in January 2020: can we blame climate change? Clim. Resil. Sust. 1, 1–15. doi: 10.1002/cli2.15.

[102] Wang, Q., Zhai, P. & Zhou, B. (2023). Attribution of tropical sea surface temperature change on extreme precipitation over the Yangtze River Valley in 2020. Clim Dyn 61, 3417–3429. https://doi.org/10.1007/s00382-023-06752-4

[103] Muñoz Sabater, J. (2019): ERA5-Land hourly data from 1950 to present. Copernicus Climate Change Service (C3S) Climate Data Store (CDS). DOI: 10.24381/cds.e2161bac [Accessed: 21/11/2023]

agreement with ERA5-land for the highest temperatures' quantiles, with some small differences for the lower percentiles. The p-value from the two sample Kolmogorov-Smirnov test (ks-test) is larger than 0.05 (0.3) suggesting that the distributions from ERA5-land and the HadGEM3-A model are not significantly different from each other for Rx6hr. However, it is important to note that the sample for ERA5-land only contains 30 data points, hence there will be significant uncertainty in the GEV fit. There is also good agreement in the trend of Rx6hr between ERA5-land and the HadGEM3-A model, with a significant increase in both.

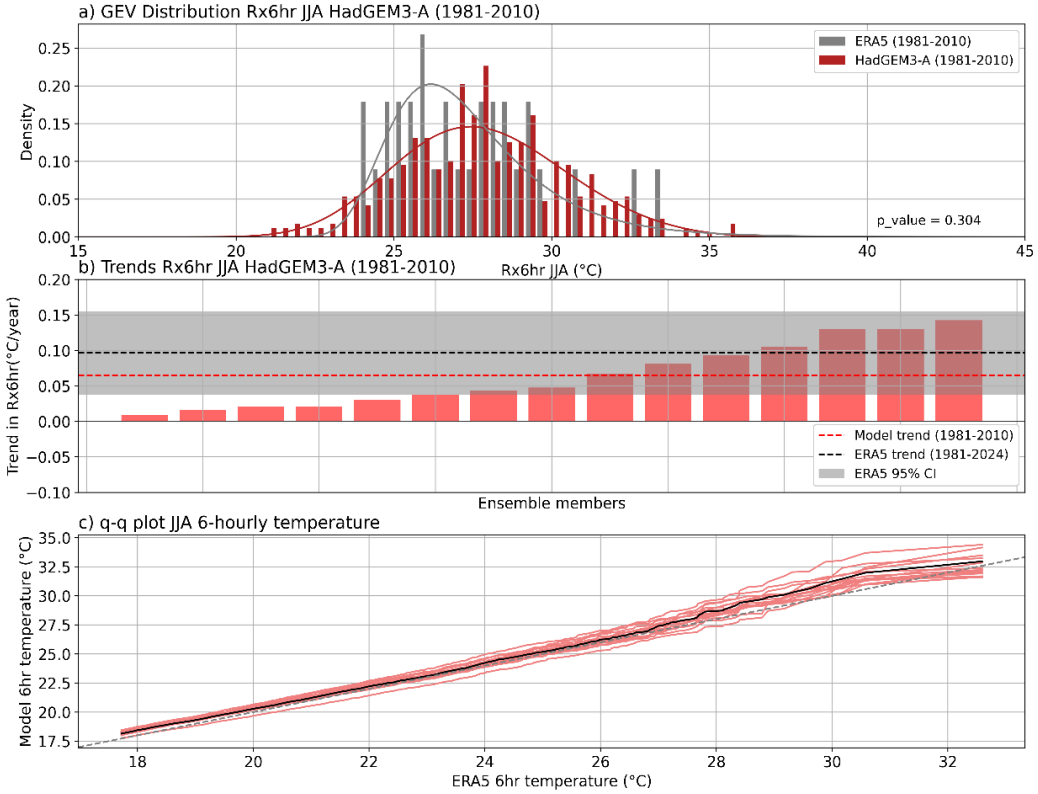

Figure 39 Validation plot comparing summer annual maximum 6-hour air temperatures (Rx6hr) over Luton Airport for ERA5-land and the HadGEM3-A attribution runs. a) A histogram of Rx6hr for ERA-5 reanalysis and 15 ensemble members between 1981-2010, fitted to general extreme value distributions. b) shows the trend in Rx6hr for the 15 ensemble members (red bars) with the overall model trend and ERA-5 trend. The 95% confidence intervals on the ERA-5 trend were calculated by bootstrapping the time series with replacement and recalculating the trend 10 000 times. c) is a quantile-quantile plot comparing 6-hour air temperatures in JJA both for ERA-5 and the attribution runs for the higher quantiles.

4.7. Results

4.7.1. Factual hazards and impacts

Using the impact metric derived from the regression model and the spatial downscaling to adjust the impact threshold for the 2022 event (average 6-hour air temperature over Luton between 0730-1330 =29.5°C in the climate model runs), we plot the distribution for the attribution runs in the current climate (Figure 40). Using the general extreme value distribution (GEV) we show that conditions that would give a high likelihood of runway melting as observed on the 18th of July 2022 had a return period of 14.5 years (CI: 11.7-19.1), based on the SST patterns of 2022.

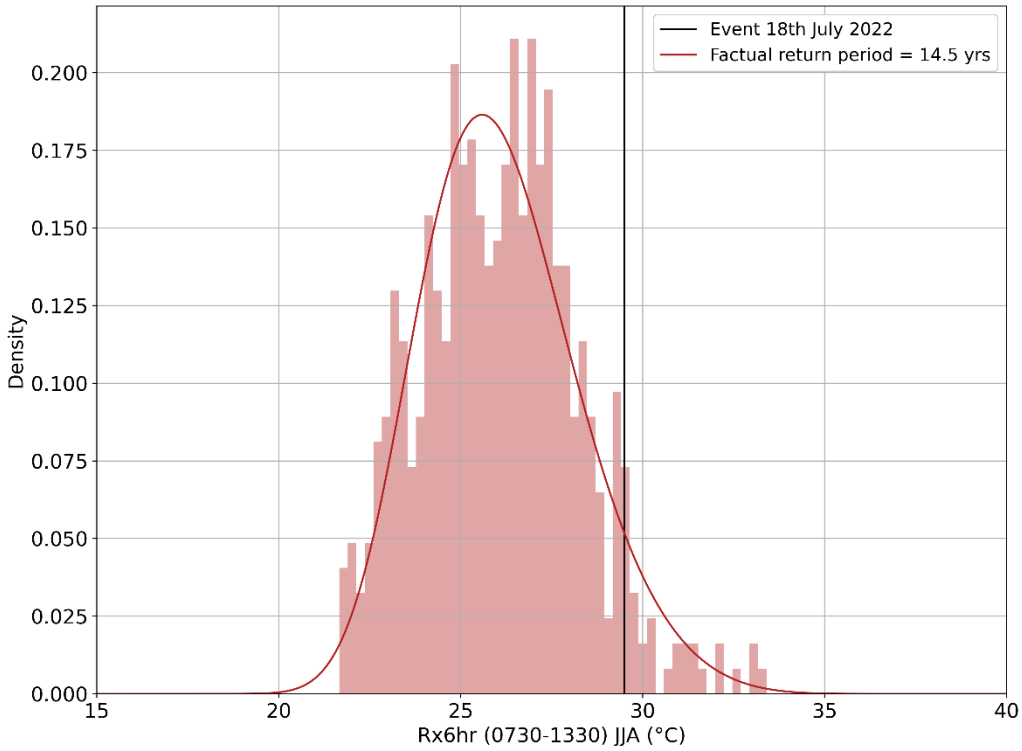

Figure 40 Histogram of 6-hour mean summer annual maximum air temperature between 0730-1330 (Rx6hr) for the HadGEM3-A attribution runs in a factual climate. A GEV is fitted to the model runs for the current climate containing 525 ensemble members conditioned on the SST patterns of 2022. The impact threshold (Event 18th July 2022) is adjusted to account for the local and grid box scale temperature differences.

Pre-conditioning soil moisture

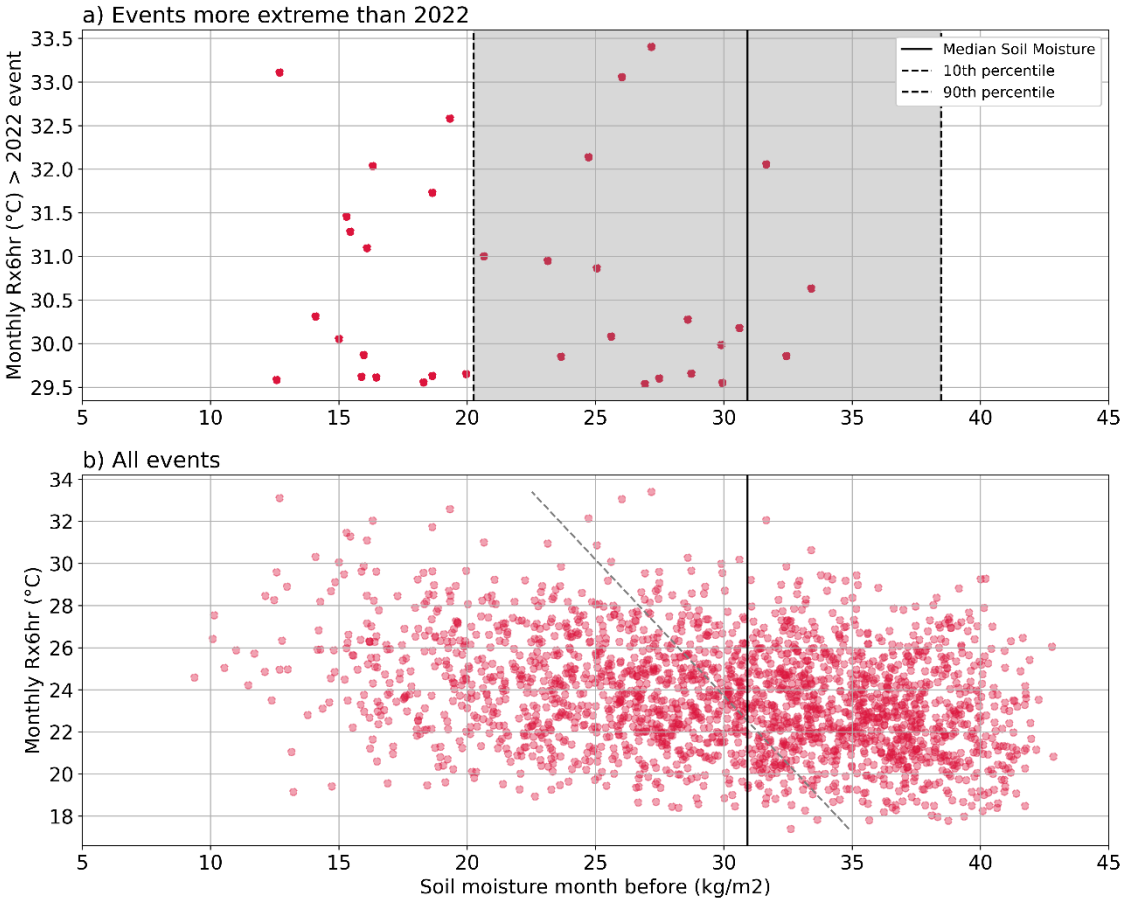

Figure 41 Scatter plot showing the relationship between 6-hour monthly maximum air temperature between (0730-1330) and the average soil moisture in the preceding month for July and August over Luton airport region. The data points come from the 525 attribution runs for current and 525 from counterfactual climate for 2022 using the months of both July and August. a) represents 6-hour air temperatures that exceed the 2022 runway melting event with b) representing all the events from the attribution runs (2100 in total). The black line represents the median monthly soil moisture during July and August.

Drought occurring alongside heatwaves (multivariate) can lead to significant impacts for many sectors such as agriculture and wildfires. Drought, however, can also be a precursor to increased intensity of temperature extremes during heatwaves (preconditioned), with studies showing that low soil moisture before/during the extreme 2003 and 2018 heatwaves in the UK exacerbated the maximum temperatures reached during the events[104+105]. Both studies use experiments with adjusted levels of soil moisture to show this impact of low soil moisture on the increased intensity of maximum daily temperature extremes. Using the soil moisture and temperature impact metric used in this study (Rx6hr), we examine the relationship between the temperature extremes seen in both July and August and the average soil moisture in the month before in our attribution runs. Figure 41 shows that for the 34 events more extreme than the observed event on the 18th July 2022, 91% of them occurred with below average soil moisture in the preceding month, and 47% of them occurred with the soil moisture in the preceding month below the 10th percentile.

[104] Fischer, E. M., Seneviratne, S. I., Vidale, P. L., Lüthi, D., & Schär, C. (2007). Soil moisture-atmosphere interactions during the 2003 European summer heat wave. Journal of Climate, 20(20), 5081–5099. https://doi.org/10.1175/JCLI4288.1

[105] Petch, J. C., Short, C. J., Best, M. J., McCarthy, M., Lewis, H. W., Vosper, S. B., & Weeks, M. (2020). Sensitivity of the 2018 UK summer heatwave to local sea temperatures and soil moisture. Atmospheric Science Letters, 21(3). https://doi.org/10.1002/asl.948

4.7.2. Attribution results

To attribute the influence of anthropogenic climate change on the likelihood of the runway melting on the 18th of July 2022, we calculate the probability of exceeding the impact threshold (local mean 6-hour air temperature between 0730-1330= 29.5°C) in both a factual and counterfactual climate for the year of 2022. The results show that anthropogenic climate change made the event 12 times more likely, with the 95% confidence intervals showing that it was at least 6 times more likely and could have been up to 32 times more likely (Figure 42). Conditioned on the SST spatial patterns of 2022, the event would have been incredibly rare in a counterfactual climate (return period of 175 years) but is much more common in the current climate (return period of 15 years). The intensity of the event with the same return period in the counterfactual climate (i.e. 15 years) is 2.1°C cooler (95% CI: 1.8-2.3) than for the same return period in the current climate. Therefore, the equivalent return period in the counterfactual climate would have resulted in no impacts, even at the bounds of the 95% confidence intervals.

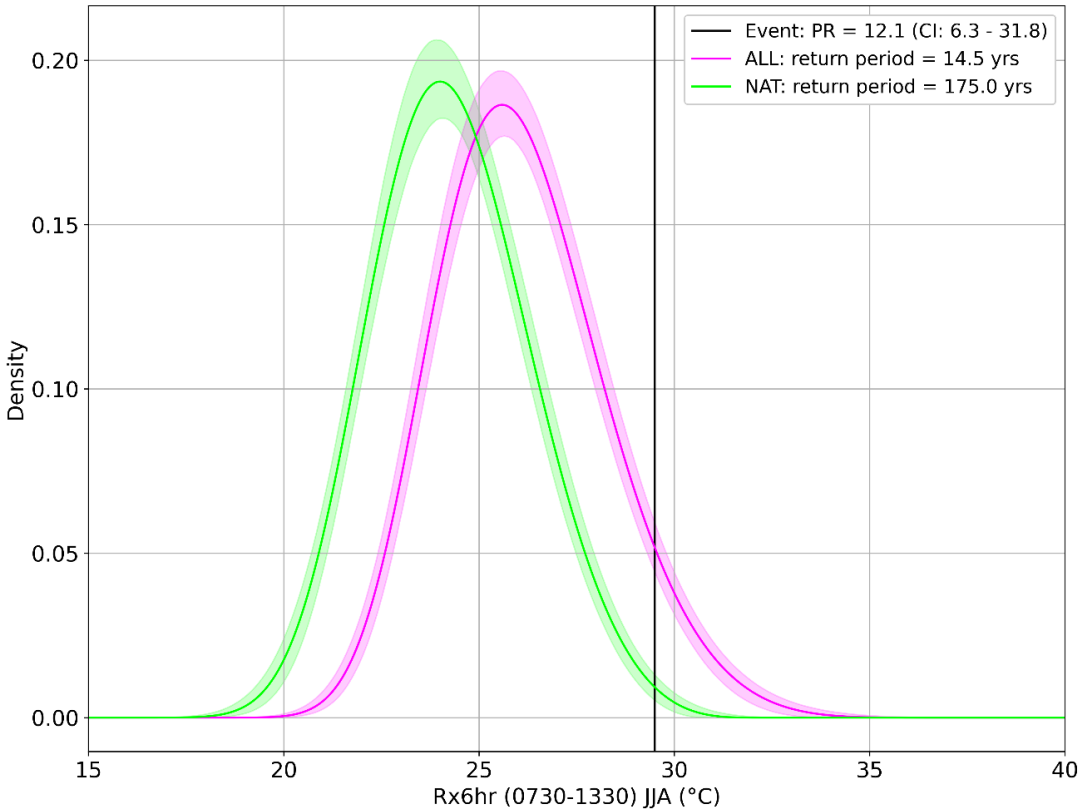

Figure 42 Comparison of 6-hour mean summer annual maximum air temperature between 0730-1330 (Rx6hr) for the HadGEM3-A attribution runs in both a factual climate (pink) and counterfactual climate (green). GEVs are fitted to both sets of attribution runs with the shaded areas representing the 95% confidence intervals, each containing 525 ensemble members conditioned on the SST patterns of 2022. The impact threshold (29.5 °C) is adjusted to account for the local and grid box scale temperature differences.

Exposure

To consider changes in exposure, we compare usage of Luton airport in 1980 with 2022. Our results indicate that increased exposure, driven by higher airport usage, has amplified the impacts of a runway melting event. In a hypothetical scenario where a 2022-type runway melting event occurred in 1980, an estimated 58 flights and 2116 passengers would have been affected. By comparison, in the factual event of 2022, 113 flights and an estimated 13,000 passengers were disrupted (Figure 43). This is equivalent to a 93% increase in affected flights and a 531% increase in affected passengers compared to 1980.

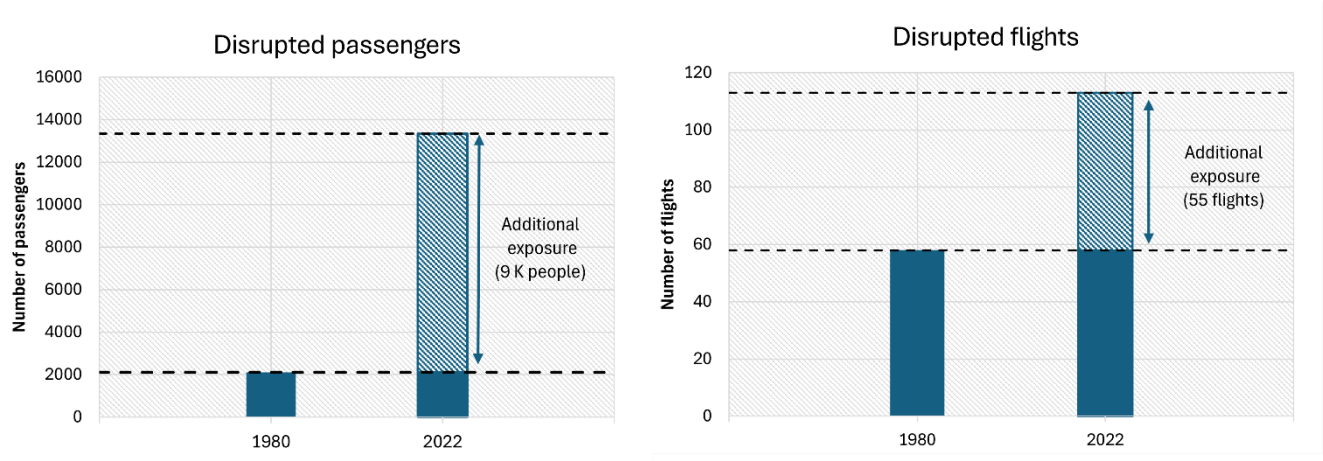

Figure 43 Estimated disrupted passengers (left) and flights (right) for a 2022-type runway melting event in 1980 compared to the actual event in 2022. Diagonal shading displays the additional passengers and flights that were affected in 2022, in comparison to if the event occurred in 1980.

As of April 2025, the UK government approved expansion plans to Luton Airport which include a new terminal, new taxiways, increased capacity of the current terminal and other supporting transport infrastructure. These changes will allow the airport to have capacity for up to 32 million passengers per annum by 2043, almost double from its current 18 million[106].

As such, we estimate that under this expansion, if a 2022-runway melting event occurred in 2043, 275 flights and over 32,000 passengers could be disrupted. This assumes the same proportion of flights and passengers impacted as 2022. This reveals that societal changes play a significant role in enhancing the impacts of climate-related events.

Vulnerability

A key vulnerability of the airport stems from the thermal tolerance of its runway, which, as evidenced in July 2022, has been shown to melt in extreme drought-heat events. Luton's runway has a rigid, concrete surface, designed to withstand the heavy loading from aircraft[107+108]. In contrast, other London airports have flexible, asphalt-based runways which bend under aircraft weight and can deal with expansion in extreme heat[108]. These structural differences may be a key reason as to why Luton was the only affected airport and highlights a critical vulnerability in its infrastructure. This identifies the need for construction materials with higher heat tolerance at Luton to cope with a warming climate.

Beyond the runway itself, Luton Airport is highly dependent on external infrastructure, particularly commercial roads, railways and pedestrian routes[73]. These networks are crucial for the transport of passengers, staff and cargo. However, they are also vulnerable to the extreme heat, with roads and pavements at risk of melting and railways bucking. Any upstream climate-induced disruptions can directly impact airport operations through flight delays, cancellations and other logistical challenges. This can have further knock-on impacts for hotels, car rentals and other commerce[73].

[106] Danny Fullbrook. (2025). Luton airport expansion approved by government. Https://Www.Bbc.Co.Uk/News/Articles/Cy4vg2d9v7no.
[107] Avion https://avion50.com/runway-pavement-types-explained-what-lies-beneath-your-smooth-takeoff/
[108] Chris Smith (2022) https://www.airwaysmag.com/legacy-posts/london-lutons-distorted-runway

At a national scale, the UK's wider airport infrastructure may be similarly exposed to the effects of extreme temperatures in the future. As the 2022 heatwave only affected Luton's runway, flights were successfully diverted to surrounding airports. However, in a future scenario involving simultaneous failures at multiple airports, the socio-economic impacts on the infrastructure sector would be far greater.

4.7.3. Summary of attribution results

We attribute that the impacts of the runway melting at Luton Airport in 2022 was 12 times more likely (95% CI: 6-32 times more likely) due to anthropogenic climate change. An event with the equivalent return period in a natural climate is unlikely to have resulted in such impacts (including the 95% confidence interval bounds), as the impact threshold for melting would not have been reached. The 6-hourly temperature extremes on the day of the event, has a return period of 15 years based off the SST patterns seen in 2022, compared to 175 years in a counterfactual climate. Consistent with other research[104+105], we find low soil moisture to be an important driver in exacerbating the maximum temperature during extreme summer heatwaves for the UK on a local scale. This underlies the importance of the preconditioning for extreme heatwaves and their corresponding impacts, as well as the multivariate nature of drought-heatwaves.

Our study reveals that societal shifts in airport usage have significantly increased population exposure to extreme temperature events and their consequential impacts. As passenger numbers continue to rise year-on-year at Luton airport, a growing number of people are now directly and indirectly affected during heat-related disruptions such as flight delays or cancellations. This increased exposure combines with the airport's operational vulnerabilities to amplify the overall impact of extreme heat events, highlighting the need for targeted adaptation and resilience measures.

Attribution studies have been carried out for this drought-heatwave event in 2022 for other impacts such as heat mortality[109] and wildfires[66]. Burton et al., 2025 found that fire weather has become six times more common in the UK due to human influence, and Beck et al., 2024 found that for the 60 000 heat related deaths over Europe during the summer of 2022, 56% of these deaths could be attributable to anthropogenic climate change. From a hazard perspective Schumacher et al., 2024 finds that soil moisture drought such as the 2022 event over western-central Europe has a return period of around 20 years in the current climate and a 100-year return period in a pre-industrial climate[110]. Zachariah et al., 2022 finds that the heatwave during the 18th-19th July 2022 where air temperatures exceeded 40°C in parts of England, was around 10 times more likely due to anthropogenic climate change[111]. The results from these are consistent with the findings in this study.

Next steps for this case study could be to expand this methodology to other areas of UK transport infrastructure, such as the road and rail network. This could include using the Met Office Road/Railway Surface Temperature model which provides site-specific forecasts of surface temperatures for operational decision-making. For the rail network, critical operating thresholds are documented within the literature and could be used as impact thresholds in future attribution studies of the 2022 heatwave. The attribution result is conditioned on the 2022 SSTs; therefore, an extension could look at the impact of the SST conditioning on the frequency and intensity of the event.

---

[109] Beck, T.M., Schumacher, D.L., Achebak, H. et al. Mortality burden attributed to anthropogenic warming during Europe's 2022 record-breaking summer. npj Clim Atmos Sci 7, 245 (2024). https://doi.org/10.1038/s41612-024-00783-2

[110] Schumacher, D. L., Zachariah, M., Otto, F., Barnes, C., Philip, S., Kew, S., Vahlberg, M., Singh, R., Heinrich, D., Arrighi, J., Van Aalst, M., Hauser, M., Hirschi, M., Bessenbacher, V., Gudmundsson, L., Beaudoing, H. K., Rodell, M., Li, S., Yang, W., … Seneviratne, S. I. (2024). Detecting the human fingerprint in the summer 2022 western-central European soil drought. Earth System Dynamics, 15(1), 131–154. https://doi.org/10.5194/esd-15-131-2024

[111] Zachariah, M., Vautard, R., Schumacher, D. L., Vahlberg, M., Heinrich, D., Raju, E., Thalheimer, L., Arrighi, J., Singh, R., Li, S., Sun, J., Vecchi, G., Yang, W., Seneviratne, S. I., Tett, S. F. B., Harrington, L. J., Wolski, P., Lott, F. C., Mccarthy, M., … Otto, F. E. L. (2022). Without human-caused climate change temperatures of 40 o C in the UK would have been extremely unlikely. https://blog.metoffice.gov.uk/2022/07/27/july-2022-a-dry-run-for-uks-future-climate/

4.7.4. Stakeholder and policy relevance

The 2022 drought-heatwave raised critical concerns over the preparedness and resilience of the UK's transport infrastructure in the context of a changing climate. Our findings demonstrate that anthropogenic climate change significantly increased the likelihood and intensity of the extreme temperatures observed in summer 2022, alongside an increase in their frequency under current climatic conditions. Our study reveals the amplifying role of socio-economic factors, particularly increased airport exposure, in determining the severity of impacts associated with such extreme events. This is of particular relevance to Luton Airport as it begins a period of major expansion. Without the implementation of adaptation and resilience measures, this growth will only enhance the airport's vulnerability to climate-related hazards. As such, future development must be climate-focused to ensure long-term operational resilience.

5. Use Case 3a: Tropical Cyclone Idai and Kenneth 2019

5.1. Summary of event

On 14 March 2019, Tropical Cyclone (TC) Idai made landfall close to Beira City in Mozambique. The storm caused major damages and ultimately affected approximately 3 million people[112]. The event is considered to be one of the Southern Hemisphere's most devastating storms on record[113]. Just six weeks later, another TC hit the region. This time, TC Kenneth made landfall in northern Mozambique. Kenneth was the strongest TC to ever make landfall in the African continent[114], and it was the first time in recorded history that Mozambique was affected by two strong TCs (at or above category 2) in the same season.

In this use case, we aim to attribute the compound flood and the flood impacts of both Idai and Kenneth to better understand the influence of climate change on the severity of the event.

5.2. Geographical context

TC Idai had a major impact in three countries: Mozambique, Malawi and Zimbabwe. TC Kenneth caused significant damage in the Comoros islands, northern Mozambique, southern Tanzania and Madagascar. For both events, our use case analysis focuses on the mainland of Mozambique.

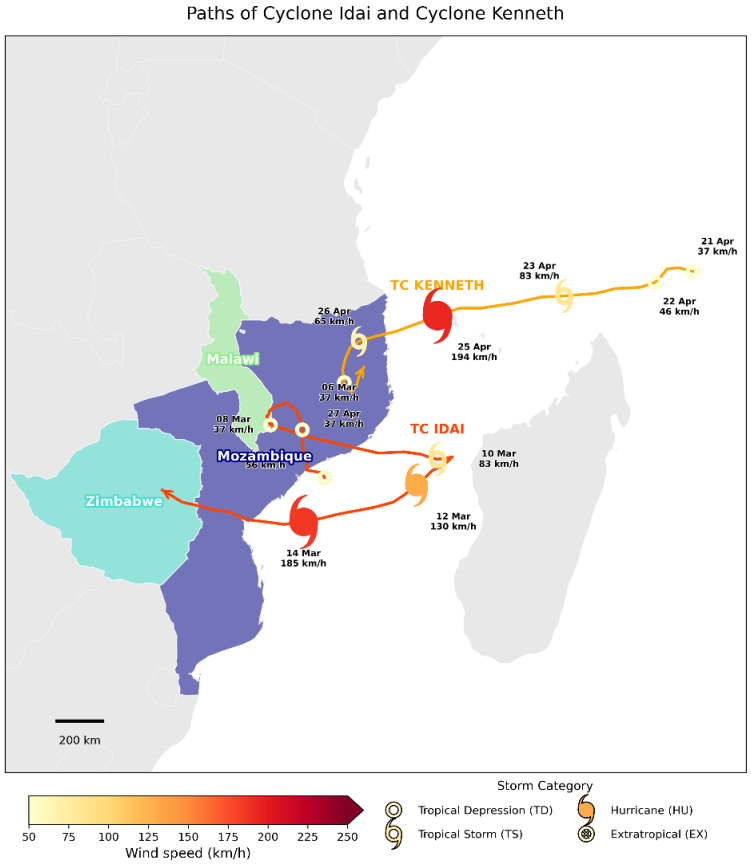

Figure 44 Path of TCs Idai and Kenneth. Markers indicate the stage of the TC, and the color of the marker indicates the wind speed (km/h). Countries affected by the TCs are highlighted.

[112] Norton, R., MacClune, K., and Szönyi, M. (2020). When the unprecedented becomes precedented: Learning from Cyclones Idai and Kenneth. Boulder, CO: ISET International and the Zurich Flood Resilience Alliance. URL: https://www.i-s-e-t.org/perc-cyclone-idai-2019

[113] Warren, M. (2019). Why Cyclone Idai is one of the Southern Hemisphere's most devastating storms. *Nature*.

[114] Cyclones Idai and Kenneth 2019 | PreventionWeb

5.3. Observed hazards

5.3.1. Type of hazards

In this use case, we focus on the compound flooding and resulting direct damages of TC Idai and TC Kenneth. Therefore, we do not consider direct damage from wind, despite evidence that it also contributed to the societal impacts in both cases.

5.3.2. Form of compounding

All TCs are *multivariate compounding* events, with drivers such as extreme rainfall and strong winds co-occurring in the same region. Strong winds can further drive high storm surge and waves at the coast, which combined with tides can cause high coastal water levels. TC Idai, followed by TC Kenneth a month later, were the first *consecutive* TCs to hit Mozambique in a single season, impacting disaster's response and increasing stress on the ongoing recovery from Idai.

5.3.3. Driving dynamics

There are several driving dynamics that contributed to TC Idai and TC Kenneth:

- The South Indian basin is an active TC basin where on average 15 named systems form per year, of which on average 4.5 are TCs with category 3 strength or higher. There is large interannual variability affected by various teleconnections[115], for example, the number of landfalling cyclones in Mozambique has been linked to La Niña events due to the zonal winds. For 2019, the seasonal forecast had no clear indication for an above-average season, but it turned out to be an exceptionally active season with more than 18 named systems of which 11 reached TC strength[116].
- For a TC to develop and be sustained, several favorable conditions are required. The main ones are sea surface temperature of 26–27 °C and a weak vertical wind shear. For both Idai and Kenneth the large-scale atmospheric and oceanic conditions were favorable. The days preceding Idai were characterized by a relatively cold ocean, but a somewhat low wind shear.[117] The days preceding Kenneth showed positive sea surface temperature anomalies up to 2°C) and weak vertical wind shear over the western tropical Indian Ocean[119]. Both TCs had a relatively slow translatory speed (< 10mph)[118], which contributed to high accumulated rainfall.
- Idai was a strong TC (Category 2 at landfall), but from a meteorological perspective it was not an exceptional event. There were some reasons that contributed to the high impacts. The storm made landfall close to Beira, which is a usual track. It hit a densely populated region and caused a significant storm surge. Moreover, the slow translatory speed contributed to high accumulated rainfall and extensive inland flooding. The looping behavior of Idai, that formed in the Mozambique Channel and made landfall in Mozambique but then strengthened again over water before making its second landfall, is rare.
- Kenneth caused less impact than Idai, but was an exceptional event from a meteorological perspective in various ways: 1) it was the strongest cyclone to make landfall in the recorded history of Mozambique; 2) it occurred unusually late in the season as most cyclones in Mozambique make landfall between January and March; 3) it made landfall exceptionally far north with the usual tracks going poleward while Kenneth went

[115] Matyas, C.J. (2015) Tropical cyclone formation and motion in the Mozambique Channel. *International Journal of Climatology*, **35**(3), 375–390.

[116] Gahtan, J., K. R. Knapp, C. J. Schreck, H. J. Diamond, J. P. Kossin, M. C. Kruk, 2024: International Best Track Archive for Climate Stewardship (IBTrACS) Project, Version 4r01. [indicate subset used]. NOAA National Centers for Environmental Information. doi:10.25921/82ty-9e16

[117] Kolstad EW. Predictionand precursors of Idai and 38 other tropicalcyclones and storms in the Mozambique Channel.Q J R Meteorol Soc. 2021;147:45–57. https://doi.org/10.1002/qj.3903

[118] Dube, K., Chapungu, L., Fitchett, J.M. (2021). Meteorological and Climatic Aspects of Cyclone Idai and Kenneth. In: Nhamo, G., Dube, K. (eds) Cyclones in Southern Africa. Sustainable Development Goals Series. Springer, Cham. https://doi.org/10.1007/978-3-030-74262-1_2

west. This was driven by the large-scale wind patterns. Warm oceanic conditions drove a rapid intensification before landfall[119].

5.3.4. Intensity

Idai

TC Idai was a category 3 TC when making landfall on March 14th near Beira, Mozambique. The TC caused heavy rainfall, strong winds and a storm surge. Idai produced high amounts of precipitation along its path. While most of the precipitation produced was over the ocean, Beira and surrounding areas received up to 700 mm during Idai's occurrence (Figure 45). The high volumes of precipitation in Mozambique led to multiple flooding events in different parts of the country.

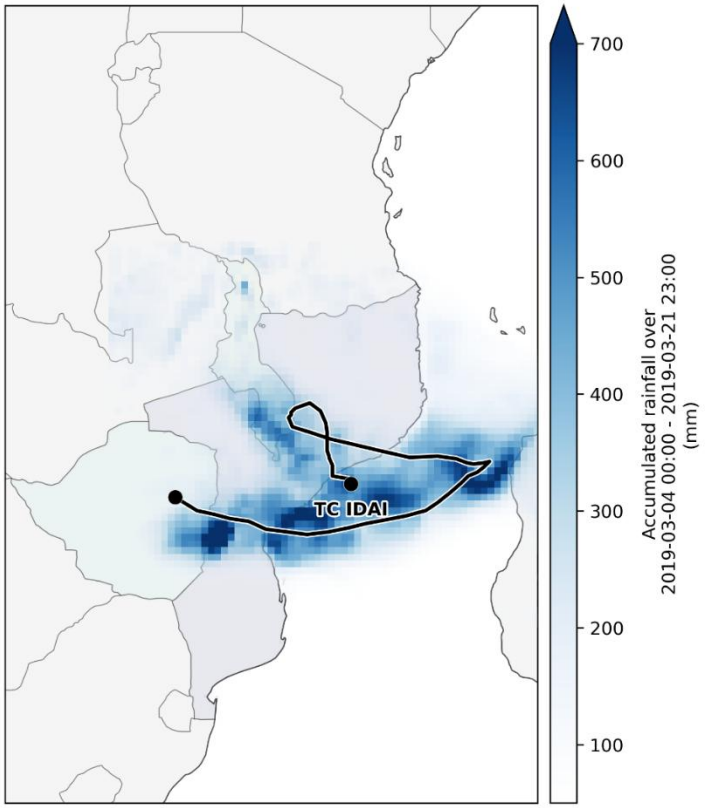

Figure 45 Map of accumulated precipitation produced by TC Idai. Black lines indicate the TC track, and blue grid cells indicate the accumulated precipitation values over time.

Wind speeds were also high, with values surpassing 30 m/s along the coast, as shown in Figure 46. In addition, mean sea level pressure reached a minimum of 950 hPa. The strong winds and low pressure generated storm surges of up to 1.75 m (Figure 47). The tide regimes in Beira are considerable, with a tidal range of up to 4 m. The landfall of Idai in Beira coincided with neap tides, leading to a reduction in impacts in the area when compared to a potential combination with spring tides[120].

[119] Mawren, D., Hermes, J., & Reason, C. J.C. (2020). Exceptional Tropical Cyclone Kenneth in the Far Northern Mozambique Channel and Ocean Eddy Influences. Geophysical Research Letters, 47, e2020GL088715. https://doi.org/10.1029/2020GL088715

[120] Goulart, H. M., Athanasiou, P., van Ginkel, K., van der Wiel, K., Winter, G., Pinto, I., & van den Hurk, B. (2025). Exploring coastal climate adaptation through storylines: Insights from cyclone Idai in Beira, Mozambique. *Cell Reports Sustainability*, *2*(1).

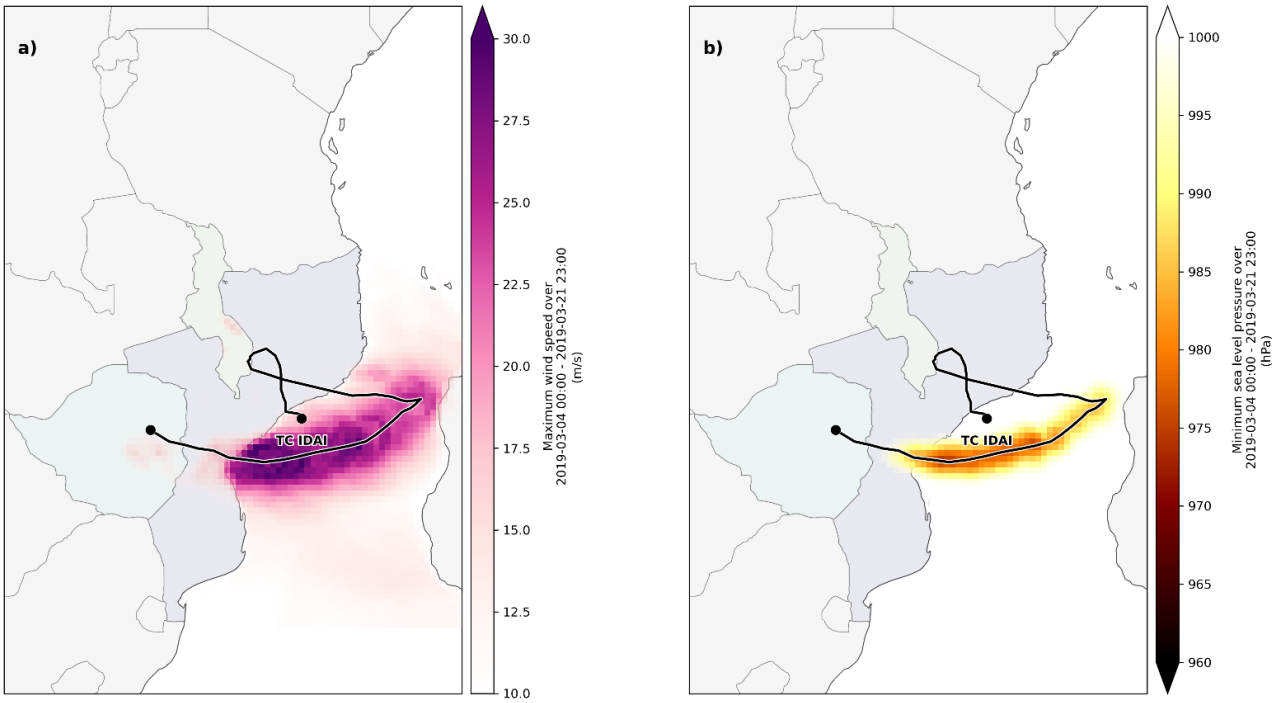

Figure 46 Map for wind speed (a) and mean sea level pressure (b) produced by TC Idai. Black lines indicate the TC track.

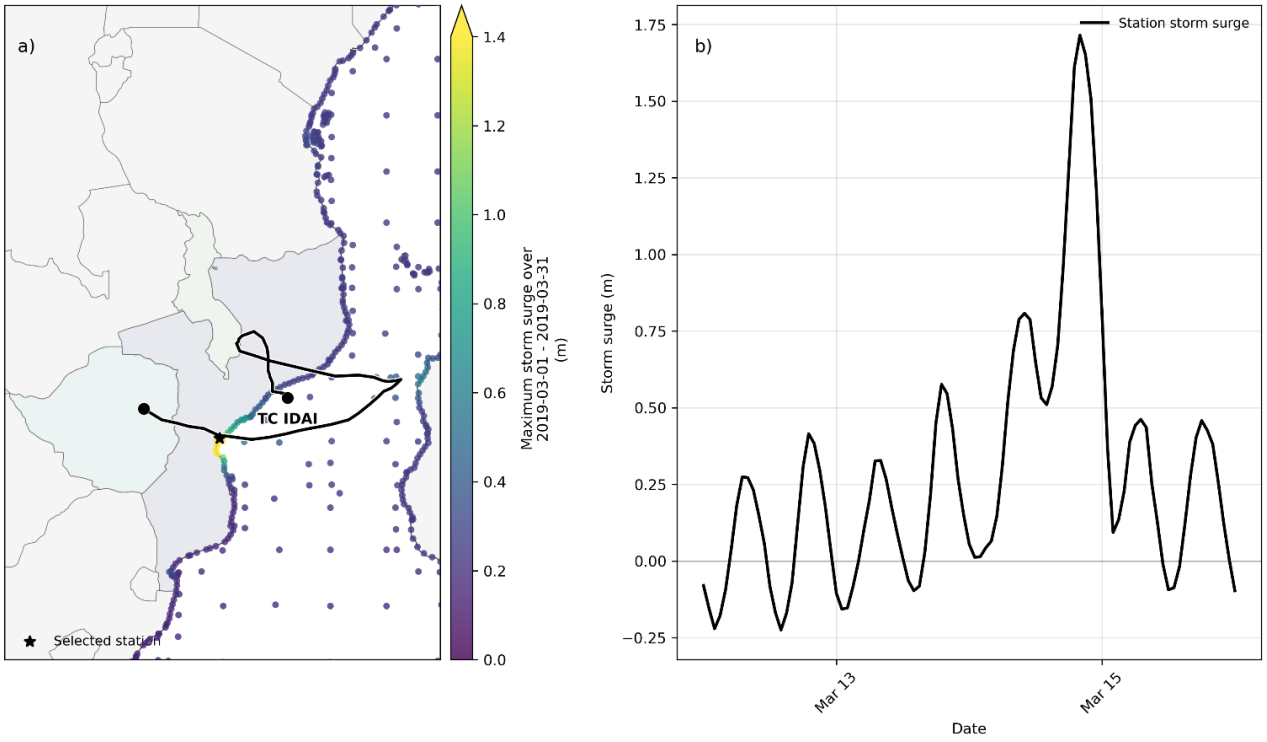

Figure 47 Storm surge as a result of TC Idai. Map of the storm surge values along the coast of Mozambique and neighboring countries (a), with the city of Beira highlighted by the black star. A time series of the storm surge values over the time that Idai made landfall in Beira (b).

Kenneth

One month later, on April 20th, TC Kenneth formed and soon later made landfall on the north of Mozambique, close to the town of Pemba. It produced significant precipitation primarily concentrated near the coastal areas.

The accumulated rainfall reached values up to 400 mm during Kenneth's occurrence (Figure 48). While less extensive than Idai, the heavy rainfall still caused flooding in the affected northern regions of Mozambique.

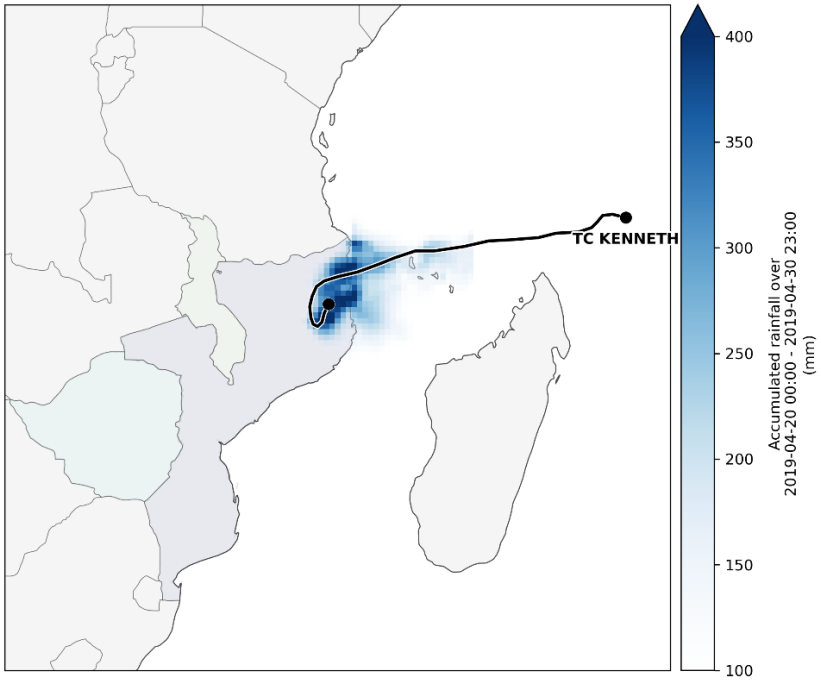

Figure 48 Similar to figure 45, but for TC Kenneth.

Wind speeds were considerable along the coast, reaching values greater than 20 m/s as shown in Figure 49. The minimum sea level pressure dropped to approximately 985 hPa, according to ERA5 data. Meteorologically, the conditions of Kenneth were less severe than those of Idai. The storm surges along the coast were not very extreme, with highest values reaching up to 0.5 m in some areas (Figure 50). Close to Pemba, maximum storm surge generated by Kenneth reached approximately 0.25 m. Similar to Idai, the timing of Kenneth's landfall occurred during relatively low tidal levels, which minimized the overall coastal impact.

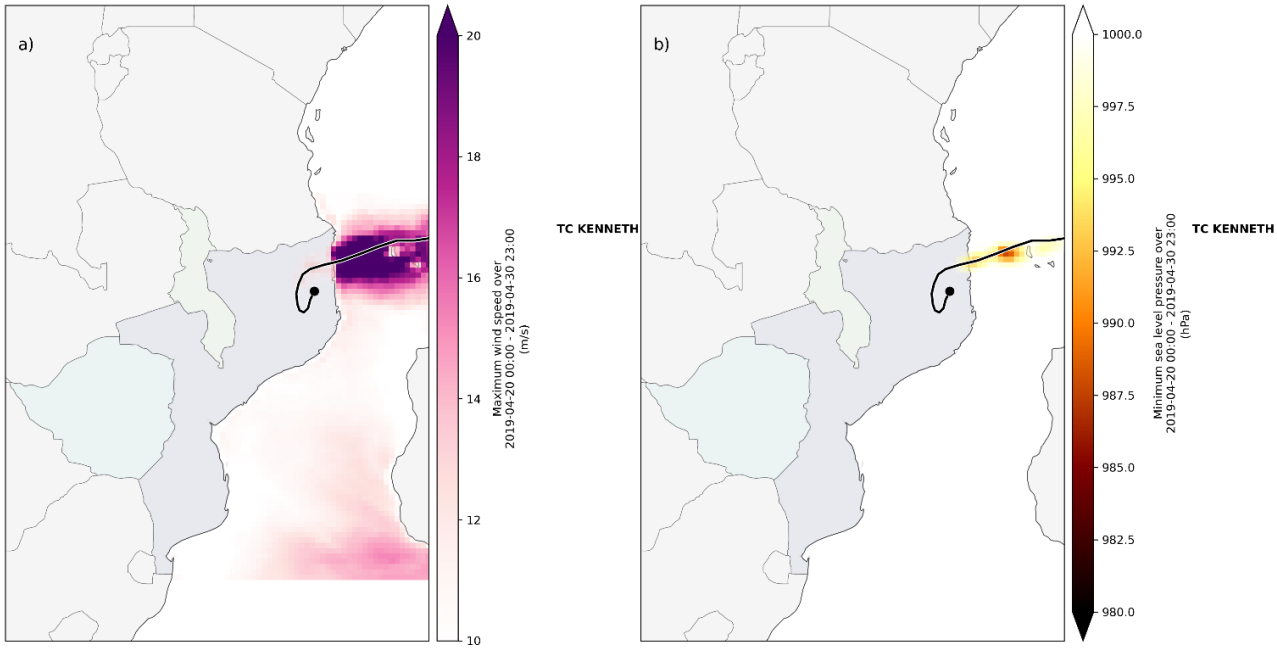

Figure 49 Similar to figure 46 but for wind speed and mean sea level pressure.

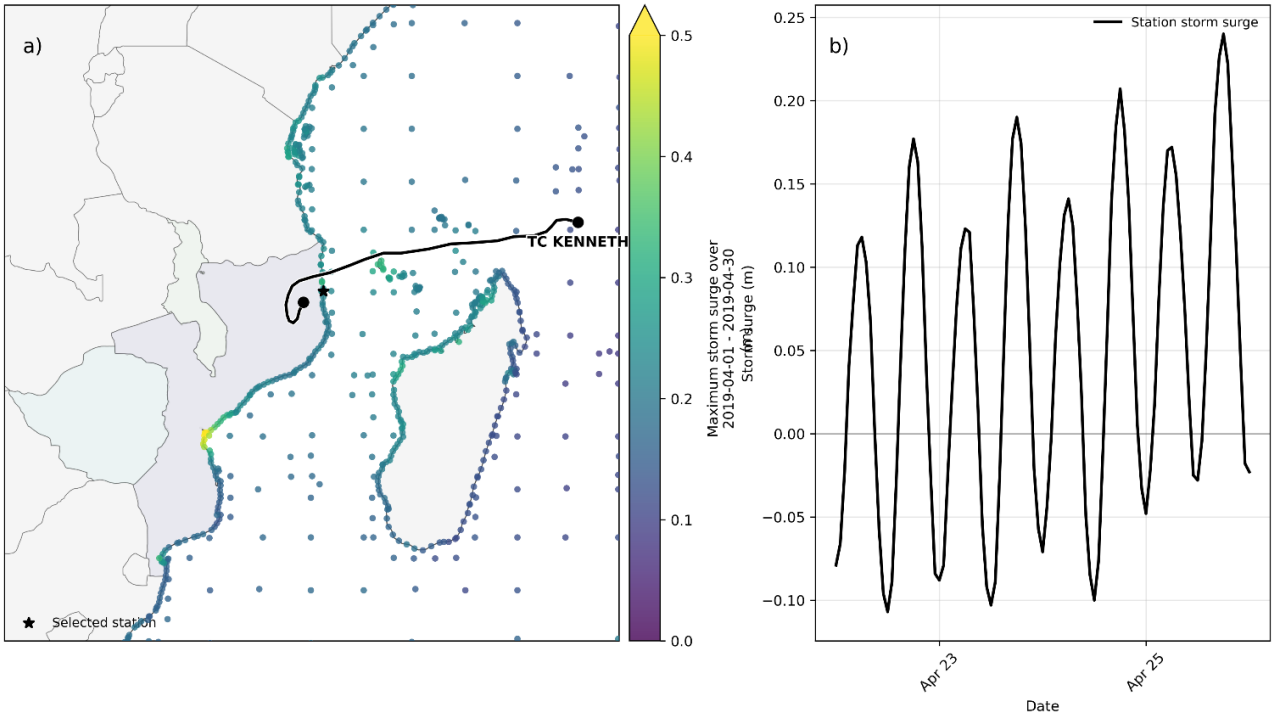

Figure 50 Similar to figure 47, but for TC Kenneth, and selected station close to the town of Pemba, north of Mozambique.

5.4. Observed impacts

5.4.1. Quantitative impacts

Idai

Table 11 Key impact data and statistics.

Impact	Magnitude/scale	Source
People	• 1303 fatalities • 3 million people affected, two-thirds in Mozambique • 240,000 homes damaged or destroyed • 1,300 fatalities	PreventionWeb, OCHA
Health impacts	• 94 hospitals affected • Outbreak of cholera and malaria	OCHA
Food security	• 715k ha of crops flooded, just before the harvest in area already affected by poverty and drought	OCHA, Mozambique after the cyclone by UN Humanitarian
Economic damages	• USD 3 billion in damages	Nhundu et al. (2021)[121]

[121] Nhundu, K., Sibanda, M., & Chaminuka, P. (2021). Economic Losses from Cyclones Idai and Kenneth and Floods in Southern Africa: Implications on Sustainable Development Goals. In G. Nhamo & D. Chikodzi (Eds.), Cyclones in Southern Africa: Volume 3: Implications for the Sustainable Development Goals (pp. 289–303). Springer International Publishing. https://doi.org/10.1007/978-3-030-74303-1_19

Kenneth

Table 12 Key impact data and statistics.

Impact	Magnitude/scale	Source
People	• 374,000 people in need • 45,000 homes damages or destroyed • 45 fatalities	OCHA
Health	• 19 health facilities damaged	OCHA
Food security	• 55,500 ha of crops were lost	OCHA
Transport	• 30% of the national road network was damaged • 20 bridges destroyed	PDNA

5.4.2. Qualitative impacts and responses

The combined impact of TCs Idai and Kenneth on Mozambique was profound. There were severe humanitarian impacts, including hundreds of casualties and millions of displaced persons. For many this was secondary displacement due to other reasons such as conflict. Mozambique has limited capacity for early warning and disaster response. Moreover, the difficulties for financing was a major constraint in recovery efforts and there were significant challenges in restoring livelihoods. There was also significant damage to the national infrastructure, with extensive damages to the road network, electricity, water, hospitals, schools and telecommunication infrastructure[114]. The floods had a severe impact on the agricultural sector and also exacerbated food insecurity and the outbreak of diseases such as cholera and malaria.

5.5. Modeling framework

5.5.1. Hazard modeling

For the hazard modelling, we use the compound flood modelling framework presented in Figure 51. For details of this framework, we refer the reader to COMPASS Deliverable D1.1[122]. In summary, to simulate compound coastal flooding, we combine various hydrological and hydrodynamic models. For river discharge and effective precipitation, we make use of the hydrological model wflow. The coastal boundaries are estimated with Delft3D-FM model that simulates tides and surge. The output of wflow and Delft3D-FM are provided as boundary conditions for the flood model SFINCS, which computes the flood depth. For TC Idai, we also include the effect of wave setup using the HurryWave and SNAPWAVE model. For TC Kenneth, we ignore the effect of waves, given that on the mainland of Mozambique the event was primarily driven by rainfall.

[122] Aleksandrova, N., Vertegaal, D., Couasnon, A., Perks, R., Cotterill, D. Vogel, M., Jack, C., Paprotny, D., Terefenko, P., Śledziowski, J. (2024): Guidelines for compound extremes modelling in current and future climates. Horizon Europe project COMPASS. Deliverable D1.1.

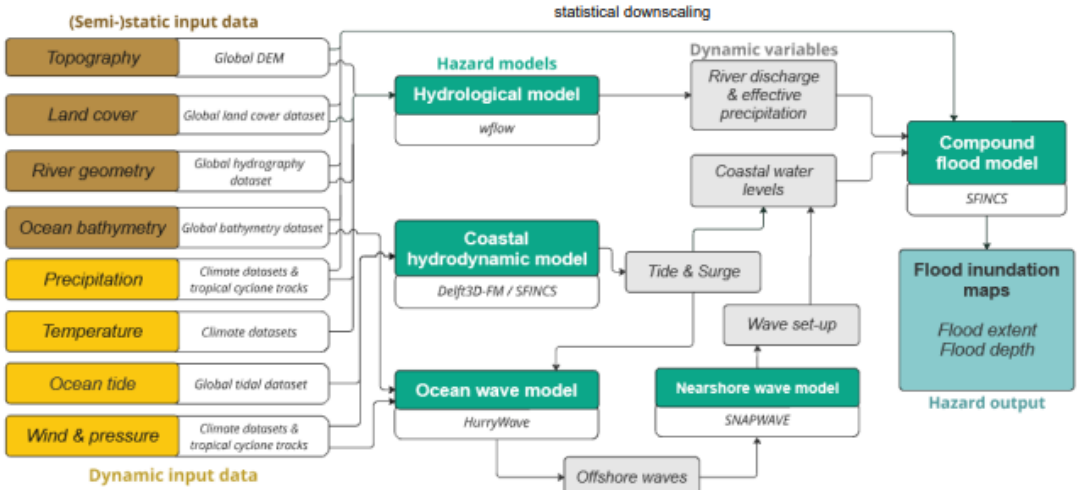

Figure 51 Flowchart of the compound modelling framework.

5.5.2. Impact modeling

To calculate the flood impacts, we use Delft-FIAT with HydroMT[123]. Impacts are calculated by overlaying the SFINCS-derived flood hazard maps with exposure and vulnerability. For exposure, we make use of building footprints from OpenStreetMap (OSM). The maximum potential damage per building type is estimated based on de Moel et al. (2016). We also assess exposed population using 100 m resolution WorldPop population data[124]. Vulnerability is represented by depth-damage curves that indicate the percent damage per flood depth[125]. The damage is expressed in US Dollars.

5.6. Attribution modeling framework

Figure 52 summarizes the main attribution modeling framework. We use a storyline approach and simulate compound flooding for TC Idai and Kenneth under factual and counterfactual scenarios. The factual simulation is based on present-day climate, whereas for the counterfactual scenarios, the long-term climate trend is removed to represent pre-industrial conditions.

[123]Deltares. (2021). *HydroMT-FIAT: Automated and reproducible Delft-FIAT model building* (0.5.4). Deltares. https://deltares.github.io/hydromt_fiat

[124] Stevens FR, Gaughan AE, Linard C, Tatem AJ (2015) Disaggregating Census Data for Population Mapping Using Random Forests with Remotely-Sensed and Ancillary Data. PLoS ONE 10(2): e0107042. https://doi.org/10.1371/journal.pone.0107042

[125] Huizinga, J., De Moel, H. and Szewczyk, W., Global flood depth-damage functions: Methodology and the database with guidelines, EUR 28552 EN, Publications Office of the European Union, Luxembourg, 2017, ISBN 978-92-79-67781-6, doi:10.2760/16510, JRC105688.

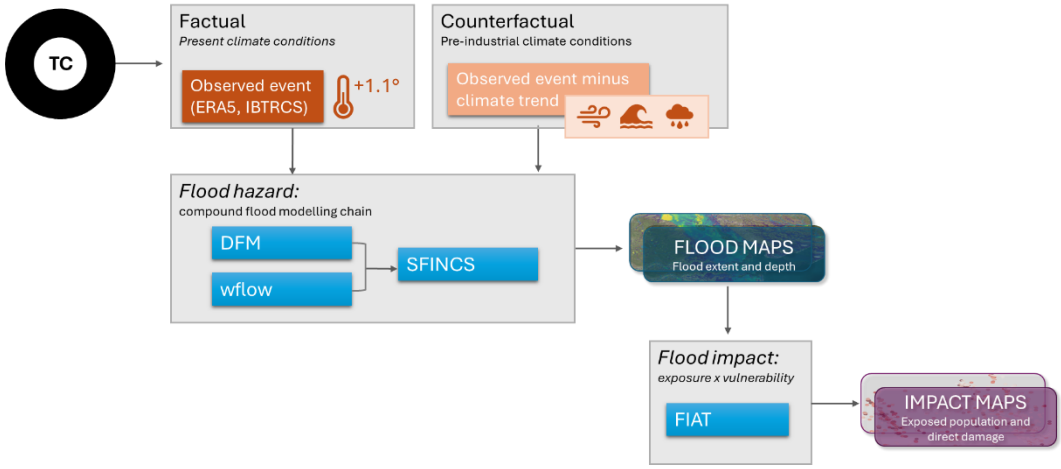

Figure 52 Flowchart of the attribution modeling framework.

5.6.1. Event definition

Our event definition for Idai and Kenneth is based on the compound flood maps. We analyse the flood events based on the maximum water extent and depth. We consider a cell as flooded if the water depth is higher than 5cm, similar to Grimley et al. (2024)[126]. We provide values of exposed population to flood depths higher than 5cm or more and 20cm or more.

5.6.2. Factual and counterfactual simulations

Factual

The factual simulations are based on observations and reanalysis datasets. To compute river runoff, the ERA5 reanalysis is used to provide total precipitation, temperature and evapotranspiration. To compute the coastal water levels, ERA5 wind and pressure forcings are combined with best track data from IBTrACS and a parametric wind model. To compute the compound flooding, SFINCS takes the runoff, coastal water levels, and ERA5 total precipitation as forcing. We refer to COMPASS D1.1 for more details[122].

Counterfactual

For the counterfactual scenario, we remove the average long-term climate trend from the flood drivers.

Idai: The counterfactual scenario includes the following changes in forcing: 1) we reduce the amount of rainfall according to Clausius-Clapeyron relation (7% per degree of warming); 2) we remove the sea-level rise from the coastal water levels, corresponding to 0.14 m of water level; 3) we reduce the maximum wind speed by 10%.

***Kenneth*:** The counterfactual scenarios only accounts for reduction in precipitation as it is reported to be the main hazard driver. The counterfactual precipitation forcing was reduced following the earlier mentioned Clausius-Clapeyron relation.

5.7. Results

5.7.1. Factual hazards and impacts

Idai

The factual simulation of TC Idai shows wide-spread flooding in the flood plains of the Sofala province, including the city of Beira (Figure 53). The deepest flooding (dark blue, > 3.5 m depths) is concentrated around the banks of the Buzi River, as well as 20-30 km northeast from Beira. Lower levels of flooding (light blue, < 1.5 m depth)

[126] Grimley, L. E., Hollinger Beatty, K. E., Sebastian, A., Bunya, S., & Lackmann, G. M. (2024). Climate change exacerbates compound flooding from recent tropical cyclones. npj Natural Hazards, 1(1), 45.

occur in the downstream flood plain of the Buzi River and Pungwe River. The spatial patterns of the flooding map suggest that flooding occurred mainly due to direct precipitation and high discharge, although coastal flooding was an important driver of the flooding in the area near the city of Beira. The total flood extent is estimated at 3591 km^2.

Figure 53 shows the factual simulation has a reasonable agreement with the satellite-derived Copernicus Emergency Management Service flood map that is based on satellite-observations[127], indicated by hit rate of 76%. However, we seem to overestimate the flood near some river inflow points. This is indicated by a false alarm rate of 13%. The overall critical success index is 68%. For a different satellite product (of Copernicus Emergency Management Service) the hit rate is 99% but the false alarm rate 60%, highlighting the variability between observed flood extent products, mainly due to different post-processing algorithms.

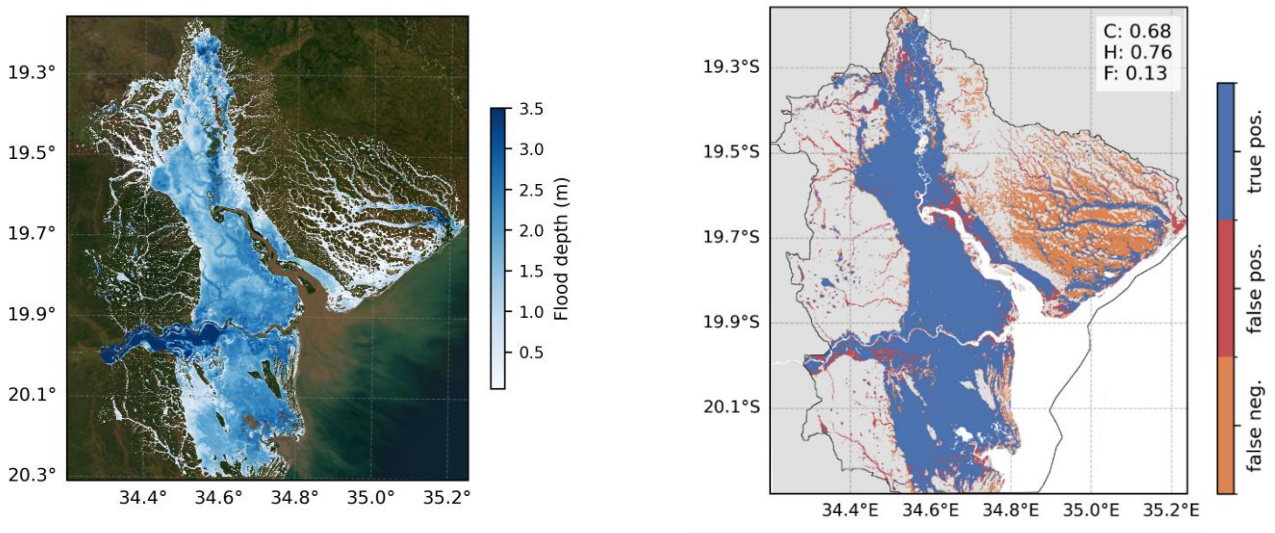

Figure 53 On the left, flood map of TC Idai (2019) along the coast of Mozambique. Blue color indicates the flood depth. On the right, comparison of the inundation maps against UNOSAT flood maps with the colors indicating the match between the satellite-derived flood map and SFINCS. The model skill is measured by the critical success index (C), the hit rate (H) and false-alarm ratio (F). The SFINCS model domain is shown in black.

For the factual simulation, the direct damage of Idai is estimated at 339 million USD, while 84k buildings are damaged. We estimate at 288k people exposed to flood depths higher than 5cm (or 190k people to flood depths higher than 20cm), Figure 54 shows where these impacts occurred, concentrating in the city of Beira and the main river flood plains.

[127] Global Flood Awareness System

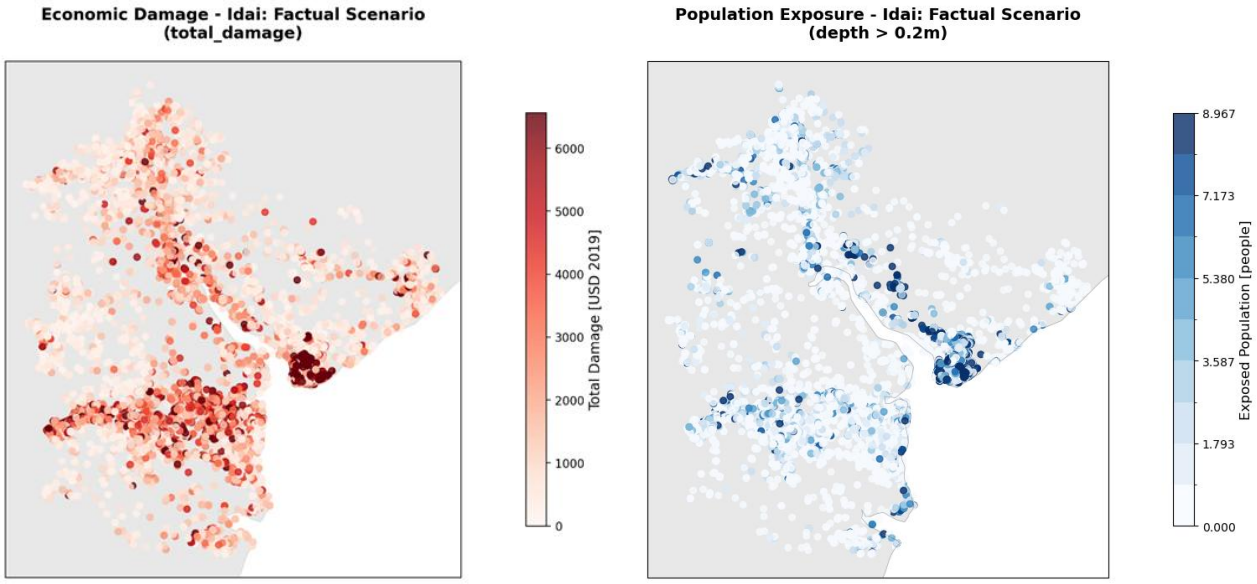

Figure 54 Economic damage in 2019 US$ (left) and exposed population (right) for TC Idai under the factual scenario.

Kenneth

The factual simulation of TC Kenneth shows flooding in the province Cabo Delgado, Northern Mozambique (Figure 55). There is extensive flooding in the rivers draining in Pemba Bay, including Lúrio and Megaruma River, although flood depths are relatively low (< 2m). Around 50 km south of Pemba, flood depths are larger (dark blue, 4-5m depths). This also applies to the area in the North, upstream of Quissanga city, which is the drainage area of Montepuez River. The total flood extent is estimated at 1014 km^2.

For TC Kenneth there are no satellite-derived flood maps available.

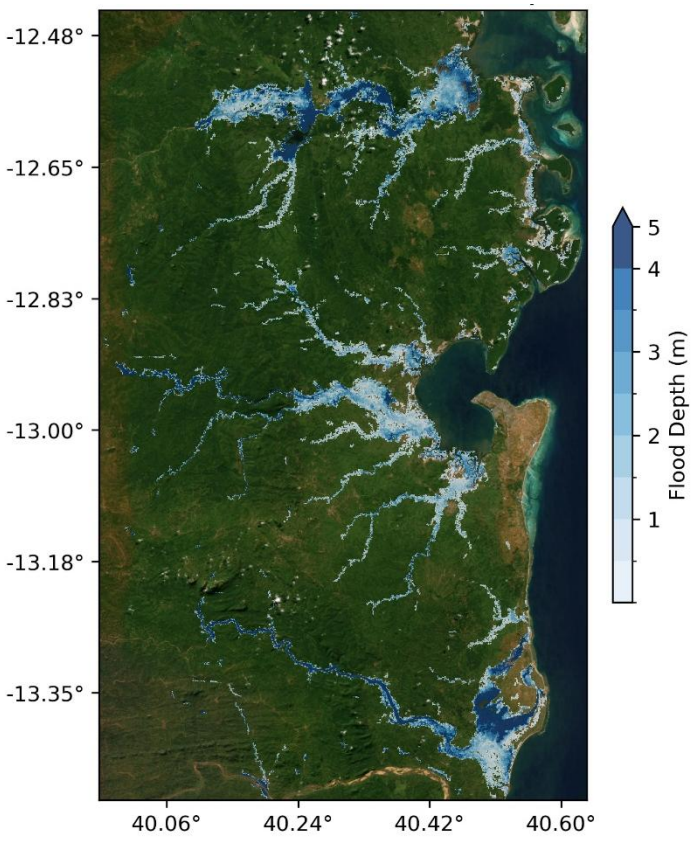

Figure 55 Modeled inundation map of TC Kenneth.

The direct damage of Kenneth is estimated at 49 million USD and 13k buildings were damaged. We estimate at 53k people exposed to flood depths higher than 5cm (or 36k people to flood depths higher than 20cm). Figure 56 shows where these impacts occurred, which are concentrated in Pemba and the other settlements near Pemba Bay.

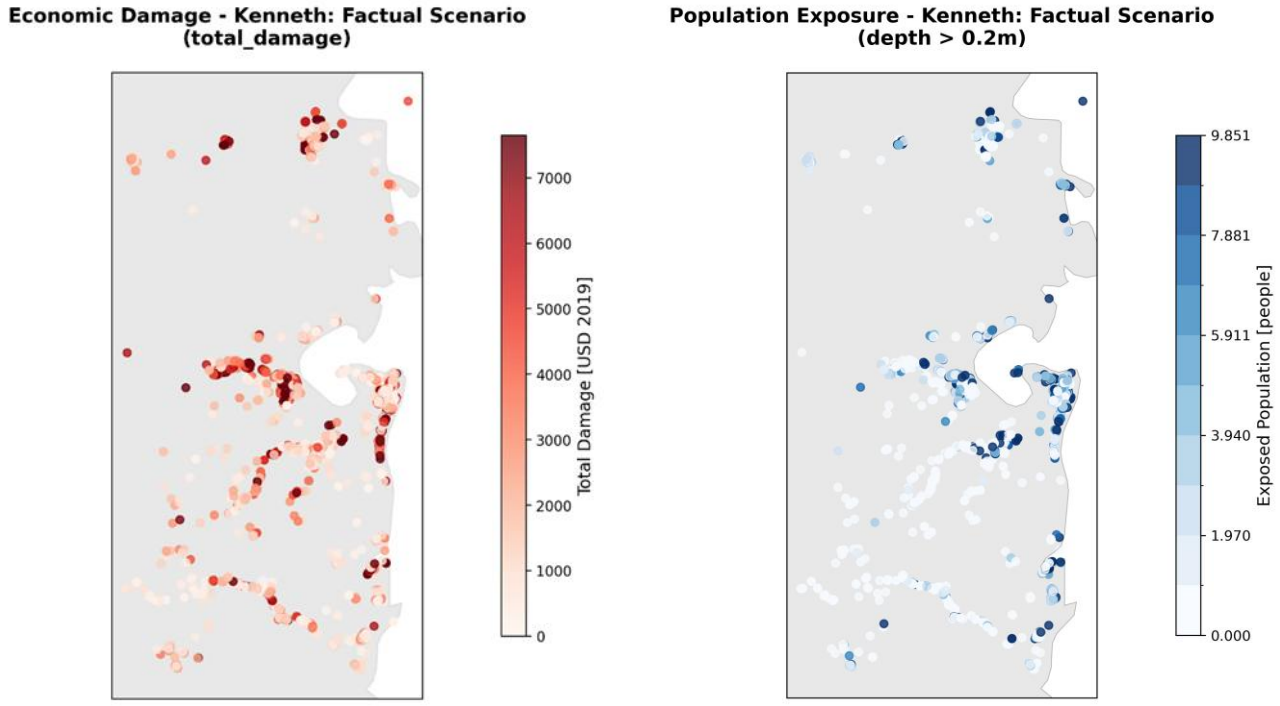

Figure 56 Economic damage in 2019 US$ (left) and exposed population (right) for TC Kenneth under the factual scenario.

5.7.2. Attribution results

Idai

Our results indicate that climate change increased the severity of the flooding due to TC Idai, as shown in Figure XX. For the counterfactual simulation, which has 8% reduction of precipitation, 10% reduction in maximum wind speeds, and 0.14 m of SLR removed, the flood extent decreases to 3507 km^2. This corresponds to an increase of 2% in flood extent that can be attributed to climate change. The mean increase in flood depth is 0.14 m, corresponding to relative increase of 14%. The areas that see the largest increases in flood depth (>0.3 m) include the banks of the Buzi River and the coastal areas east and west of Beira. The total flood volume increases with 9% due to climate change.

When comparing the factual against the counterfactual, the total damages increase with $63 million USD, which corresponds to a 29% increase. The total number of buildings that experienced damages increases with 9k, corresponding to an 11% increase. This indicates that that most of the additional damage under the factual scenario is due to larger flood depths and not due to increase in flood extent. When analyzing the exposed population to flood depths higher than 20cm, there is an 18% increase under the factual scenario, corresponding to an additional 34k people exposed to severe flooding that can be attributed to climate change.

Kenneth

Figure 57 shows that the flooding for TC Kenneth is also less severe under the counterfactual scenario, indicating an increase in flood hazard under climate change. For the factual simulation, which has 8% increase in precipitation, the flood extent is 3% larger than for the counterfactual. The mean increase in flood depth is 0.14 m. The areas that see the largest increases in flood depth (>0.3 m) include upstream of Pemba Bay and the flooding in the North.

For the counterfactual, the total damage is 42 million USD. This means that for the counterfactual there is an increase with $7 million USD, which corresponds to a 14% increase that can be attributed to climate change. The total number of buildings that experienced damages increases with about 800 buildings, corresponding to

a 6% increase. This indicates that most of the additional damage under the factual scenario is due to larger flood depths and not due to increase in flood extent. When analyzing the exposed population to flood depths higher than 20cm, there is a 10% increase under the factual scenario, corresponding to an additional 3.5k people exposed to severe flooding that can be attributed to climate change.

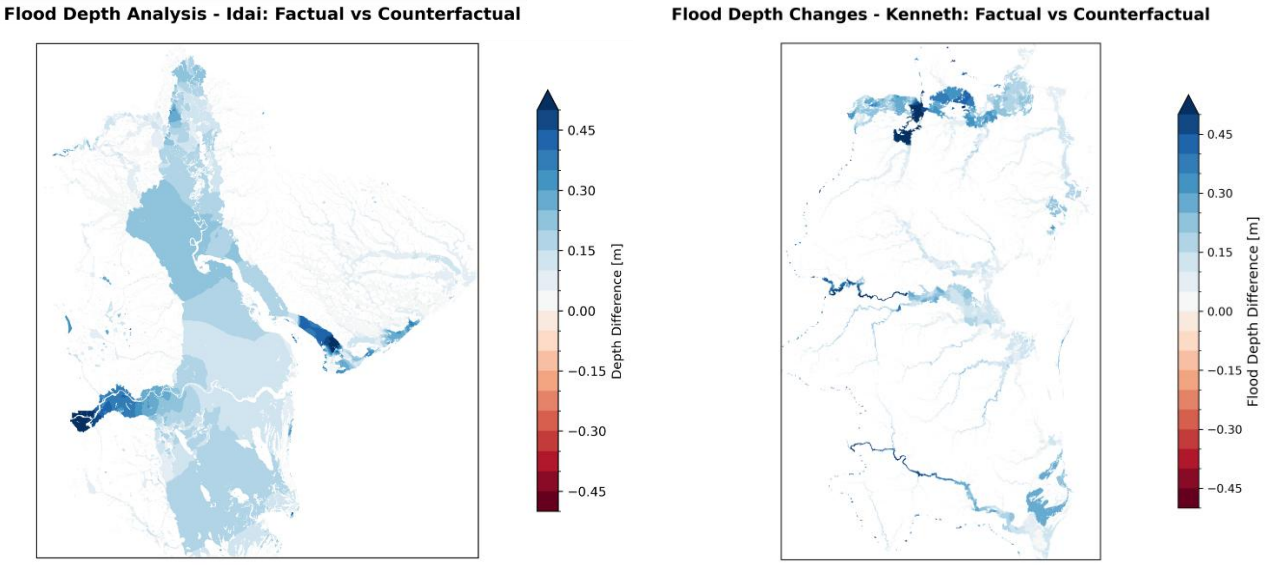

Figure 57 Change in flood depth for TC Idai (left) and TC Kenneth (right) when comparing the factual against the counterfactual.

5.7.3. Summary of attribution results

Figure 58 summarizes the attribution results for total damages and exposed population that can be attributed to climate change.

***Idai*:** We attribute an increase in flood hazard as a result of climate change. Our results show a 2% increase in flood extent, which is driven by an 8% increase in precipitation in current climate conditions compared to preindustrial levels compounding with higher coastal water levels driven by a 10% increase in maximum wind speeds and 0.14 m of regional SLR. Flood depths increased by 0.14 m on average, driving larger damages. For the flood impacts, climate change led to 29% higher damages and 18% more exposed population to flood depths higher than 20cm.

***Kenneth*:** We attribute an increase in flood hazard as a result of climate change. Our results show a 3% increase in flood extent, which is driven by an 8% increase in precipitation in current climate conditions compared to preindustrial levels. Flood depths increased by 0.14 m on average, driving larger damages. For the flood impacts, climate change led to 14% higher damages and 10% more exposed population to flood depths higher than 20cm.

When synthesizing the results for the two TCs, we find that the impact of climate change on flood damage is more profound than on flood hazard. It shows that the societal consequences of TCs can be amplified, even for relatively small increases in individual flood drivers.

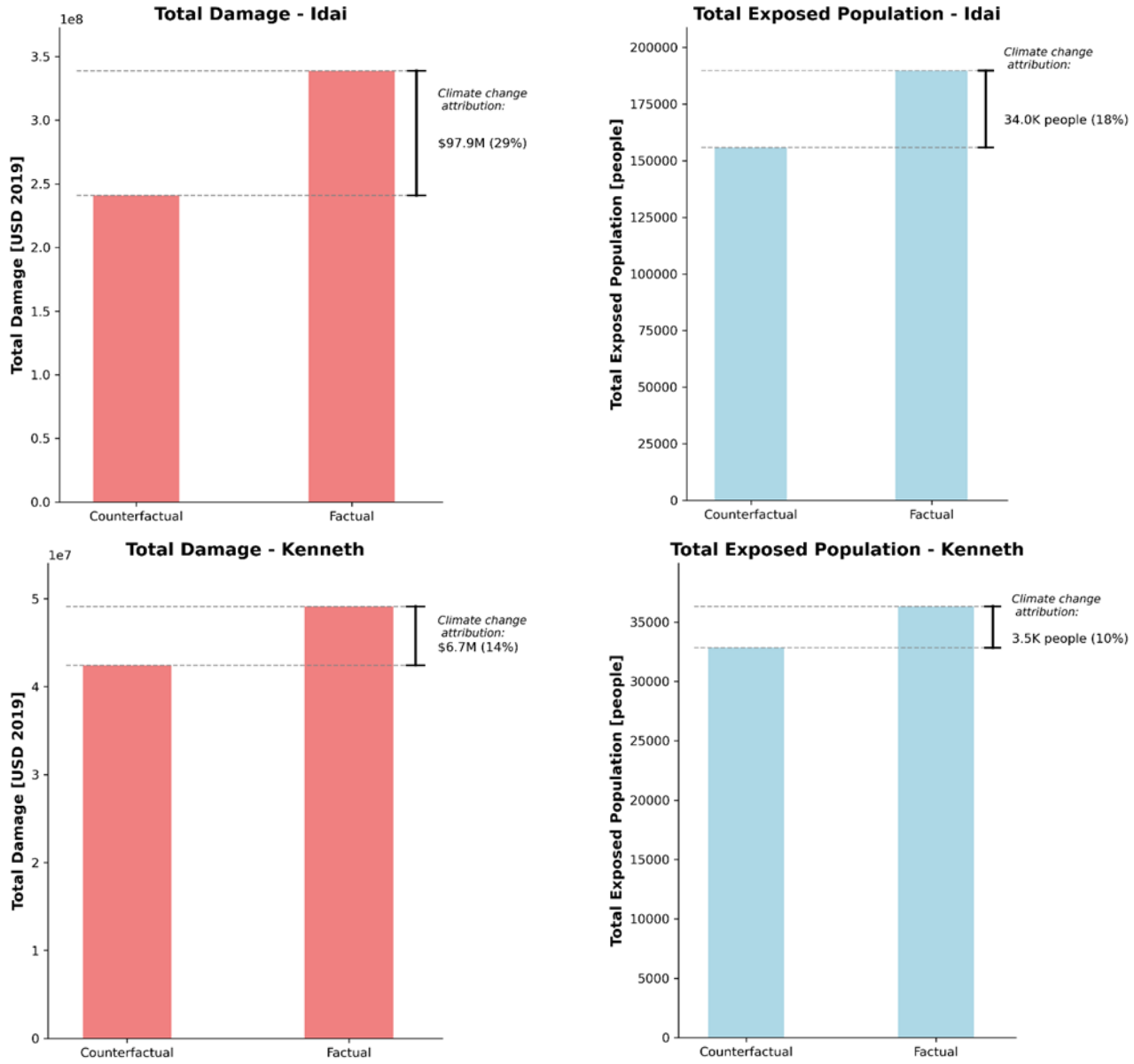

Figure 58 Climate attribution of the flood impacts of TC Idai (top) and TC Kenneth (bottom) for total damage (left) and total exposed population (right).

Idai is a well-studied event in literature with various studies investigating the main meteorological drivers and the societal impacts. There are also past studies that have simulated the flood hazard and impact using similar approaches as applied here[128,129,130]. For example, Mester et al. (2023) shows that climate change drives increased human displacement, corresponding to 28,000 to 52,000 additional displaced persons, depending on the considered flood depth threshold. This is in line with our estimates of 34,000 more exposed population. Kenneth is less studied, and we cannot compare our results against literature.

[128] Eilander, D., Couasnon, A., Leijnse, T., Ikeuchi, H., Yamazaki, D., Muis, S., Dullaart, J., Haag, A., Winsemius, H. C., and Ward, P. J.: A globally applicable framework for compound flood hazard modeling, Nat. Hazards Earth Syst. Sci., 23, 823–846, https://doi.org/10.5194/nhess-23-823-2023, 2023.

[129] Mester, B., Vogt, T., Bryant, S., Otto, C., Frieler, K., and Schewe, J.: Human displacements from tropical cyclone Idai attributable to climate change, EGUsphere [preprint], https://doi.org/10.5194/egusphere-2022-1308, 2023.

[130] Exploring coastal climate adaptation through storylines: Insights from cyclone Idai in Beira, Mozambique - ScienceDirect

More generally, the climate attribution of TC-induced flooding in a data-scarce country is extremely challenging: 1) TCs are low-probability events, that are poorly-represented in climate models and climate change can have opposing influences on the various aspects of the TC (genesis, track, intensity, translation speed, etc.); and 2) due to data scarcity it is difficult to validate our modelling framework. We fully rely on global data and while satellite-derived flood models show reasonable agreement with our data, uncertainties are considered to be relatively high.

5.7.4. Stakeholder and policy relevance

The 2019 TC season highlighted the vulnerability of Mozambique and the larger eastern Africa region to the devastating impacts of TCs. Our results indicate that climate change may increase the severity of TCs, putting additional pressure on the governments to invest in early warning systems, resilient infrastructure and better protect vulnerable communities. When synthesizing the results for the two TCs, we find that the impact of climate change on flood impact is more profound than on flood hazard. It shows that the societal consequences of TCs can be amplified, even for relatively small increases in individual flood drivers, which highlights the added value of flood impact modelling in the field of climate attribution. These results are possibly more meaningful to policymakers and the public because they link to real-world impacts.

While climate change may have led to additional flood impacts, TC Idai struck Mozambique in a context of high poverty levels, food insecurity, weak infrastructure, political fragility, and social inequality. The 2019 TC season underscored the urgent need for socially inclusive climate resilience and disaster preparedness. To study what socio-economic drivers were influential in the impact of TC Idai, key informant interviews with stakeholders working in Mozambique were used to construct Causal Loop Diagrams[131]. This result, presented in Figure 59, highlighted the difference between urban and rural impacts. Moreover, it explained the underlying drivers of land use changes such as charcoal production, driving deforestation and informal urban expansion, which in turn enhance flooding. It emphasizes that impacts of TC Idai were not only the result of intense climatic hazards but were amplified by complex, deeply rooted socio-economic processes, that create reinforcing cycles of vulnerability and exposure**.**

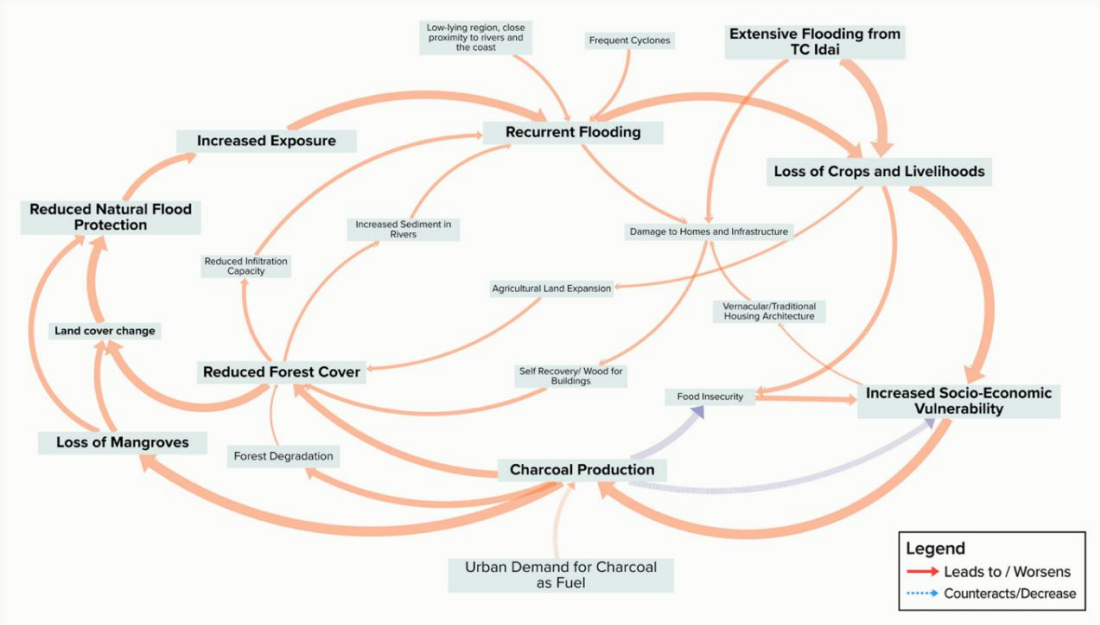

[131] Webb, P. (2025). Impact attribution of compound flooding from Tropical Cyclone Idai: Assessing the influence of socio-economic drivers using a mixed-methods approach. MSc Thesis Earth Sciences: Global Environmental Change and Policy, Vrije Universiteit Amsterdam.

Figure 59 A causal loop diagram highlighting some of the main drivers and feedback loop of flood impacts in rural areas. Source: (Webb, P., 2025).

6. Use Case 3b: Tropical Cyclone Freddy 2023

6.1. Summary of event

In 2023 Mozambique faced a period of severe flooding as the result of Tropical Cyclone (TC) Freddy, which with 35 days was one of the longest-lasting TC on record. In the period between February and mid-March, the country received heavy rain, totalling more than a year's worth of rainfall[132]. At its peak, there was a flooded area of 18,500 km2 (UNOSAT). The first landfall of Freddy was on February 24. There was between 250-300 mm of rain in 3 days. Two weeks after its first landfall, on 11 March 2023, Freddy made a rare trajectory change and made a second landfall in Mozambique. Freddy brought intense rains (over 200mm per day) on the provinces of Zambezia, Sofala, Manica, Tete and Niassa, causing flooding across the various provinces which were already affected by floods since early February. About 1.1 million people have been cumulatively affected by Freddy, while close to two hundred thousand houses were destroyed[133].

In this use case, we aim to attribute the compound flood and the flood impacts of TC Freddy to better understand the influence of climate change on the severity of the event. Note that this use case is less detailed than use case 3a. The main goal was to apply our attribution workflow in another setting, but less effort has been spent on understanding the full context of the event.

6.2. Geographical context

TC Freddy impacted Mozambique, Zimbabwe and Malawi (Figure 60). Freddy started south of Indonesia on February 2nd 2023 and moved westward across the Indian Ocean. It took 19 days to make its first landfall in Madagascar After this, Freddy re-intensified over the Mozambique Channel, making landfall in Mozambique and dissipating on 24 February 24th. However, on March 2nd, Freddy regenerated over the Mozambique Channel and changed course toward Madagascar before turning back toward Mozambique. After making landfall, it finally dissipated at March 13th after making landfall.

[132] Mozambique - Floods and Tropical Cyclone Freddy DREF Operational Update (MDRMZ020) - Mozambique | ReliefWeb
[133] Southern Africa: Snapshot of Tropical Cyclone Freddy's Impact (February - March 2023) | OCHA

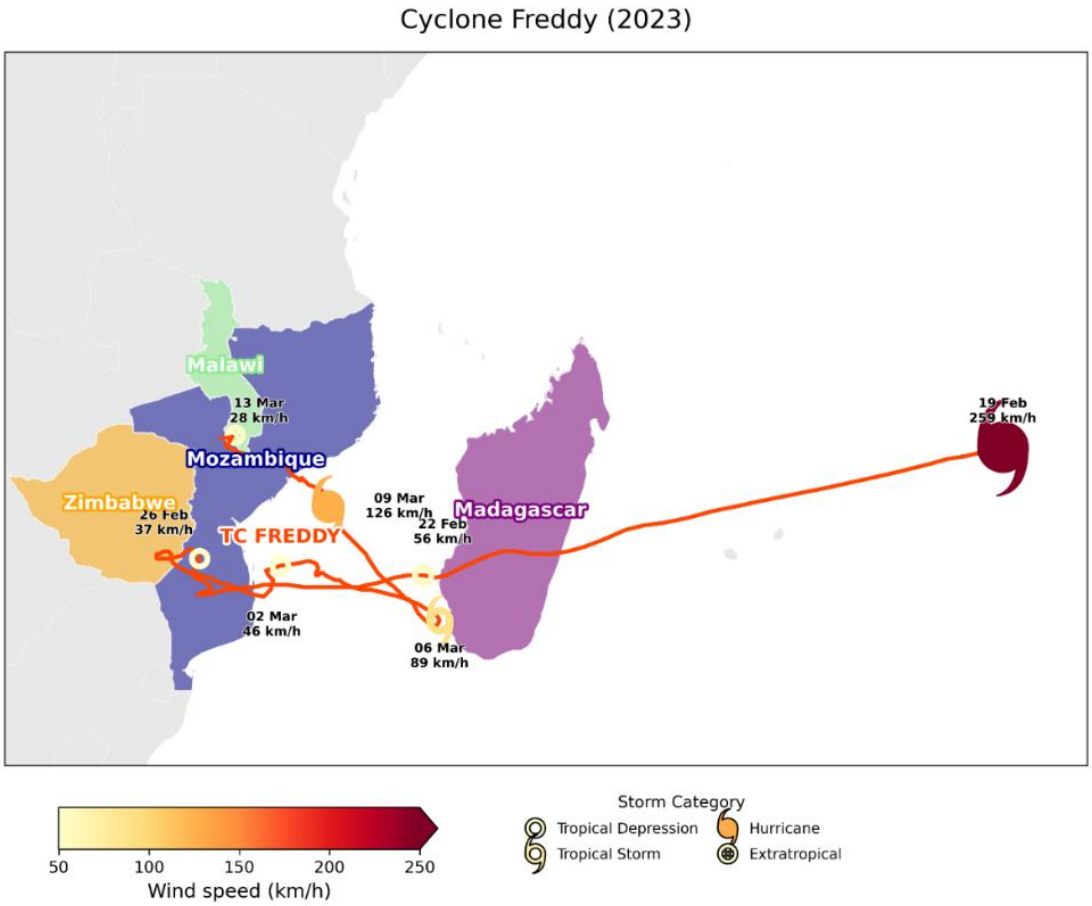

Figure 60 Path of TC Freddy. Markers indicate the stage of the TC, and the color of the marker the wind speed (km/h). Countries affected by the TC are highlighted.

6.3. Observed hazards

6.3.1. Type of hazards

In this use case, we focus on the (compound) flooding of TC Freddy, although the strong wind may have also contributed to the impacts.

6.3.2. Form of compounding

As most TCs, Freddy impacted the coastal areas of Mozambique through a combination of high precipitation, storm surges and, in some areas, high discharges, making it a multivariate compound event. In addition, the two landfalls in different areas of the country could be defined as a spatially compound event.

6.3.3. Driving dynamics

TC Freddy had multiple contributing drivers:

- In terms of accumulated cyclone energy, Freddy was the most energetic storm on record. It went through cycles of weakening and re-intensifying, and may have been the longest-lasting cyclone in recorded history.[134] Along the entire track of Freddy, sea surface temperatures were above 27 °C, which allowed for intensification. Freddy experienced rapid intensification, which was driven by sea surface temperatures, weak vertical wind shear, high potential intensity, and high relative humidity that were all more favorable

[134] Why is Cyclone Freddy a record-breaking storm? | Reuters

than historical averages[135]. The re-intensification by 6 March, after re-entering the Mozambique Channel was likely due to high TC heat potential and a moisture flux from the northern Mozambique Channel[136].

- For a TC to develop and be sustained, several favorable conditions are required. An important one is sea surface temperature of 26–27 °C. Also, a weak vertical wind shear is needed for the TC to sustain. The ocean conditions were favorable with high sea surface temperatures above 29.5 °C, while atmospheric conditions were also favorable with a weak vertical wind shear of 15 m/s[136].
- The synoptic conditions and climate models played a major role in the usual trajectory of Freddy. There was a positive Sub-tropical Indian Ocean Dipole (SIOD) and Southern Annular Mode (SAM) phase while transitioning from a La Niña to a neutral ENSO phase[136]. This combined with the presence of a second TC and a high-pressure system in the Indian Ocean, steered Freddy westward. The double landfall in Mozambique was steered by subtropical anticyclones, which act as blocking system and prevented the southward movement out of the Mozambique Channel[137].

6.3.4. Intensity

Freddy made two landfalls along the coast of Mozambique, which led to considerable meteorological hazards and impacts in the country. Freddy produced substantial precipitation along its path, affecting Mozambique, Malawi, Zimbabwe and Madagascar. And the heaviest rainfall concentrated near the coastal areas of Mozambique where it made landfall, and over the border with Malawi where it stalled (Figure 61). Precipitation values reached up to 1700 mm over the time period analyzed, and considerable regions faced more than 1000 mm of precipitation (dark blue in the figure).

[135] Wang, Q., Guan, S., Can, L., Zhao, W., Zhang, L., & Yang, S. (2025). Record-breaking lifespan, rapid intensification, and long-lasting coastal activity of Tropical Cy-clone Freddy (2023) in the South Indian Ocean. *Environmental Research Letters*.
[136] Perry, Z., Rapolaki, R., Roffe, S., & Ragoasha, M. (2024). Analysing the atmospheric-oceanic conditions driving the sustained long track and intensity of Tropical Cyclone Freddy. *Tropical Cyclone Research and Review*, *13*(4), 356-388.
[137] Xulu, N. G., Chikoore, H., Bopape, M. J. M., & Nethengwe, N. S. (2020). Climatology of the mascarene high and its influence on weather and climate over Southern Africa. *Climate*, *8*(7), 86.

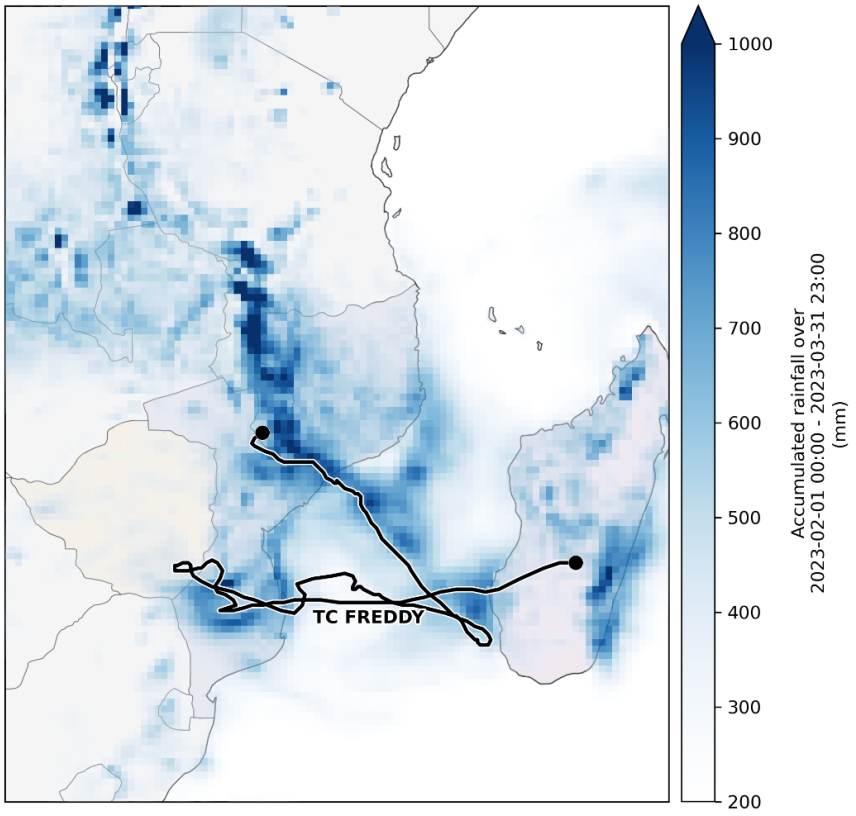

Figure 61 Map of accumulated precipitation produced by TC Freddy. Black lines indicate the TC track, and blue grid cells indicate the accumulated precipitation values over time.

Albeit less intense than during its passage through the Indian Ocean, wind speeds were still considerable, especially on the east coast of Madagascar and before the two landfalls in Mozambique, near the storm's center (Figure 62a). Similar patterns are observed for minimum sea level pressure, where the lowest values were observed just before the landfall in Madagascar (960 according to ERA5, Figure 62b), and subsequently, before the landfalls in Mozambique.

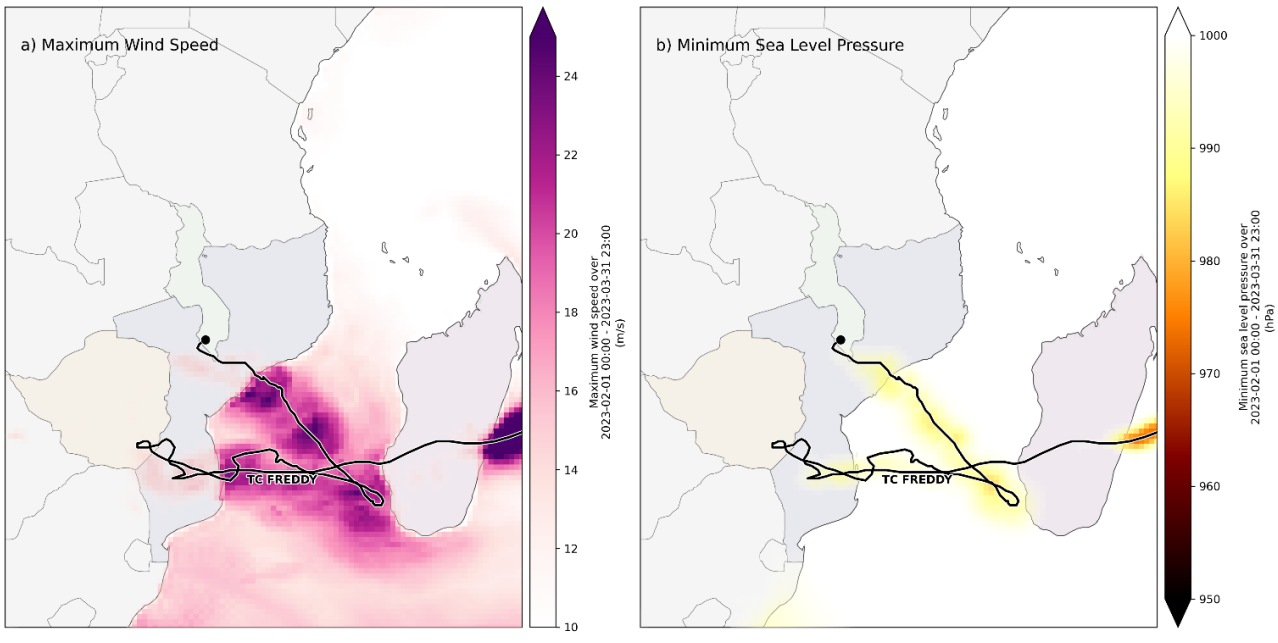

Figure 62 Map of maximum wind speed (left) and minimum sea level pressure (right) produced by TC Freddy.

The storm surge generated by Freddy along the Mozambican coast is illustrated in Figure 63, showing the spatial distribution and time series of storm surges during the event. Near Beira, where the highest values were recorded, the storm surge values reached 0.3m during Freddy's passage, which is similar to the TC Kenneth but lower than TC Idai.

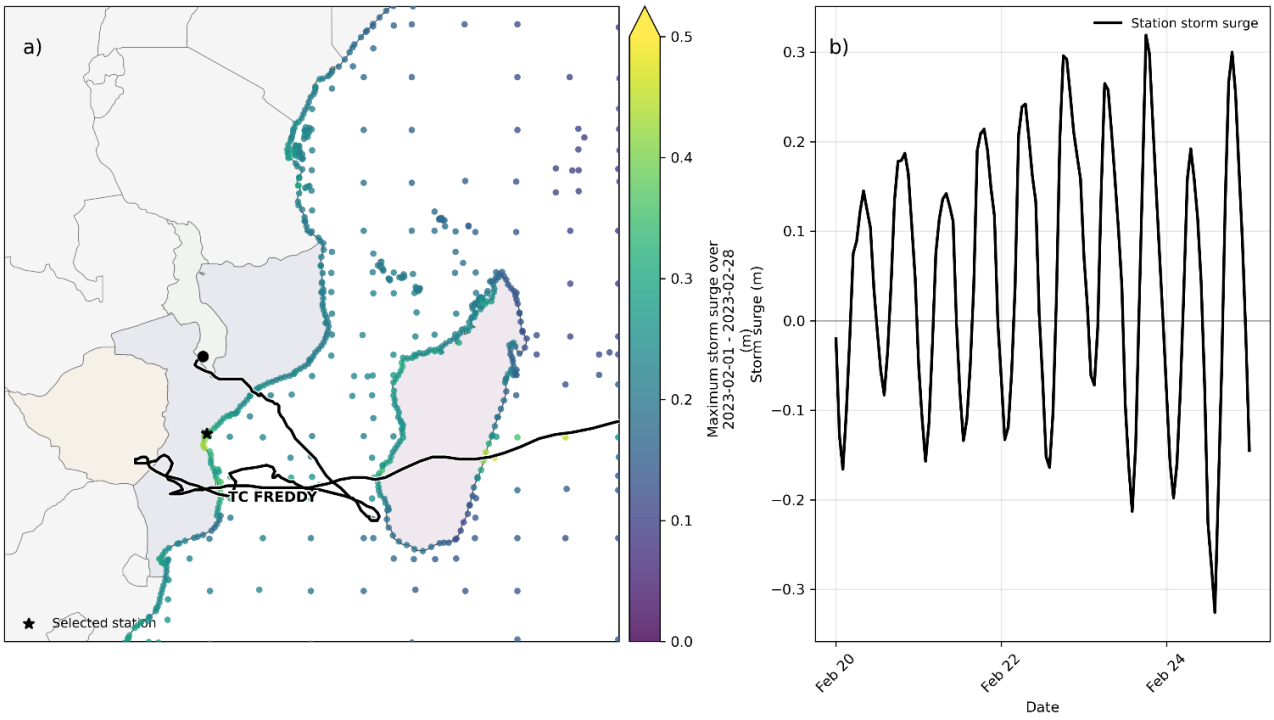

Figure 63 Storm surge as a result of TC Freddy. Map of the storm surge values along the coast of Mozambique (a), with the city of Beira highlighted by the black star. A timeseries of the storm surge values over the time that Idai made landfall in Beira (b).

6.4. Observed impacts

6.4.1. Quantitative impacts

Table 13 Key impact data and statistics.

Impact	Magnitude/scale	Source
People	• 2.7 million people affected • 876 fatalities • 2,925 injured • 916k people displaced	OCHA (2023)[138]
Health	• 223 health facilities affected across 3 countries • Cholera outbreak in Mozambique, creating a compounding effect of damage, floods, and an increased spread of diseases	OCHA (2023)
Transport	• 5,967 km of road damages	OCHA (2023)
Agricultural	• 660k of land affected and 285k of livestock affected • In Malawi, over 204,800 hectares of crops were flooded, just before harvest, prompting concerns regarding food insecurity	OCHA (2023)
Education	• 1.9 k school affected, access to education was interrupted as schools were used as emergency shelters for displaced people	OCHA (2023)

[138] Southern Africa: Snapshot of Tropical Cyclone Freddy's Impact (February - March 2023) | OCHA

6.4.2. Qualitative impacts and responses

Qualitive impacts and responses has not been addressed for TC Freddy.

6.5. Modeling framework

6.5.1. Hazard modeling

For the hazard modelling, we use the compound flood modelling framework presented in Figure 64. For details of this framework, we refer the reader to COMPASS Deliverable D1.1[139]. In summary, to simulate compound coastal flooding, we combine various hydrological and hydrodynamic models. For river discharge and effective precipitation, we make use of the hydrological model wflow. The coastal boundaries are estimated with Delft3D FM model that simulates tides and surge. In this use case, we ignore the effect of waves, given that on the mainland of Mozambique the event was primarily driven a rainfall.

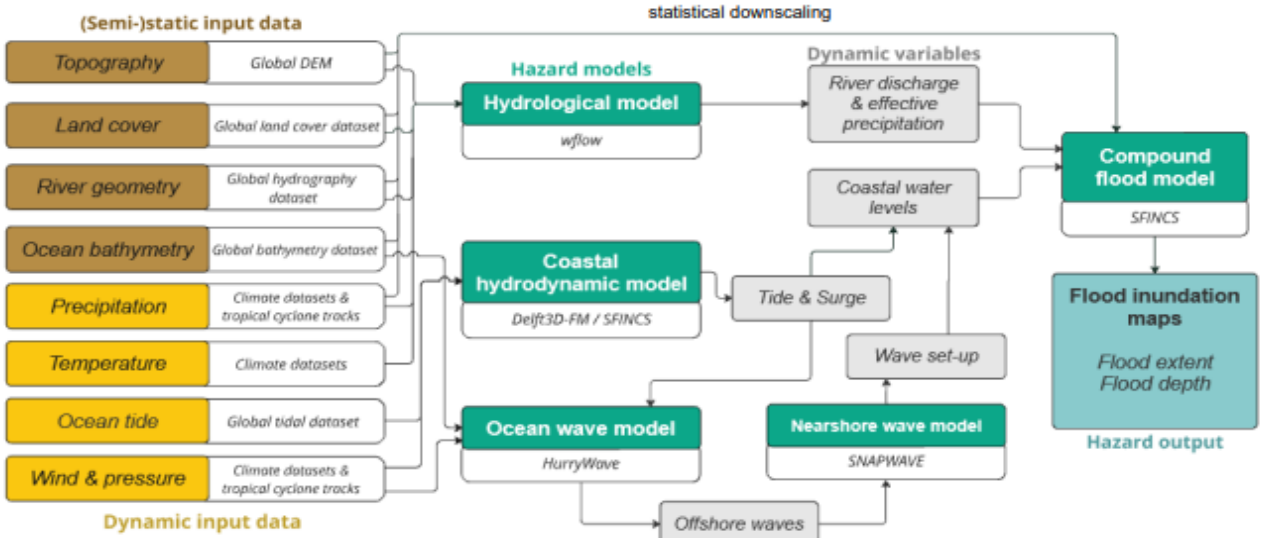

Figure 64 Flowchart of the compound flooding modelling framework.

6.5.2. Impact modeling

To calculate the flood impacts, we use Delft-FIAT with HydroMT[140]. Impacts are calculated by overlaying the SFINCS-derived flood hazard maps with exposure and vulnerability. For exposure, we make use of building footprints from OpenStreetMap (OSM). The maximum potential damage per building type is estimated based on de Moel et al. (2016)[141]. We also assess exposed population using 100 m resolution WorldPop population data[142]. Vulnerability is represented by depth-damage curves that indicate the percent damage per flood depth[143]. The damage is expressed in US Dollars.

---

[139] Aleksandrova, N., Vertegaal, D., Couasnon, A., Perks, R., Cotterill, D. Vogel, M., Jack, C., Paprotny, D., Terefenko, P., Śledziowski, J. (2024): Guidelines for compound extremes modelling in current and future climates. Horizon Europe project COMPASS. Deliverable D1.1.

[140] Deltares. (2021). *HydroMT-FIAT: Automated and reproducible Delft-FIAT model building* (0.5.4). Deltares. https://deltares.github.io/hydromt_fiat

[141] de Moel, H., Huizinga, J., & Szewczyk, W. (2016). Global flood depth-damage functions – Methodology and the database with guidelines. Publications Office. https://doi.org/doi/10.2760/16510

[142] Stevens FR, Gaughan AE, Linard C, Tatem AJ (2015) Disaggregating Census Data for Population Mapping Using Random Forests with Remotely-Sensed and Ancillary Data. PLoS ONE 10(2): e0107042. https://doi.org/10.1371/journal.pone.0107042

[143] Huizinga, J., De Moel, H. and Szewczyk, W., Global flood depth-damage functions: Methodology and the database with guidelines, EUR 28552 EN, Publications Office of the European Union, Luxembourg, 2017, ISBN 978-92-79-67781-6, doi:10.2760/16510, JRC105688.

6.6. Attribution modeling framework

Figure 65 summarizes the main attribution modeling framework. We use a storyline approach and simulate compound flooding for TC Freddy under factual and counterfactual scenarios. The factual simulation is based on present-day climate, whereas for the counterfactual scenarios, the long-term climate trend is removed to represent pre-industrial conditions.

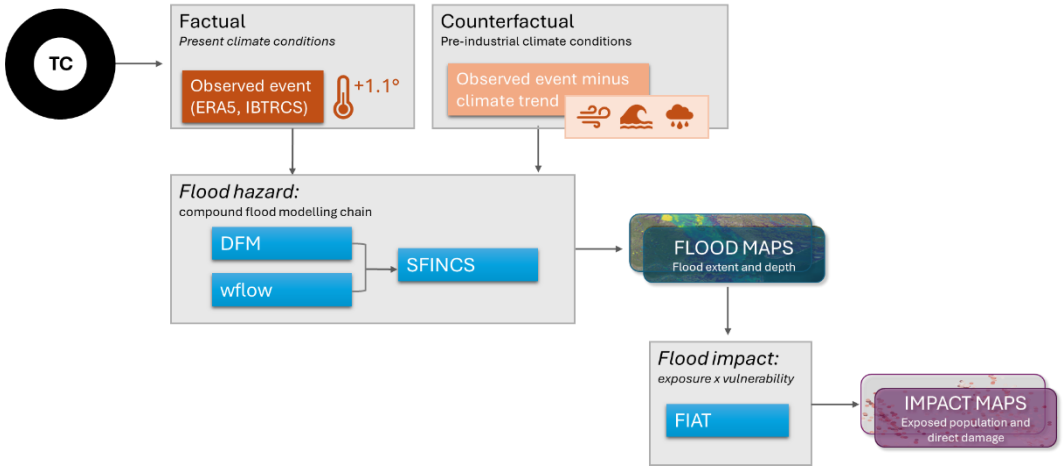

Figure 65 Flowchart of the attribution modelling framework.

6.6.1. Event definition

Our event definition for TC Freddy is based on the compound flood maps. We analyse the flood events based on the maximum water extent and depth. We consider a cell as flooded if the water depth is higher than 5 cm, similar to Grimley et al. (2024)[126]. We provide values of exposed population to flood depths higher than 5cm or more and 20cm or more.

6.6.2. Factual and counterfactual simulations

Factual

The factual simulations are based on observations and reanalysis datasets. To compute river runoff, the ERA5 reanalysis is used to provide total precipitation, temperature and evapotranspiration. To compute the coastal water levels, ERA5 wind and pressure forcings are combined with best track data from IBTrACS and a parametric wind model. To compute the compound flooding, SFINCS takes the runoff, coastal water levels, and ERA5 total precipitation as forcing. We refer to COMPASS D1.1 for more details about the used forcing[122].

Counterfactual

For the counterfactual scenario, we remove the average long-term climate trend from the flood drivers. For this use case, the counterfactual scenarios only accounts for reduction in precipitation as it is reported to be the main hazard driver. The counterfactual precipitation forcing was reduced following the Clausius-Clapeyron relation, which is equivalent to 7% reduction for 1 degree of warming. More details are provided in Vertegaal et al. (in prep.)[144].

6.7. Results

6.7.1. Factual hazards and impacts

The factual simulation of TC Freddy shows the extensive inundation that occurred in central Mozambique during TC Freddy's second landfall near Quelimane between March 11 and 14, 2023 (Figure 66). The deepest flooding

[144] Vertegaal et al. (in prep). Comparing climate and impact attribution for compound events: a case study for tropical cyclone Idai in Mozambique. To be submitted.

(dark blue, 4-5m depths) appears concentrated in low-lying inland areas leading to deltas, and along major drainage channels, while most of the flat lands around Quelimane present lower levels of flooding (<2m). The spatial patterns of the flooding map suggest that flooding occurred mainly due to direct precipitation and high discharge, with limited influence of coastal flooding. The total flood extent is Figure 66 shows the factual simulation has a reasonable agreement with the satellite-derived UNOSAT flood map, indicated by hit rate of 83%. We may overestimate the flood extent upstream as well as close to the coast.

For the factual simulation, the direct damage of Freddy is estimated at 114 million USD, and about 27k buildings damaged. We estimate at 187k people exposed to flood depths higher than 5cm (or 128k people to flood depths higher than 20cm). Figure 67 shows where these impacts occurred, which are concentrated along the rivers and include communities such as Quelimane.

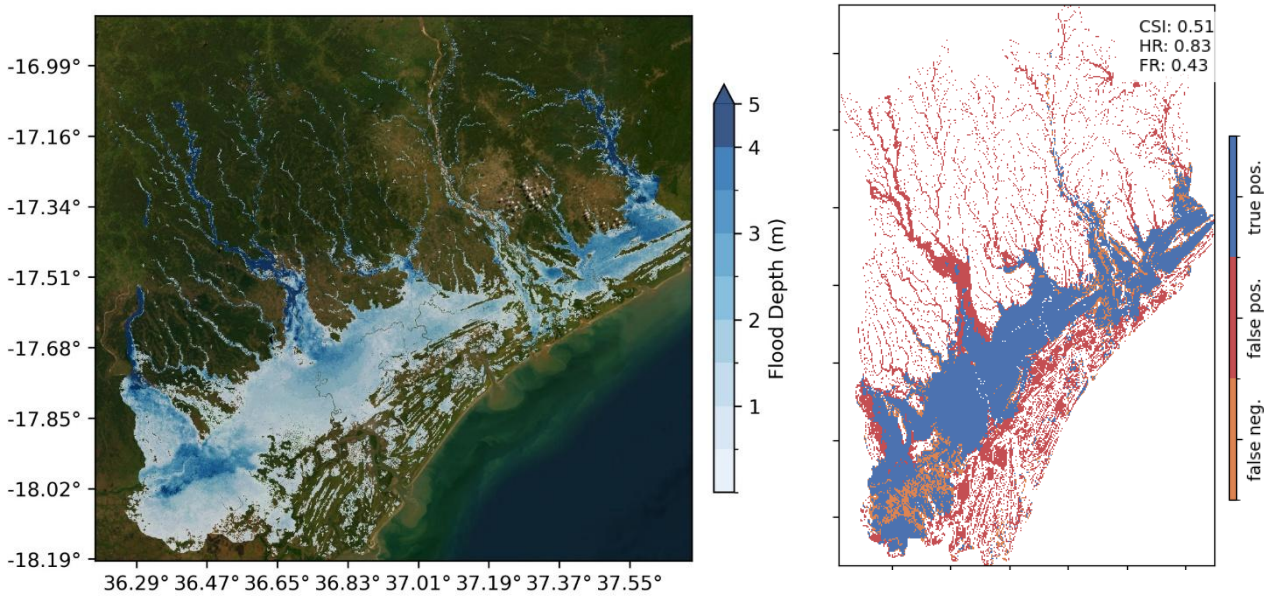

Figure 66 On the left, flood map of TC Freddy along the coast of Mozambique. Blue color indicates the flood depth. On the right, comparison of the inundation maps against UNOSAT flood maps with the colors indicating the match between the satellite-derived flood map and SFINCS.

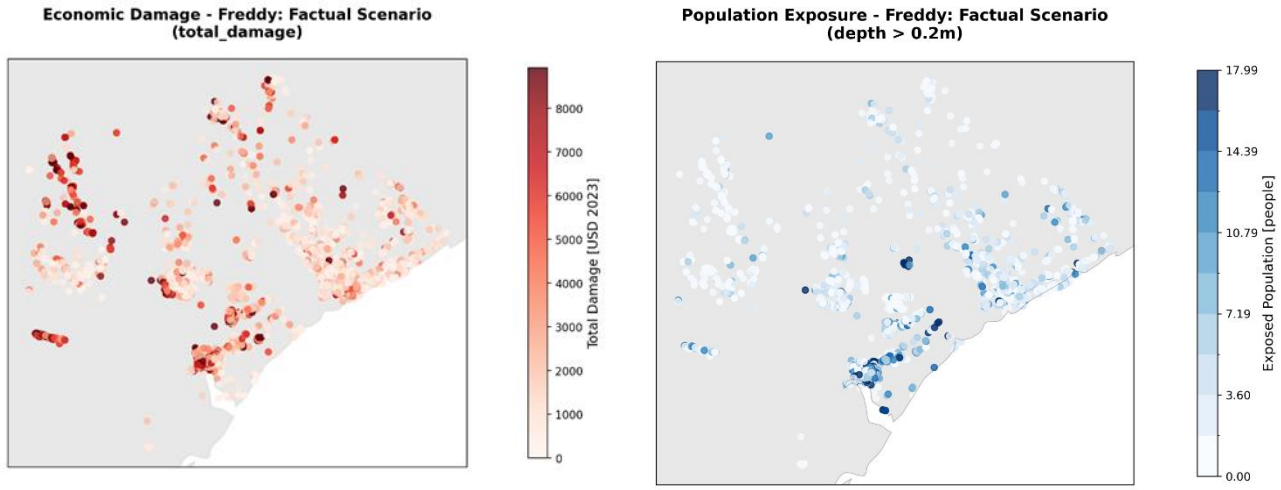

Figure 67 Economic damage in 2023 US$ (left) and exposed population (right) for TC Freddy under the factual scenario.

6.7.2. Attribution results

Climate change increased the severity of the flooding due to TC Freddy, as shown in Figure 68. For the factual simulation, which has 8% increase of precipitation, the flood extent increases with 3% compared to the counterfactual. The largest increase in flood depth (>0.5m) occurs upstream of one of the tributaries of the Licungo River. The mean increase in flood depth is 0.15 m, which drives higher damage. When comparing the factual against the counterfactual, the total damages increase with $21 million USD, which corresponds to 19%. The total number of buildings that experienced damage increases with 8%, indicating that most of the damage is due to larger flood depths and not due to an increase in flood extent. When analyzing the exposed population to flood depths higher than 20cm, there is a 13% increase under the factual scenario, corresponding to an additional 16k people exposed to severe flooding that can be attributed to climate change.

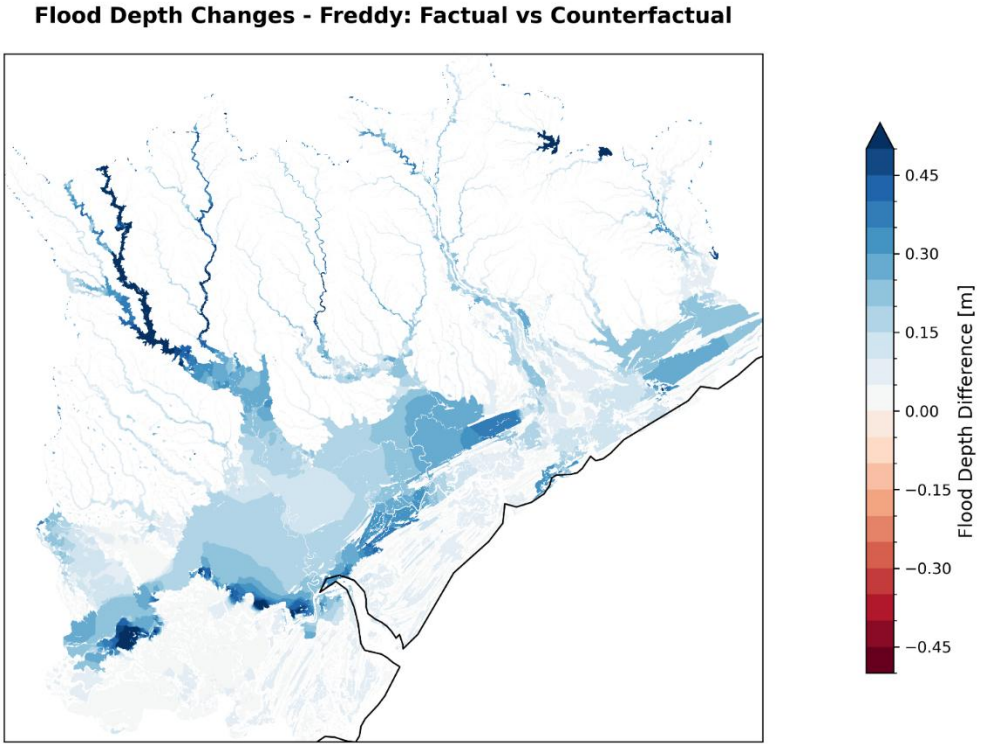

Figure 68 Change in flood depth for TC Freddy when comparing the factual against the counterfactual.

6.7.3. Summary of attribution results

We attribute the flood hazard as 3% in flood extent as a result of climate change. This increase in severity driven by an 8% reduction in precipitation under pre-industrial levels. For the flood impacts, climate change led to 19% higher damages and 13% higher exposed population to flood depths higher than 20cm (Figure 69). This highlights that the influence of climate change can be more pronounced on the flood impacts than on the flood hazard.

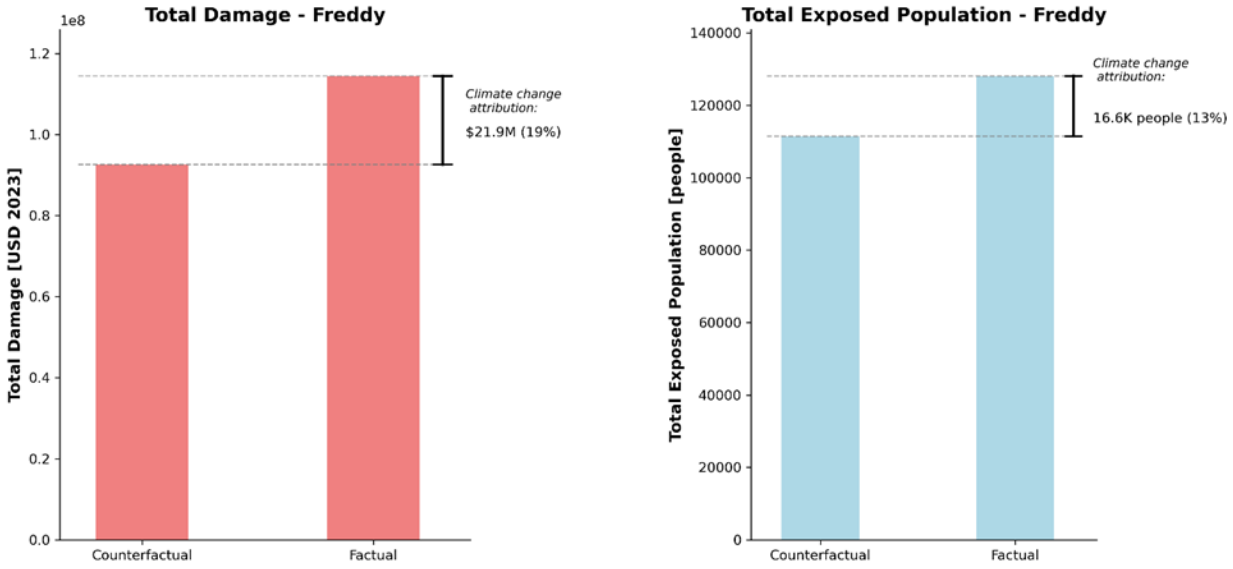

Figure 69 Climate attribution of the flood impacts of TC Freddy for total damage (left) and total exposed population (right).

To the best of our knowledge, the impact of climate change on TC Freddy has not been studied in detail in previous studies. In this use case, we apply a storyline approach based on Clausius-Clapeyron relation to provide insights into the changes in rainfall in a warmer climate, given that rainfall was the main flood driver on the mainland of Mozambique. Probabilistic attribution studies, for example those by World Weather Attribution, do indicate that climate changes make extreme rainfall induced by TC more likely[145,146] but these results are not directly comparable to our results. The 8% reduction in rainfall is a conservative estimate, and studies have shown that the impact on extreme rainfall may go beyond the Clausius-Clapeyron rate[147,148]. Moreover, there are other climate change aspects that we did not consider, including a change in track, wind speed, and sea-level rise.

More generally, the climate attribution of TC-induced flooding in a data-scarce country is extremely challenging: 1) TCs are low-probability events, that are poorly-represented in climate model and climate change can have opposing influences on the various aspects of the TC (genesis, track, intensity, translation speed, etc.); and 2) due to data scarcity it is difficult to validate our modelling framework. We fully rely on global data and while satellite-derived flood models show reasonable agreement with our data, uncertainties are considered to be relatively high.

6.7.4. Stakeholder and policy relevance

For the case of TC Freddy, we did not carry out any stakeholder engagement activities or investigate the policy context.

[145] Rapid attribution of the extreme rainfall in Texas from Tropical Storm Imelda – World Weather Attribution

[146] Climate change added $4bn to damage of Japan's Typhoon Hagibis – World Weather Attribution

[147] Climate change increased Typhoon Gaemi's wind speeds and rainfall, with devastating impacts across the western Pacific region – World Weather Attribution

[148] Lenderink, G., de Vries, H., van Meijgaard, E., de Rooy, W., van Ulft, L., Thompson, V., ... & Fowler, H. J. (2025). A pseudo global warming based system to study how climate change affects high impact rainfall events. *Weather and Climate Extremes*, 100781.

7. Use Case 4: Honduras tropical cyclones Eta and Iota

7.1. Summary of event

The analysis of impacts and drivers of risk in this case study build on research done by the Red Cross Red Crescent Climate Centre for the World Bank. This involved key informant interviews, literature research and data analysis. Full results unpublished, executive summary accessible through:

https://storymaps.arcgis.com/stories/8fd49dccaf0f4b719a7aa6b5a2e0201a

In the midst of the COVID-19 pandemic, in November 2020, two hurricanes hit Honduras in the span of two weeks[149]. Hurricane Eta made landfall on November 4th, causing widespread damage across Central America, and particularly in Honduras. There was heavy rainfall, primarily occurred in the northwest of the country, with widespread riverine flooding, landslides and flashfloods. The storm tragically caused at least 74 deaths. On 17 November, while the country was still responding to the immediate impacts of Eta, Hurricane Iota made landfall. While the track was different, heavy rainfall affected the same area where Eta had already triggered floods and landslides – further exacerbating the impacts and causing 13 additional deaths. The most severely affected rivers included the Ulúa and Chamelecón rivers in the Sula Valley, the Choluteca River in the south, the Aguán Valley in Colón, and the León Valley in Atlántida.

According to CEPAL[150], the storms had a direct impact on 437,000 people and indirectly affected 4.5 million, forcing the displacement of around 937,000 individuals. Humanitarian needs surged, with 2.8 million people requiring assistance[151]. The economic toll was severe, with losses reaching $1.9 billion USD and national economic growth declining by 0.8%[152] . The disasters claimed 95 lives—primarily due to drowning and structural collapses—and left more than 300,000 people cut off because of damaged infrastructure[153]. Over 90,000 homes were damaged by flooding and landslides, with approximately 170,000 people needing to be evacuated[154].

Acting on forecasts, COPECO (the Honduran disaster management agency) and humanitarian actors called for emergency evacuations. However, this was hampered for a variety of reasons including a national holiday just before Eta made landfall, ongoing violence and insecurity, and the COVID-19 pandemic[155]. Immediate response included search and rescue efforts, data collection and support to affected households with humanitarian assistance[156]. Learning from this and given the scale of cascading impacts from these dual hurricanes, there has been a stronger focus in the country around preparedness planning and early action.

[149] CEPAL. (2021). Evaluación de los efectos e impactos de la tormenta tropical Eta y el huracán Iota en Honduras. https://www.cepal.org/es/publicaciones/46853-evaluacion-efectos-impactos-causados-la-tormenta-tropical-eta-huracan-iota

[150] CEPAL. (2021). Evaluación de los efectos e impactos de la tormenta tropical Eta y el huracán Iota en Honduras. https://www.cepal.org/es/publicaciones/46853-evaluacion-efectos-impactos-causados-la-tormenta-tropical-eta-huracan-iota

[151] IFRC. (2020). Honduras: Hurricane Eta and Iota - Emergency appeal n° MDR43007 operation update no. 2. https://reliefweb.int/report/honduras/honduras-hurricane-eta-and-iotaemergency-appeal-n-mdr43007-operation-update-no-2

[152] World Bank. (2021). Poverty & equity brief Honduras. www.worldbank.org/poverty

[153] IFRC. (2020). Honduras: Hurricane Eta and Iota - Emergency appeal n° MDR43007 operation update no. 2. https://reliefweb.int/report/honduras/honduras-hurricane-eta-and-iotaemergency-appeal-n-mdr43007-operation-update-no-2

[154] CEPAL. (2021). Evaluación de los efectos e impactos de la tormenta tropical Eta y el huracán Iota en Honduras. https://www.cepal.org/es/publicaciones/46853-evaluacion-efectos-impactos-causados-la-tormenta-tropical-eta-huracan-iota

[155] World Bank and Red Cross Red Crescent Climate Centre (2022).

[156] IFRC. (2020). Honduras: Hurricane Eta and Iota - Emergency appeal n° MDR43007 operation update no. 2. https://reliefweb.int/report/honduras/honduras-hurricane-eta-and-iotaemergency-appeal-n-mdr43007-operation-update-no-2

7.2. Geographical context

Countries and or sub-regions impacted.

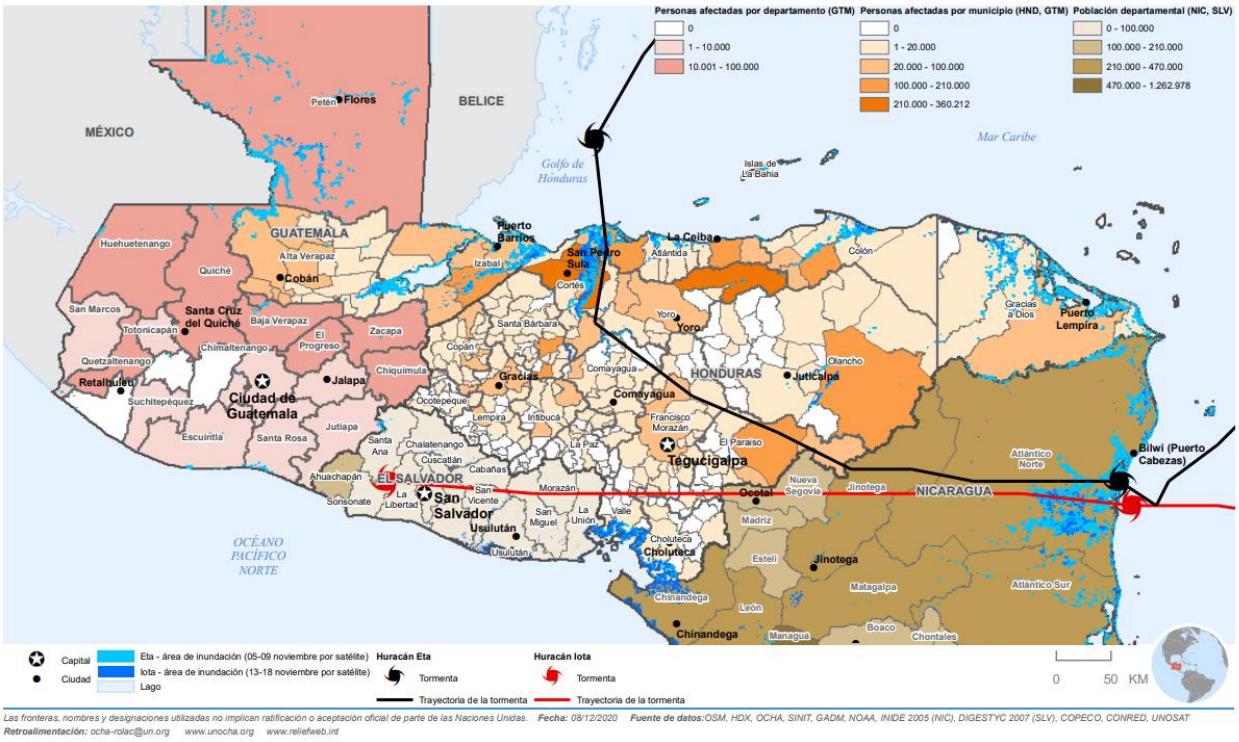

Figure 70 Map of Eta and Iota storm tracks and population affected across the region (Mapaction)[157].

7.3. Observed hazards

7.3.1. Type of hazards

High wind speeds, intense rainfall, storm surge, flooding

In this case study, the hazards being analyzed are two consecutive tropical storms, Hurricane Eta and Hurricane Iota. Eta reached Category 4 and Iota reached Category 5. Both were tropical storm strength when they reached Honduras with high windspeeds. There was also intense rainfall from both these storms, as well as storm surge along the coast creating additional impacts.

7.3.2. Form of compounding

Storms Eta and Iota were spatially compounding, consecutive events. The storms caused cascading hazards, including riverine flooding, landslides and mudslides.

Intersecting with these impacts, were previous factors which compounded the impacts from Eta and Iota. Compounding physical factors include heavy rainfall from a preceding cold front, saturated soils from earlier storms and reservoirs at almost full capacity.[158] Heavy rainfall, was a significant factor in creating the pre-

157 ma718_ocha_centralamerica_eta_iota_adm2_affd-300dpi.pdf

158 Álvarez, D. (2020). Primer frente frío dejaría temperaturas de 5 y 7 grados en algunas zonas de Honduras. HRN. https://www.radiohrn.hn/primer-frente-frio-dejaria-temperaturas-de-5-y-7-grados-en-algunas-zonas-de-honduras

conditions for flooding of several major rivers, and landslides. La Niña conditions amplified rainfall levels and together with river sedimentation, intensified flooding[159].

In addition, the two storms spatially and temporally compounded with the COVID-19 pandemic, a severe dengue epidemic in 2019 and ongoing violence by organized crime groups. These elements limited households' capacity to act due to economic limitations and exposure to violence. While the two storms were disconnected in time and space from the drought of 2014-2019, reverberating impacts were still present as populations which had migrated because of the drought were living in areas severely affected by the storms.

7.3.3. Driving dynamics

There are several driving dynamics which contributed to the compounding impacts of tropical cyclones Eta and Iota. Hurricane Eta began as a tropical wave off the western coast of Africa, traveling westward due to a high-pressure system over the northern Caribbean as well as a combination of other factors. Its rapid intensification was supported by favorable conditions over the Caribbean Sea with minimal vertical wind shear and high ocean heat content. The storm's slow movement—caused by a mid-level ridge over the Gulf of Mexico, eyewall replacement processes, and the upwelling of cooler shelf waters—led to intense and prolonged rainfall over Honduras[160].

Similarly, Hurricane Iota also formed from a west African tropical wave. Its western trajectory was influenced by a southeasterly cross-equatorial wind surge and the southern divergent section of a broad mid- to upper-level trough. Although initially hindered by high vertical wind shear, Iota underwent rapid intensification over the southwestern Caribbean thanks to low shear, warm sea-surface temperatures, and abundant atmospheric moisture. The storm later weakened as it moved through waters cooled by Eta's passage[161].

Meanwhile, prolonged drought in Honduras—driven by a mix of El Niño–Southern Oscillation (ENSO) dynamics and human-induced climate change—reflected a complex interaction of shifting rainfall patterns, rising temperatures, land use changes, and water management practices[162].

In the lead-up to Hurricane Eta, northern Honduras had already experienced intense rainfall, largely due to a preceding cold front[163]. Earlier in the season, an unusually high number of storms had passed through the region,

---

[159] CENAOS. (n.d.). *El Niño Oscilación del Sur (ENOS)*. http://cenaos.copeco.gob.hn/elnino.html ; key informant interviews

[160] Pasch, R. J., Reinhart, B. J., Berg, R., & Roberts, D. P. (2021). National Hurricane Center Tropical Cyclone Report Hurricane Eta. https://www.nhc.noaa.gov/data/tcr/AL292020_Eta.pdf

[161] Stewart, S. R. (2021). National Hurricane Center Tropical Cyclone Report Hurricane Iota (AL312020). https://www.nhc.noaa.gov/data/tcr/AL312020_Iota.pdf

[162] Pascale, S., Kapnick, S. B., Delworth, T. L., Hidalgo, H. G., & Cooke, W. F. (2021). Natural variability vs forced signal in the 2015–2019 Central American drought. *Climatic Change*, *168*(3–4), 1–21. https://doi.org/10.1007/S10584-021-03228-4/FIGURES/9

[163] Álvarez, D. (2020). Primer frente frío dejaría temperaturas de 5 y 7 grados en algunas zonas de Honduras. HRN. https://www.radiohrn.hn/primer-frente-frio-dejaria-temperaturas-de-5-y-7-grados-en-algunas-zonas-de-honduras

leaving the soil heavily saturated even before Eta arrived[164]. The situation was further exacerbated by reservoirs nearing full capacity—despite having been previously low due to a prolonged drought[165]. The excessive rainfall during the fall of 2020 was also linked to the La Niña phase of the El Niño–Southern Oscillation (ENSO), which is known to bring above-average precipitation and heightened storm activity to the region[166]. The intense rainfall during Eta and Iota also triggered widespread landslides across multiple regions[167].

Additional dynamics which affected the way in which Tropical Hurricanes Eta and Iota impacted Honduras include health conditions such as dengue and significant levels of violence. As for the dengue outbreak, extended periods of high heat and humidity, coupled with excessive rainfall, created ideal conditions for mosquito breeding, prolonging the transmission season[168]. This affected both the capacity of health structures and the economic security of many households. Finally, violence was an important factor with serious impacts on vulnerability, affecting how many households were affected by and could respond to the events. However, it did not have identifiable environmental drivers.

7.3.4. Intensity

Tropical Hurricane Eta: This storm had a Category 4 intensity, weakening to a tropical storm and then a tropical depression. The rainfall totals during 1-7 November were 31.63 inches in Tela and 29.25 inches in La Ceiba[169]. The return period was one-in-100/150 years[170].

Tropical Hurricane Iota: This storm was a Category 5 hurricane, and then weakened to a tropical depression[171]. The rainfall over 7 days was up to 11.85 inches[172]. The return period was one-in-100/150 years[173].

---

[164] Conde, M. (2021). Real time decisions during Hurricanes ETA and IOTA GEOGloWS-ECMWF, Honduras. *AmeriGEO Week 2021*. ; Thompson, A., & Montañez, A. (2020). *In 2020, Record-Breaking Hurricanes Arrived Early and Often*. Scientific American. https://www.scientificamerican.com/article/in-2020-record-breaking-hurricanes-arrived-early-and-often1/

[165] Conde, M. (2021). Real time decisions during Hurricanes ETA and IOTA GEOGloWS-ECMWF, Honduras. *AmeriGEO Week 2021*. ; Thompson, A., & Montañez, A. (2020). *In 2020, Record-Breaking Hurricanes Arrived Early and Often*. Scientific American. https://www.scientificamerican.com/article/in-2020-record-breaking-hurricanes-arrived-early-and-often1/

[166] CENAOS. (n.d.). El Niño Oscilación del Sur (ENOS). http://cenaos.copeco.gob.hn/elnino.html

[167] Pasch, R. J., Reinhart, B. J., Berg, R., & Roberts, D. P. (2021). National Hurricane Center Tropical Cyclone Report Hurricane Eta . https://www.nhc.noaa.gov/data/tcr/AL292020_Eta.pdf

[168] Zambrano, L. I., Rodriguez, E., Espinoza-Salvado, I. A., Fuentes-Barahona, I. C., Lyra de Oliveira, T., Luciano da Veiga, G., Cláudio da Silva, J., Valle-Reconco, J. A., & Rodríguez-Morales, A. J. (2019). Spatial distribution of dengue in Honduras during 2016–2019 using a geographic information systems (GIS)–Dengue epidemic implications for public health and travel medicine. Travel Medicine and Infectious Disease, 32, 101517. https://doi.org/10.1016/J.TMAID.2019.101517 ; Martheswaran, T. K., Hamdi, H., Al-Barty, A., Zaid, A. A., & Das, B. (2022). Prediction of dengue fever outbreaks using climate variability and Markov chain Monte Carlo techniques in a stochastic susceptible-infected-removed model. Scientific Reports 2022 12:1, 12(1), 1–17. https://doi.org/10.1038/s41598-022-09489-y

[169] Pasch, R. J., Reinhart, B. J., Berg, R., & Roberts, D. P. (2021). National Hurricane Center Tropical Cyclone Report Hurricane Eta . https://www.nhc.noaa.gov/data/tcr/AL292020_Eta.pdf

[170] Pasch, R. J., Reinhart, B. J., Berg, R., & Roberts, D. P. (2021). National Hurricane Center Tropical Cyclone Report Hurricane Eta . https://www.nhc.noaa.gov/data/tcr/AL292020_Eta.pdf

[171] Stewart, S. R. (2021). *National Hurricane Center Tropical Cyclone Report Hurricane Iota*. https://www.nhc.noaa.gov/data/tcr/AL312020_Iota.pdf

[172] Pasch, R. J., Reinhart, B. J., Berg, R., & Roberts, D. P. (2021). National Hurricane Center Tropical Cyclone Report Hurricane Eta . https://www.nhc.noaa.gov/data/tcr/AL292020_Eta.pdf

[173] Pasch, R. J., Reinhart, B. J., Berg, R., & Roberts, D. P. (2021). National Hurricane Center Tropical Cyclone Report Hurricane Eta . https://www.nhc.noaa.gov/data/tcr/AL292020_Eta.pdf

Floods: The maximum flood extent for Tropical Hurricane Eta was 21827.4 hectares and 18351.8 hectares for Iota. The water depth in flood areas ranged between 0.15 and 4 meters, with an average of 1.8 meters[174]

Landslides: In total there were 174 instances of landslides reported as a result of conditions created by Eta and Iota[175].

Drought: Over the 5-year anomaly May-September (MJJAS) Summer Rainfall Index (SRI) precipitation was found to be 37 mm/month lower across the entire Dry Corridor of Central America, as compared to 1921-2019[176].

Dengue outbreak: Epidemic level - incidence rate of 312.32 cases/100,000 population[177].

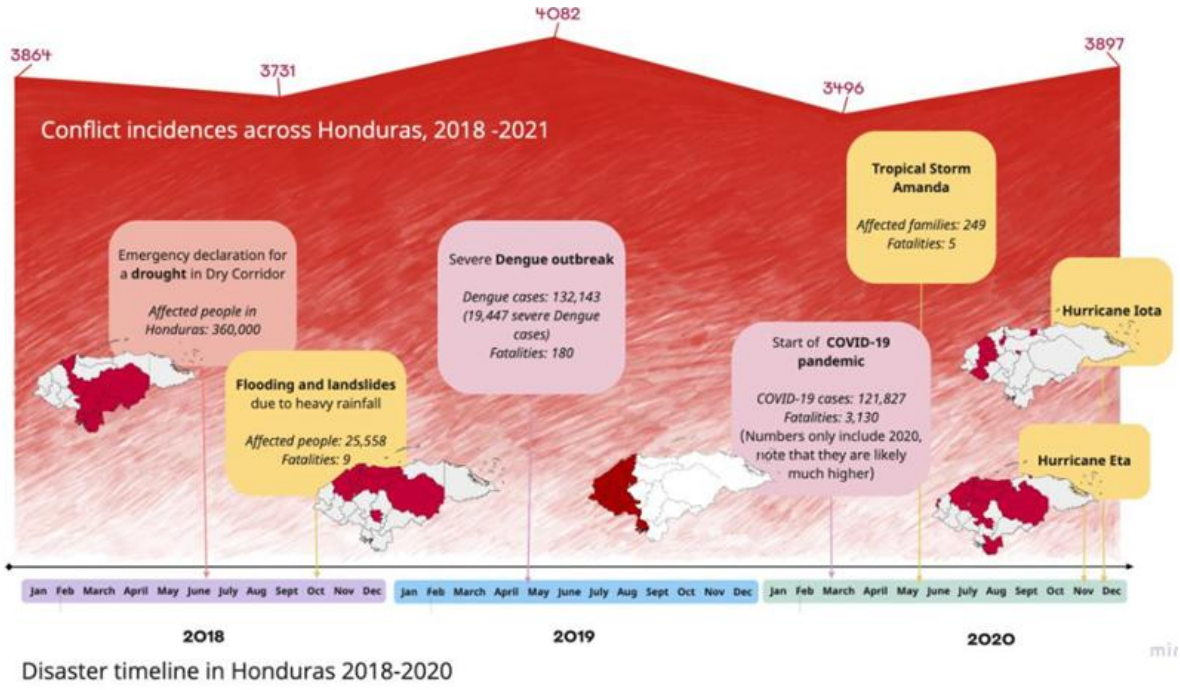

Disaster timeline in Honduras 2018 - 2020.

Figure 71 Disaster timeline for Honduras 2018-2020 (based on unpublished World Bank study by Red Cross Red Crescent Climate Centre).

7.4. Observed impacts

Table 14 Key impact data and statistics.

[174] European Commission, Joint Research Centre (JRC) (2020): ETA and IOTA hurricanes effects in Honduras (2020-12-03). European Commission, Joint Research Centre (JRC) http://data.europa.eu/89h/7eaa3330-7cb7-41fc-a765-684b3e2f9093

[175] CEPAL. (2021). Evaluación de los efectos e impactos de la tormenta tropical Eta y el huracán Iota en Honduras. cepal.org/es/publicaciones/46853-evaluacion-efectos-impactos-causados-la-tormenta-tropical-eta-huracan-iota

[176] Pascale, S., Kapnick, S. B., Delworth, T. L., Hidalgo, H. G., & Cooke, W. F. (2021). Natural variability vs forced signal in the 2015–2019 Central American drought. Climatic Change, 168(3–4), 1–21. https://doi.org/10.1007/S10584-021-03228-4/FIGURES/9

[177] Zambrano, L. I., Rodriguez, E., Espinoza-Salvado, I. A., Fuentes-Barahona, I. C., Lyra de Oliveira, T., Luciano da Veiga, G., Cláudio da Silva, J., Valle-Reconco, J. A., & Rodríguez-Morales, A. J. (2019). Spatial distribution of dengue in Honduras during 2016–2019 using a geographic information systems (GIS)–Dengue epidemic implications for public health and travel medicine. Travel Medicine and Infectious Disease, 32, 101517. https://doi.org/10.1016/J.TMAID.2019.101517

Impact	Magnitude/Scale	Source
Homes affected	90,000	CEPAL, 2021
People evacuated	437,000	CEPAL, 2021
Roads damaged	927	CEPAL, 2021
Bridges damaged	72 damaged, 62 destroyed	CEPAL, 2021
Health facilities	400 damaged, 120 inoperative	CEPAL, 2021
Cold chain equipment losses	Not quantified	CEPAL, 2021
Schools damaged	3% of all buildings	CEPAL, 2021
Sanitation infrastructure destroyed	Not quantified	IFRC, 202; CEPAL, 2021
Agricultural losses	Up to 80% (coffee, banana, plantain, sugarcane)	CEPAL, 2021
Fatalities	95	CEPAL, 2021
Missing persons	10 (mainly fishermen)	CEPAL, 2021
Isolation of communities	Weeks of isolation	IFRC, 2020
Healthcare services disrupted	Not quantified	IFRC, 2020; CEPAL, 2021
Education disrupted	Schools used as shelters	IFRC, 2020; CEPAL, 2021
Supply chain disruptions	Not quantified	IFRC, 2020
Emergency response and repair costs	Not quantified	CEPAL, 2021
Public health risks	Not quantified	IFRC, 2020
Mental health consequences	Not quantified	IFRC, 2020
Learning loss	Not quantified	IFRC, 2020
Increase in COVID-19 cases	The spread of COVID-19 increased with San Pedro Sula as one of the highest reported cases, especially because of the overcrowded and undersupplied shelters and lack of personal protection equipment	IDB, 2021; UNICEF, 2020
Economic losses	1.9 billion United States dollars, with a 0.8 per cent reduction in economic growth in Honduras during 2020	World Bank, 2021a

Observed flood extent and impact – Figure 72 below shows an estimate of the maximum flood extent and population exposed based on Sentinel satellite data. Sentinel satellite data analysis enables mapping of water body extent and flood extent can be derived by differentiating pre-flood water body extent with water body extent during flooding. Limitations include the irregular and relatively infrequent timing of satellite overpass which means that maximum flood extent can occur between satellite image acquisition dates. Image processing can also create spurious water body detection resulting from changing shadows in mountain regions and other sources of noise. Sentinel flood extent analysis was obtained from the Copernicus EMS Rapid Mapping service [178] which provides flood mapping data for significant flood events in support of emergency response and recovery.

178 https://mapping.emergency.copernicus.eu/activations/EMSR481/

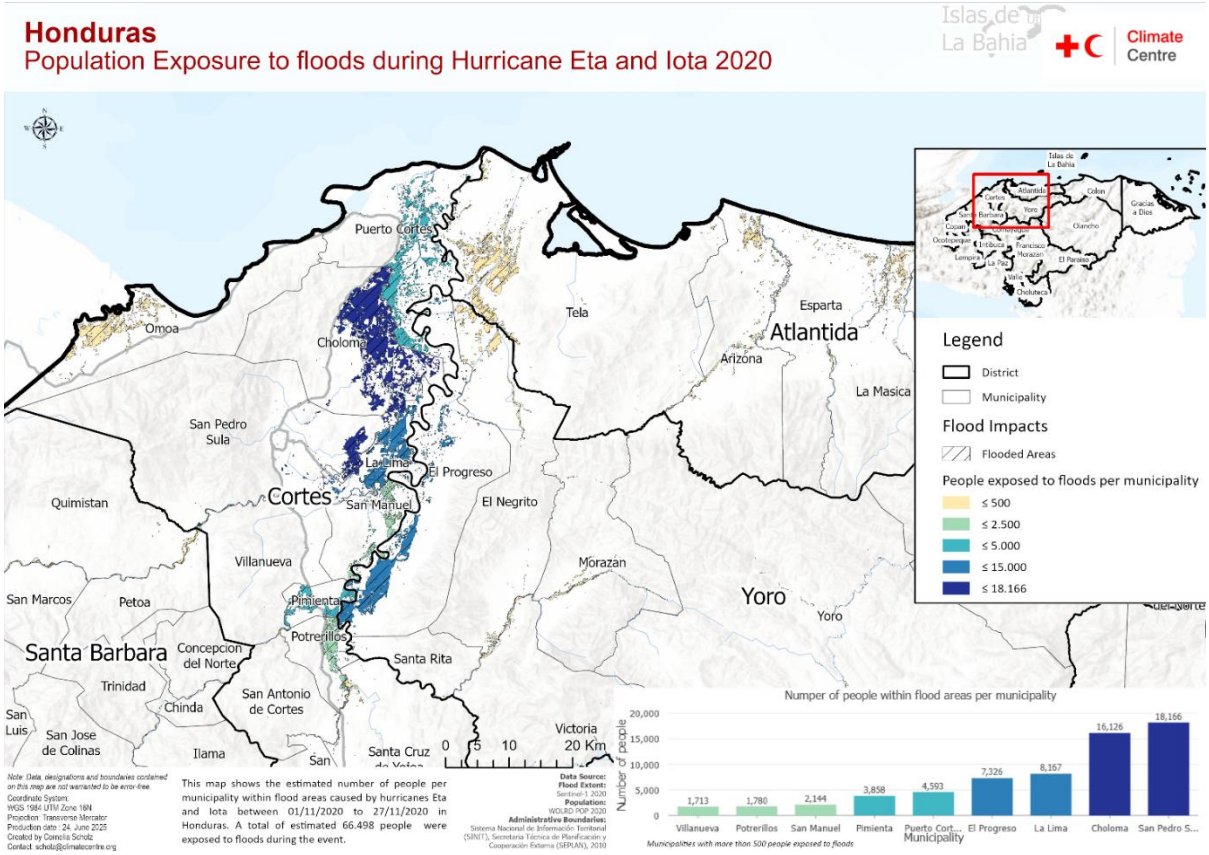

Figure 72 Population exposure to floods during Hurricane Eta and Iota 2020 – Sentinel 1 flood analysis 2020; Map – Climate Centre 2025.

Figure 73 shows the same flood extent but assesses the building exposure to provide an indication of the number of buildings potentially flooded which is strongly associated with displacement of populations to temporary accommodation.

Estimates of population and buildings exposed to flooding through the Sentinel based mapping are much lower than reported figures. Total population exposed, based on Sentinel flood mapping is 85,704, and buildings exposed is 2,543, whereas the reported number of people evacuated was 437,000 and homes affected was 90,000 (see Table 14 above). It is plausible that the Sentinel based flood mapping is an underestimate due to some of the limitations described above, in particular the satellite image acquisition timing relative to the timing of the peak flood extent. However, it is also very likely that many people were evacuated even if their homes were not flooded. These two factors combined could explain some of the discrepancy between reported impacts and the mapping analysis.

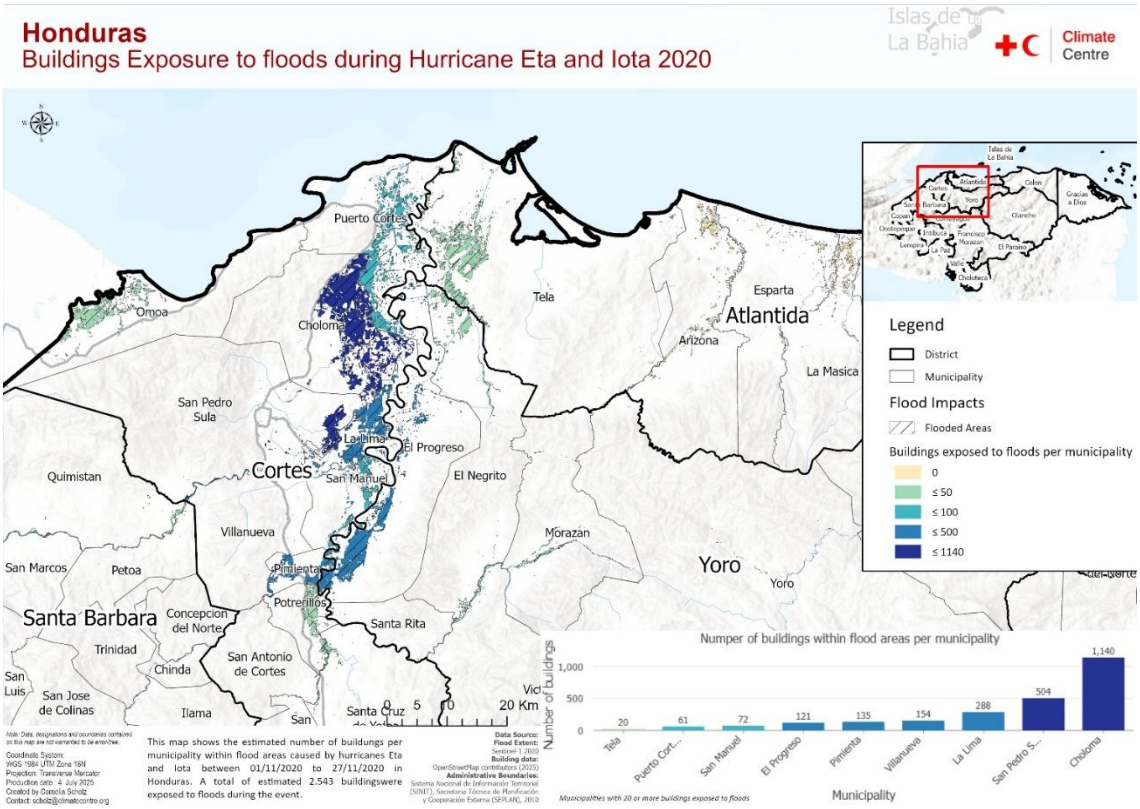

Figure 73 Population exposure to floods during Hurricane Eta and Iota 2020 – Sentinel 1 flood analysis 2020; Map – Climate Centre 2025.

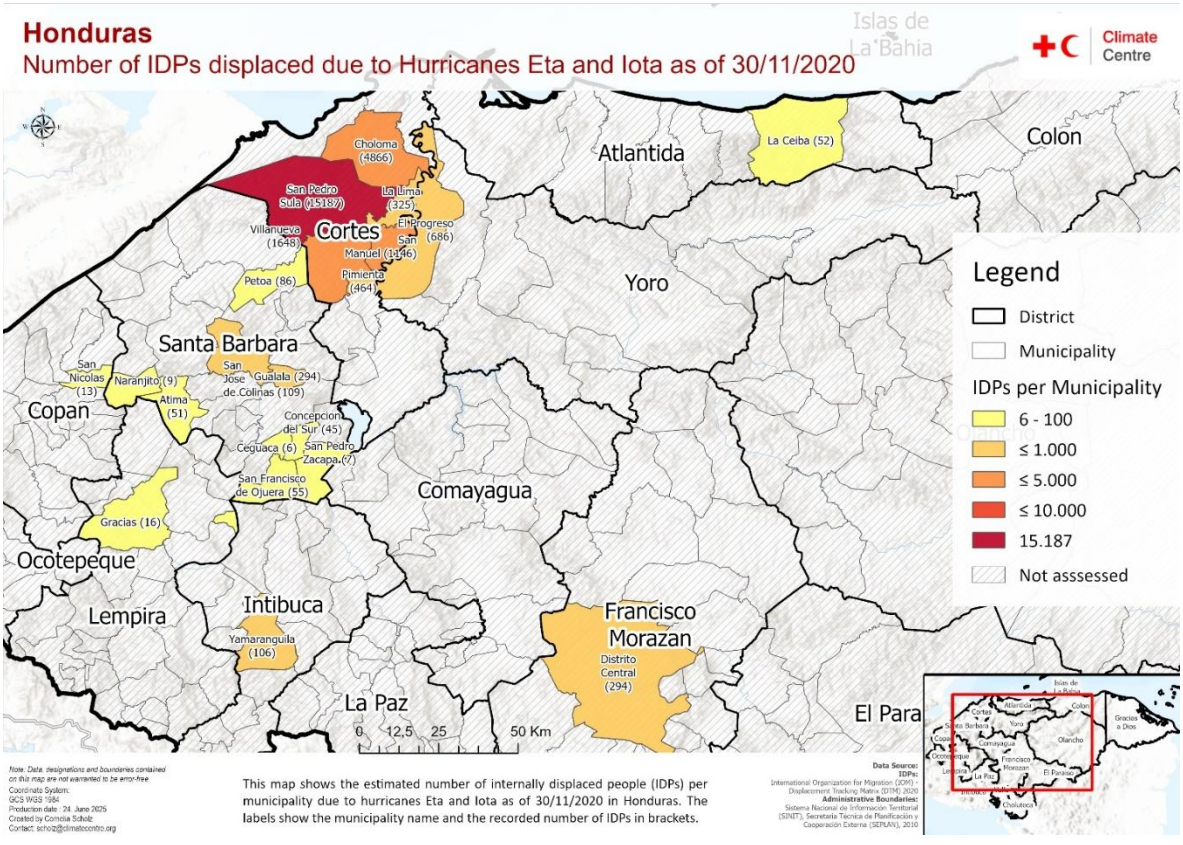

Figure 74 Number of IDPs displaced due to Hurricane Eta and Iota as of 30/11/2020 – IDP data: IOM 2020; Map - Climate Centre 2025.

7.4.1. Qualitative impacts and responses

Analyses of the combined effects of Hurricanes Eta and Iota indicate widespread human suffering and damage to infrastructure. This is due in large part to the flooding and landslides which took place as a result of Eta and Iota. Around 95 people lost their lives, with an additional 10 reported missing, mostly fishermen. The areas most significantly affected were the departments of Cortés, Santa Bárbara, and Lempira[179]. The main impacts of Eta and Iota included physical damage to housing and infrastructure, direct and indirect impacts to health services, agriculture loss and food insecurity, as well as increases in violence.

Housing and Essential Infrastructure

Physical damage to housing and essential infrastructure including roads, bridges, schools and sanitation systems, was extensive. Approximately 90,000 homes were affected, and more than 437,000 individuals had to be evacuated. The Atlantic coast and the region surrounding San Pedro Sula, especially areas along the Chamelecón and Ulúa rivers, sustained particularly heavy damage[180]. In the wake of flooding and landslides, 927 roads were destroyed and 72 bridges were damaged, 62 of which were completely destroyed[181]. As a result, nearly 369,000 people were cut off from surrounding areas for weeks, with the Colón department being the most affected[182].

Sanitation systems, particularly along the Chamelecón and Ulúa rivers, were nearly wiped out, and widespread damage to community wells further worsened living conditions[183]. In addition, it was reported that 3% of schools were damaged and another 3% repurposed as emergency shelters. While only a few schools were permanently destroyed, the impacts were most pronounced in Cortés, Atlántida, and Francisco Morazán[184]. Beyond physical damage, this would also result in more long-term impacts on children's education due to interruptions.

Health Services

The health system faced significant disruptions, while simultaneously needing to address secondary health consequences. Around 400 healthcare facilities sustained damage, with 120 rendered non-operational. Damage to cold chain equipment further compromised the storage of critical medicines and vaccines. The Cortés department was particularly affected, with 70% of its health facilities reporting damage[185].

---

[179] CEPAL. (2021). Evaluación de los efectos e impactos de la tormenta tropical Eta y el huracán Iota en Honduras. https://www.cepal.org/es/publicaciones/46853-evaluacion-efectos-impactos-causados-la-tormenta-tropical-eta-huracan-iota

[180] CEPAL. (2021). Evaluación de los efectos e impactos de la tormenta tropical Eta y el huracán Iota en Honduras. https://www.cepal.org/es/publicaciones/46853-evaluacion-efectos-impactos-causados-la-tormenta-tropical-eta-huracan-iota

[181] CEPAL. (2021). Evaluación de los efectos e impactos de la tormenta tropical Eta y el huracán Iota en Honduras. https://www.cepal.org/es/publicaciones/46853-evaluacion-efectos-impactos-causados-la-tormenta-tropical-eta-huracan-iota

[182] IFRC. (2020a). Central America: Dengue Outbreak Emergency Plan of Action, 6-months Operations update (MDR42005). https://reliefweb.int/report/honduras/central-america-dengue-outbreak-emergency-plan-action-6-months-operations-update

[183] IFRC. (2021). Communities affected by Hurricanes Eta and Iota are threatened by food insecurity, displacement and the climate crisis. https://www.ifrc.org/press-release/communities-affected-hurricanes-eta-and-iota-are-threatened-food-insecurity

[184] CEPAL. (2021). Evaluación de los efectos e impactos de la tormenta tropical Eta y el huracán Iota en Honduras. https://www.cepal.org/es/publicaciones/46853-evaluacion-efectos-impactos-causados-la-tormenta-tropical-eta-huracan-iota

[185] CEPAL. (2021). Evaluación de los efectos e impactos de la tormenta tropical Eta y el huracán Iota en Honduras. https://www.cepal.org/es/publicaciones/46853-evaluacion-efectos-impactos-causados-la-tormenta-tropical-eta-huracan-iota ; Project HOPE. (2020). Hurricanes Eta & Iota. https://www.projecthope.org/hurricanes-eta-iota-contaminated-water-honduras/12/2020/

Tropical Hurricanes Eta and Iota also led to far-reaching indirect health consequences. Around 2 million people faced restricted access to healthcare due to fewer health services because of damage and increased demand post disaster. This took place in a health system still recovering from the dengue outbreak and the current COVID19 pandemic. Overcrowded, under-resourced shelters, particularly in San Pedro Sula, contributed to the spread of COVID-19[186]. Conditions in these shelters also led to increased risks of sexual violence, especially for women and girls, with a documented rise in gender-based violence[187]. In addition, the breakdown of water, sanitation, and hygiene (WASH) infrastructure, combined with stagnant water and unsanitary shelter environments, fueled outbreaks of waterborne illnesses and dengue fever, primarily in the Sula Valley[188].

Agriculture and Food Insecurity

Losses in agriculture were substantial—up to 80% in certain areas—affecting key crops such as coffee, banana, plantain, and sugarcane. The damage spanned a wide geographic area, from the Sula Valley and northern Atlantic departments to southern, western, and northeastern regions like Gracias a Dios[189].

Food insecurity significantly worsened after the 2020 disasters due to physical damage to agricultural infrastructure, as well as loss of livelihoods from direct and indirect consequences of Eta and Iota. By August 2022, an estimated 2.6 million people were projected to be experiencing high levels of acute food insecurity[190]. Damage to the agricultural sector disrupted livelihoods across the country, with coastal Indigenous communities—especially those reliant on fishing—facing pronounced challenges. However, data from sparsely populated Indigenous areas remains limited[191]. Displacement and loss of livelihoods and employment simultaneously contributed to food insecurity by diminishing households' purchasing power.

Violence

The post-disaster period saw an uptick in localized violence, particularly gang-related[192]. Monthly homicide statistics show a clear increase in killings after Eta and Iota compared to earlier in 2020, with homicide rates

---

[186] CEPAL. (2021). Evaluación de los efectos e impactos de la tormenta tropical Eta y el huracán Iota en Honduras. https://www.cepal.org/es/publicaciones/46853-evaluacion-efectos-impactos-causados-la-tormenta-tropical-eta-huracan-iota ; UNICEF. (2020). Over 1.2 million children affected by ETA across Central America. https://www.unicef.org/press-releases/over-12-million-children-affected-eta-across-central-america-unicef

[187] CARE, & UN Women. (2020). Latin America and the Carribaen Rapid Gender Analysis for COVID-19. https://reliefweb.int/report/brazil/latin-america-and-carribean-rapid-gender-analysis-covid-19

[188] CEPAL. (2021). Evaluación de los efectos e impactos de la tormenta tropical Eta y el huracán Iota en Honduras. https://www.cepal.org/es/publicaciones/46853-evaluacion-efectos-impactos-causados-la-tormenta-tropical-eta-huracan-iota ; IFRC. (2021). Communities affected by Hurricanes Eta and Iota are threatened by food insecurity, displacement and the climate crisis. https://www.ifrc.org/press-release/communities-affected-hurricanes-eta-and-iota-are-threatened-food-insecurity

[189] CEPAL. (2021). Evaluación de los efectos e impactos de la tormenta tropical Eta y el huracán Iota en Honduras. https://www.cepal.org/es/publicaciones/46853-evaluacion-efectos-impactos-causados-la-tormenta-tropical-eta-huracan-iota ; IFRC. (2020a). Central America: Dengue Outbreak Emergency Plan of Action, 6-months Operations update (MDR42005). https://reliefweb.int/report/honduras/central-america-dengue-outbreak-emergency-plan-action-6-months-operations-update

[190] IPC. (2022). Honduras: Integrated Food Security Phase Classification Snapshot, December 2021 - August 2022. https://reliefweb.int/report/honduras/honduras-integrated-food-security-phase-classification-snapshot-december-2021-august

[191] CEPAL. (2021). Evaluación de los efectos e impactos de la tormenta tropical Eta y el huracán Iota en Honduras. https://www.cepal.org/es/publicaciones/46853-evaluacion-efectos-impactos-causados-la-tormenta-tropical-eta-huracan-iota ; FEWS NET. (2021). El Salvador, Honduras, and Nicaragua - Key Message Update: Fri, 2021-01-29. https://fews.net/central-america-and-caribbean/el-salvador-honduras-and-nicaragua/key-message-update/january-2021 ; IFRC. (2020b). Honduras: Hurricane Eta and Iota - Emergency appeal n° MDR43007 Operation Update no. 2 - Honduras. https://reliefweb.int/report/honduras/honduras-hurricane-eta-and-iota-emergency-appeal-n-mdr43007-operation-update-no-2

[192] Armed Conflict Location & Event Data Project (ACLED). (2020). Central America and COVID-19: The Pandemic's Impact on Gang Violence. https://acleddata.com/2020/05/29/central-america-and-covid-19-the-pandemics-impact-on-gang-violence/

continuing to rise into 2021[193]. While the COVID-19 pandemic and other existing crises played a role, anecdotal evidence indicates that the impact of Eta and Iota significantly contributed to this deterioration[194].

The compounding of hazards over time and space only partially explains the extensive losses from Eta and Iota. Root causes were a significant contributing factor to the way in which impacts from Eta and Iota were experienced, such as persistent high poverty rates, urban planning deficiencies, inadequate disaster risk management systems, and violence.

Responses

The response to Hurricanes Eta and Iota in Honduras was largely reactive and marked by significant challenges across all levels of the disaster risk management system.

Life-Saving Responses

In the immediate aftermath of Eta, the response centered on urgent life-saving measures. Evacuations were carried out in flood- and landslide-affected areas, and humanitarian agencies provided food assistance, shelter, and WASH support to affected communities[195]. However, these efforts were hampered by widespread infrastructure damage including roads and bridges, leaving over 368,000 people isolated for weeks, particularly in Colón department.

Early Warning Systems

At the operational level, flood and landslide forecasting systems were limited in capacity. Monitoring was based primarily on manual observation of river levels, without integration of rainfall data. Early warning efforts were mostly localized and disconnected from national systems, resulting in fragmented communication between communities and central authorities. Organizational issues—including staffing shortages, inadequate funding, and poor coordination across national, regional, and municipal levels—further weakened early action efforts. Further, by the time forecasts for Iota became available, the response to Eta was still ongoing. Limited preparedness and strained response capacity meant that there was little time or ability to transition from relief to risk reduction.

Early warning messages were limited in both scope and clarity. Communities in high-risk areas often did not understand the implications of the forecasts or the likelihood of secondary impacts such as landslides and flooding. Low levels of risk awareness—especially among younger populations who had not experienced major hurricanes before—further reduced the effectiveness of preventive messaging. In northern Honduras, a lack of clear guidance contributed to underestimation of the risk and uncertainty about how to act. Some improvements were noted in the lead-up to Iota. Early warning messages included more specific guidance on evacuation routes and protective measures. A second wave of evacuations was carried out, and efforts were made to mitigate the risk of COVID-19 transmission in shelters through hygiene measures, distancing, and mask use. However, according to interviews, these health measures were generally considered inadequate.

[193] CEPAL. (2021). Evaluación de los efectos e impactos de la tormenta tropical Eta y el huracán Iota en Honduras. https://www.cepal.org/es/publicaciones/46853-evaluacion-efectos-impactos-causados-la-tormenta-tropical-eta-huracan-iota

[194] Olson, J. (2020). Honduran storm survivors form US-bound migrant caravan. The New Humanitarian. https://www.thenewhumanitarian.org/news-feature/2020/12/11/honduras-hurricane-survivors-migrant-caravan

[195] IFRC. (2021). Communities affected by Hurricanes Eta and Iota are threatened by food insecurity, displacement and the climate crisis. https://www.ifrc.org/press-release/communities-affected-hurricanes-eta-and-iota-are-threatened-food-insecurity

Critical Gaps

Throughout both events, the absence of a multi-hazard early warning system was a critical gap. Hazard monitoring was not integrated with information on vulnerabilities such as food insecurity, health risks, housing, violence, and migration. This hindered the ability of responders to anticipate the full scope of impacts. Certain high-risk areas were known anecdotally, but the lack of a formal risk monitoring framework limited coordination between government agencies, communities, and humanitarian actors. Information gaps remained particularly acute for rural, Indigenous, and migrant populations.

Table 15 Details of response measures and associated benefits and tradeoffs as a result of Eta and Iota.

Measure	Hazard(s) Targeted	Structural/ Non-Structural	Timing	Synergies / Trade-offs
Research and information sharing on hurricane risk (e.g., SINAGER/COPECO/UNAH collaboration, INFORM index)	Hurricanes / Tropical storms	Non-structural	Before	Strengthens understanding of flood and landslide risks; enhances risk databases.
Sharing early warning information and advisories	Hurricanes / Tropical storms / Floods	Non-structural	Before Eta and Iota (better before Iota)	Improvements noted between Eta and Iota. However, warnings were single-hazard focused and didn't address local vulnerabilities or compounding risks.
Establishment and training of emergency committees (CODEM, CODECE, CODEL)	General	Non-structural	Before Eta	Strengthened local response capacities, but effectiveness was undermined by violence, corruption, and COVID-19 disruptions.
Development of Emergency and Risk Management Plans (World Bank-funded project)	Flooding, landslide, wildfires	Non-structural	Before Eta	Limited integration of biological and multi-risk scenarios; implementation challenges due to governance issues and lack of adaptation to dynamic population movements and vulnerabilities.
Designation of shelter locations	Floods, tropical storms	Non-structural	Before, during, and after Eta and Iota	Implemented inconsistently; more effective in areas with lower violence exposure.
Building and maintenance of flood barriers, bridges, and stormwater canals	Floods	Structural	Before and after Eta and Iota	Maintenance was poor, especially in vulnerable areas, creating a false sense of security.
Introduction of Ley del Sistema Nacional de Gestión de Riesgos (2009)	General	Non-structural	Before Eta and Iota	— *(no synergy or trade-off described in the original)*
COVID-19 spread prevention measures	COVID-19	Non-structural	Before Eta and Iota	Focus on pandemic response reduced preparedness for hurricane season. Led to distrust in authorities, decreased

(curfews, mobility restrictions, closures)				willingness to act on early warnings, and disrupted DRM efforts. Holiday mobility just before Eta further undermined preparedness—many people were traveling, especially to the north (perceived as low-risk), and missed early storm warnings.

7.5. Modeling framework

7.5.1. Hazard modeling

For the hazard modelling, we use the compound flood modelling framework presented in Figure 75. For details of this framework, we refer the reader to COMPASS Deliverable D1.1[196]. In summary, to simulate compound coastal flooding, we combine various hydrological and hydrodynamic models. For river discharge and effective precipitation, we make use of the hydrological model wflow. Initial analysis demonstrated that coastal flooding was minimal and so the final modeling did not include the SFINCS component of the model.

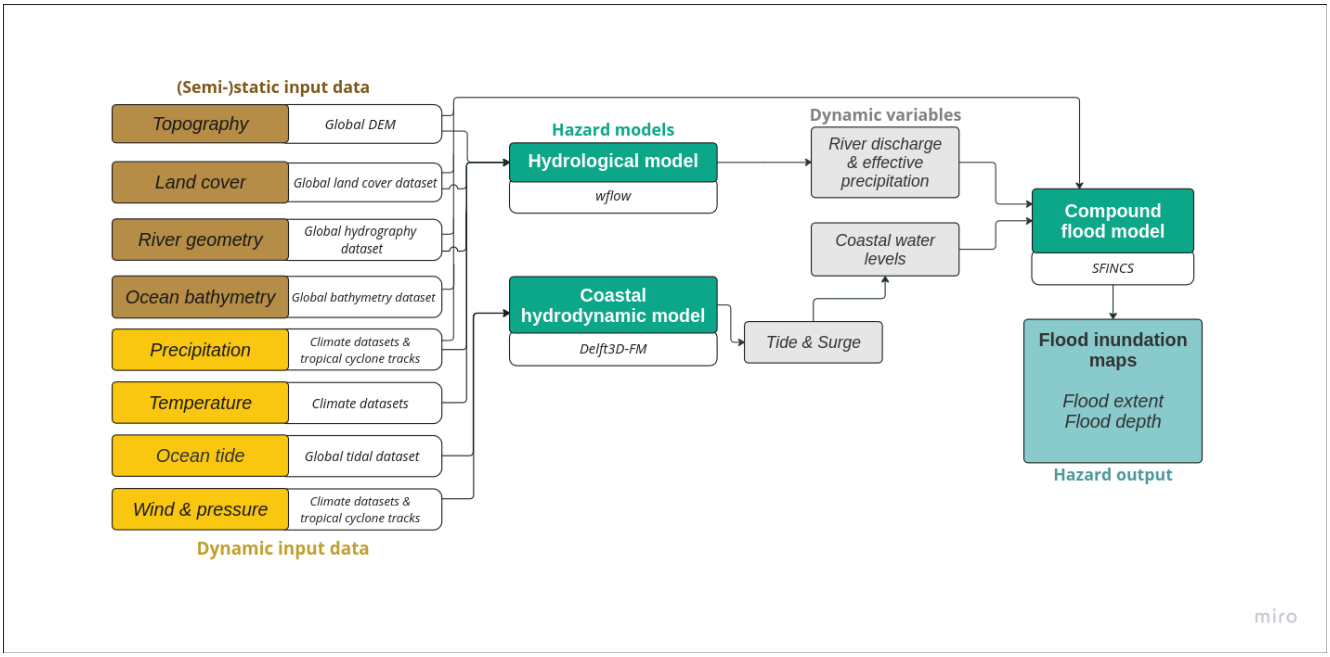

Figure 75 Flowchart of the compound flooding modelling framework for Eta and Iota flood modeling

7.5.2. Impact modeling

Flood Exposure Analysis – Population Affected by Hurricanes Eta and Iota To assess population exposure to flooding caused by Hurricanes Eta and Iota, a geospatial analysis was conducted using the WorldPop 2020 Population Count dataset. The flood extent model was first reclassified into a binary raster format, where values of 1 represented flooded areas and 0 denoted non-flooded areas. This binary flood raster was then converted into vector polygons representing the flooded zones. These polygons were intersected with an administrative level 2 (municipality) shapefile to spatially aggregate flood extents by municipality boundaries of the 30 assessed municipalities. Subsequently, the WorldPop population raster and all vector layers were reprojected to a common coordinate reference system: WGS 1984 UTM Zone 16N. Using the Zonal Statistics tool, the total

[196] Aleksandrova, N., Vertegaal, D., Couasnon, A., Perks, R., Cotterill, D. Vogel, M., Jack, C., Paprotny, D., Terefenko, P., Śledziowski, J. (2024): Guidelines for compound extremes modelling in current and future climates. Horizon Europe project COMPASS. Deliverable D1.1.

population within the flooded areas was calculated for each municipality by overlaying the flood extent polygons with the population raster. The resulting dataset quantified the number of people exposed to flooding per municipality. This was visualized through a choropleth map symbolizing exposure levels, and a bar chart highlighting municipalities with more than 5,000 exposed individuals was produced.

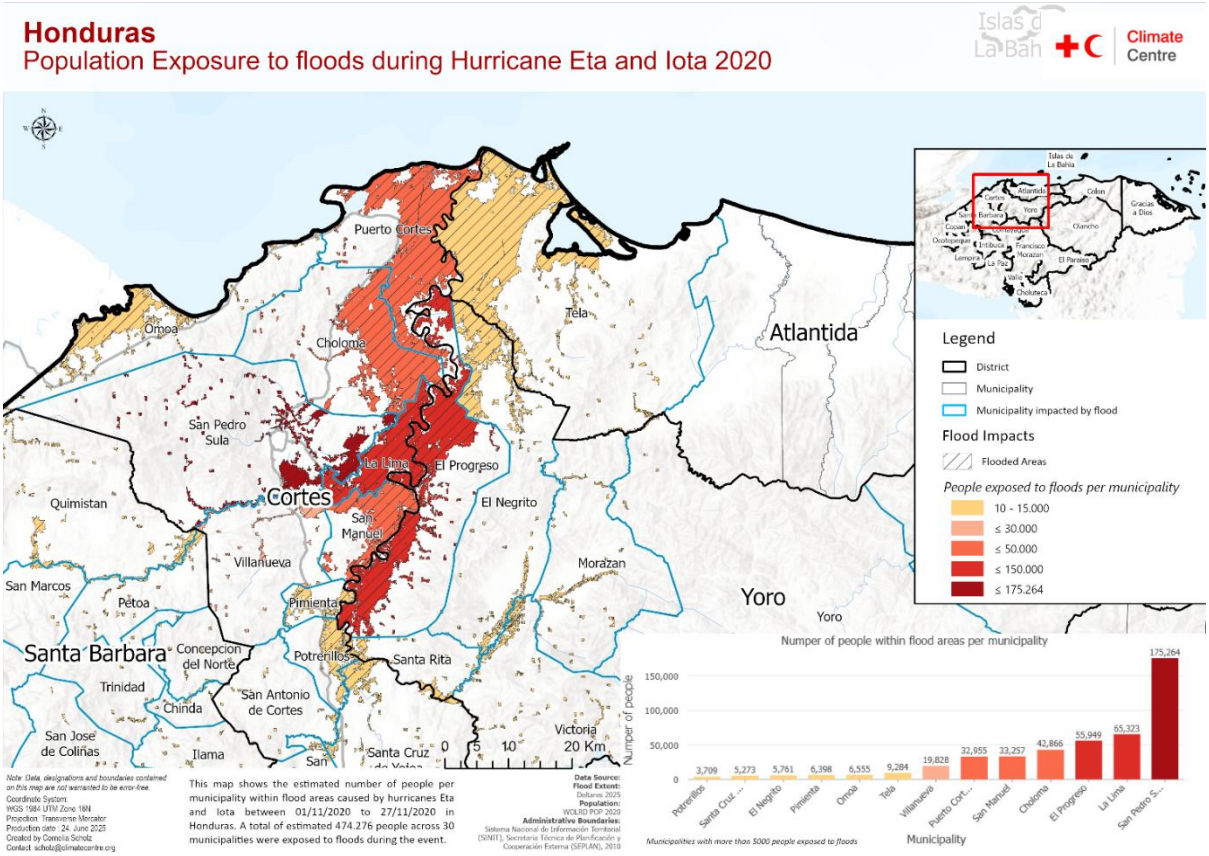

Figure 76 Population exposure to floods during Hurricane Eta and Iota 2020 – Deltares flood model 2025; Map – Climate Centre 2025.

Flood Exposure Analysis – Buildings Affected by Hurricanes Eta and Iota To assess building exposure to flooding caused by Hurricanes Eta and Iota, a geospatial analysis was carried out using OpenStreetMap (OSM) building footprint data. The flood extent model was first reclassified into a binary raster format, where values of 1 represented flooded areas and 0 denoted non-flooded areas. This binary raster was then converted into vector polygons representing flooded zones. The OSM building footprints were exported, reprojected to WGS 1984 UTM Zone 16N, and spatially intersected with the flood extent polygons. The analysis was aggregated at the administrative level 2 (municipality) using a boundary shapefile to calculate the number of buildings falling within flooded areas per municipality (if a building polygon intersected two municipality polygons, it was assigned to the municipality with greatest overlap). The resulting dataset quantified the estimated number of exposed buildings to floodwaters across affected municipalities. These figures were visualized using a choropleth map, illustrating relative exposure levels. However, it is important to note that OSM building footprint coverage is not complete across all regions, and therefore the results represent a minimum estimate of exposed structures. The absolute number of exposed buildings is likely underrepresented, especially in areas with limited mapping coverage.

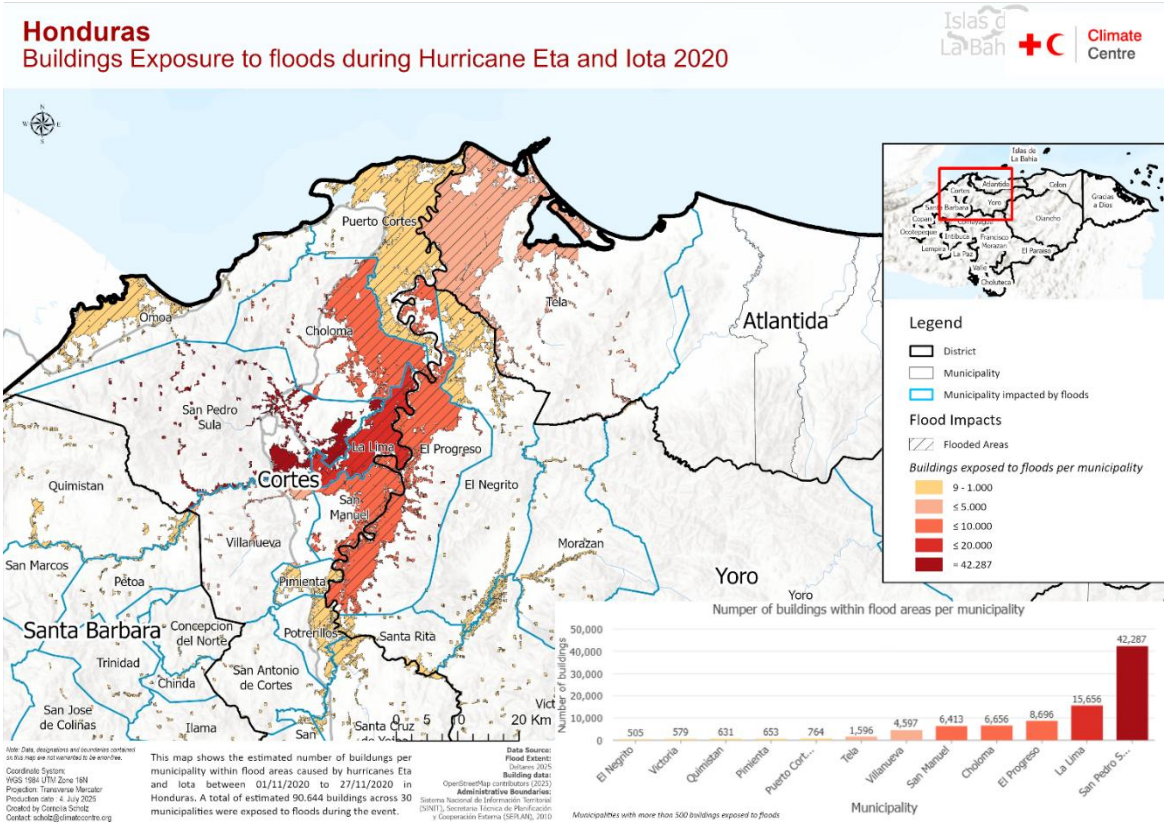

Figure 77 Building exposure to floods during Hurricane Eta and Iota 2020 – Deltares flood model 2025; Map – Climate Centre 2025.

Choropleth Map of Internally Displaced Persons (IDPs) by Municipality – Hurricanes Eta and Iota[SEP]To visualize internal displacement caused by Hurricanes Eta and Iota, data from the IOM Displacement Tracking Matrix (DTM), specifically the response dataset dated 30 November 2020, was used. The tabular data containing IDP figures per municipality (admin level 2) was joined to a corresponding administrative boundary shapefile. Following the join, a choropleth map was produced to display the number of assessed internally 197 displaced persons (IDPs) per municipality. The visualization highlights the spatial distribution of displacement and supports analysis of the most affected areas across the country.

Vulnerability modeling

Aligning with COMPASS Deliverable 3.2[198] a qualitative vulnerability assessment approach using stakeholder engagement, document analysis, and causal mapping, is used. This assessment highlights key impact pathways and the contributing vulnerability factors and allows for a rich and comprehensive analysis of vulnerability as well as how hazards and risks cascade and compound within a particular context.

The resultant causal map is presented in Figure 78 below.

197 Singh, R., Vogel, M. M., Vahlberg, M., Periera Marghidan, C., Santos Vega, M., Izquierdo, K., Gale, S., Jack, C. (2025): Guidance note on qualitatively assessing vulnerability factors, including non- climate compounding factors, in attribution studies. Horizon Europe project COMPASS. Deliverable D3.2.

198 Roop et. al. (2025), Qualitative vulnerability assessment for attribution studies, COMPASS Deliverable 3.2

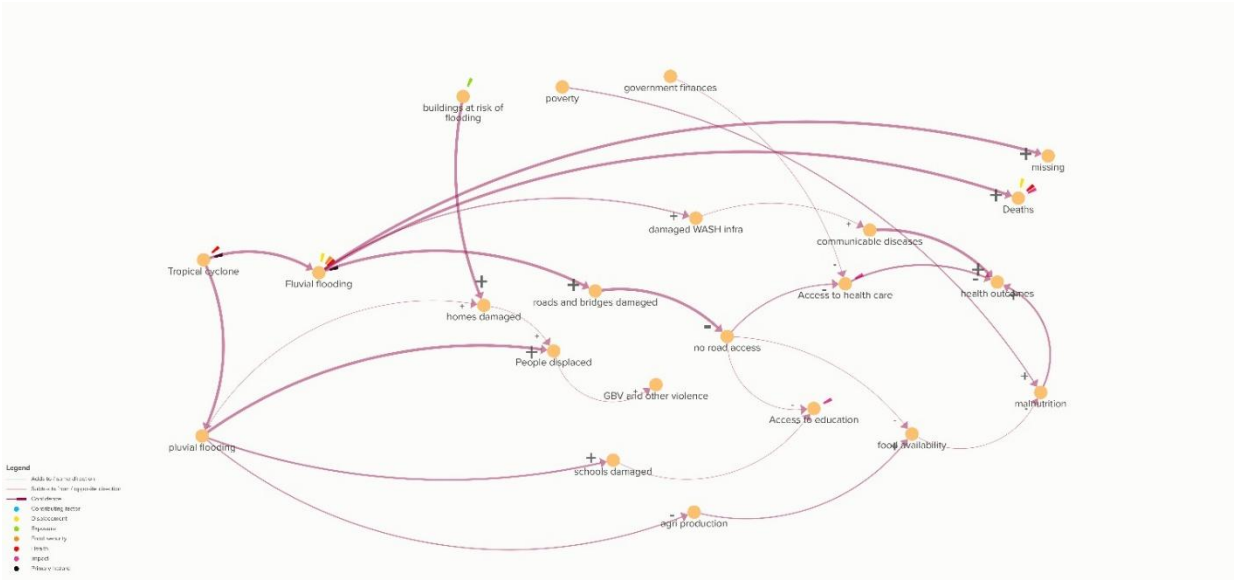

Figure 78 Causal map of impact pathways and vulnerability factors based on retrospective analysis of Eta and Iota impacts.

7.6. Attribution modeling workflow

Figure 79 summarizes the main attribution modeling framework. We use a storyline approach and simulate compound flooding for TC Idai and Kenneth under factual and counterfactual scenarios. The factual simulation is based on present-day climate, whereas for the counterfactual scenarios, the long-term climate trend is removed to represent pre-industrial conditions.

7.6.1. Event definition

The event definition for the combined Eta and Iota is based on the modeled flood maps. We represent the flood event by maximum water extent and depth.

7.6.2. Factual and counterfactual simulations

Factual simulations

The factual simulations are based on observations and reanalysis datasets. To compute river runoff, the ERA5 reanalysis is used to provide total precipitation, temperature and evapotranspiration. To compute the coastal water levels, ERA5 wind and pressure forcings are combined with best track data from IBTrACS and a parametric wind model. To compute the compound flooding, SFINCS takes the runoff, coastal water levels, and ERA5 total precipitation as forcing. We refer to COMPASS D1.1 for more details.

Counterfactual simulations

For the counterfactual simulations we reduce the observed rainfall intensities according to the Clausius-Clapeyron relation (7% per degree of warming). This results in a reduction in rainfall intensity of 9% which resulted in a counterfactual rainfall dataset used to drive the same modeling framework as for the factual simulations.

7.7. Results

7.7.1. Factual hazards and impacts

The difference in flood extent between the factual and counterfactual simulations are complex with some areas flooded under the counterfactual simulation that are not flooded under the factual simulation. Some challenges with the modeling of very high river flows through very narrow river channels were noted during the development of the simulations. In some cases, this led to unrealistically high-water levels which had to be

removed through filtering. In Figure 79 below the difference between to the two modeling extents are visualized to highlight areas of agreement and disagreement.

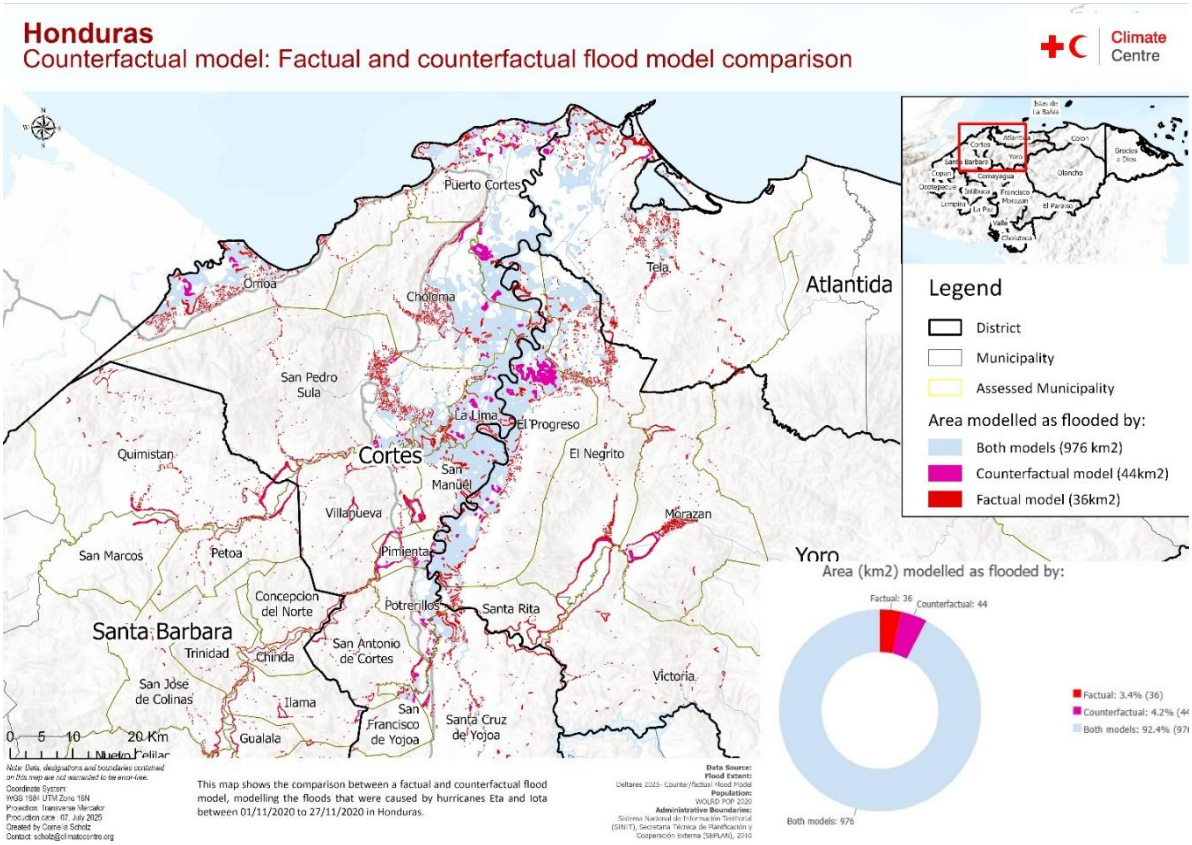

Figure 79 Comparison of flooding extent between factual and counterfactual simulations

The factual simulation results in the population exposure detailed in the Figure 80 below. Interestingly, the estimate of population exposure derived from the factual modeling (462,693) is much closer to the documented number of people evacuated (437,000)[199] suggesting that the modeling flood extents may be more accurate than the satellite derived flood extent.

[199] CEPAL. (2021). Evaluación de los efectos e impactos de la tormenta tropical Eta y el huracán Iota en Honduras. https://www.cepal.org/es/publicaciones/46853-evaluacion-efectos-impactos-causados-la-tormenta-tropical-eta-huracan-iota

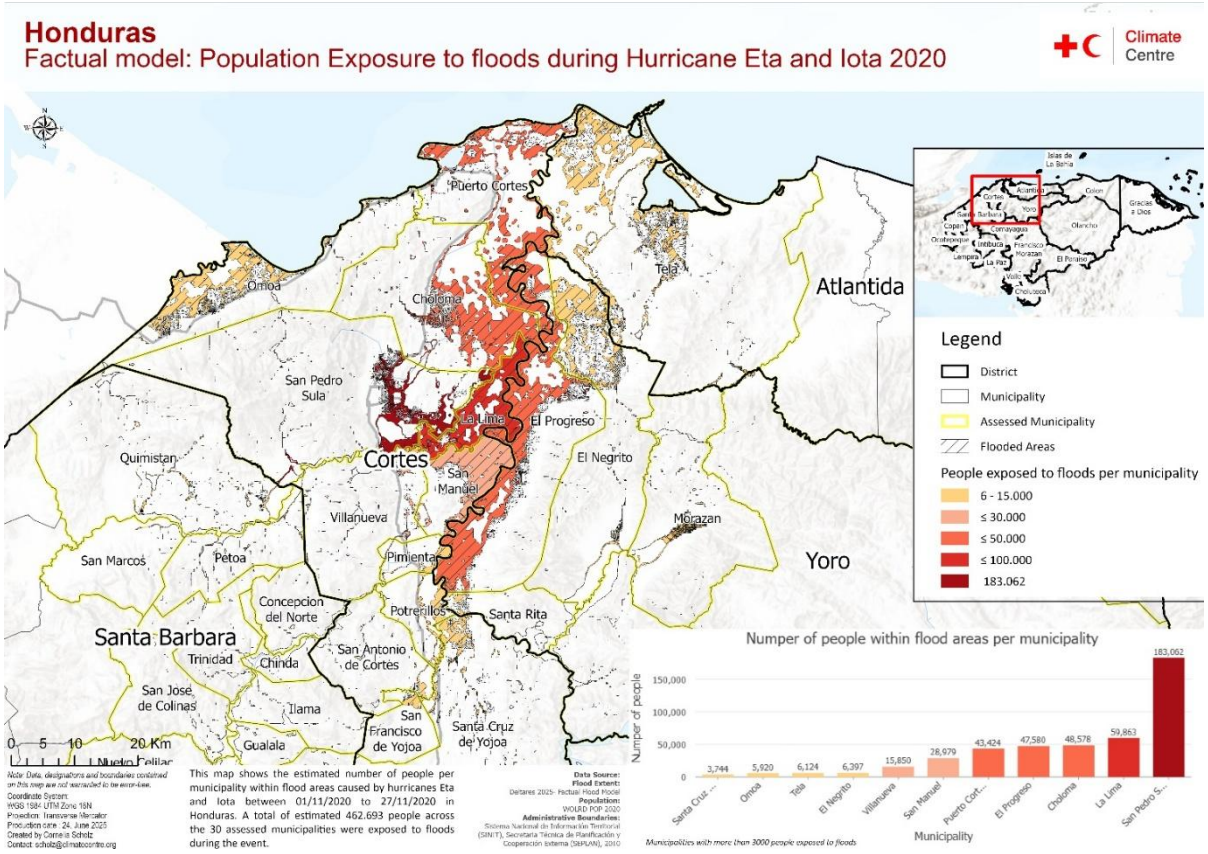

Figure 80 Factual model simulation of flood extent and population exposure during Hurricanes Eta and Iota, 2020.

As noted above, the difference between the factual and counterfactual flood extent is minimal. Figure 81 below maps the counterfactual flood extent and associated population exposure resulting in a slightly lower total population exposed (454,498) which is a reduction of around 1.8%. Given the modeling challenges this result should not be considered confident is likely conditional on post processing steps.

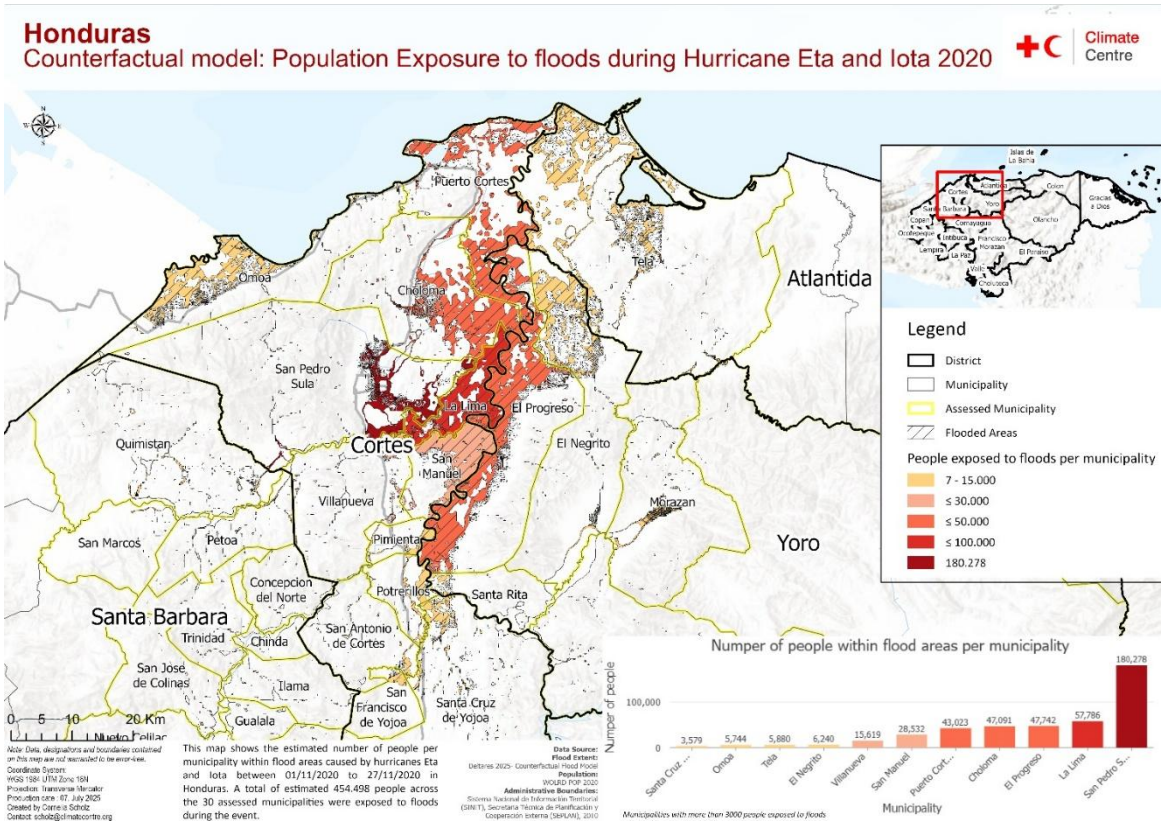

Figure 81 Counterfactual model simulation of flood extent and population exposure during Hurricanes Eta and Iota, 2020.

The factual modeling of buildings impacted also aligns more closely to the reported number of buildings affected than to the Sentinel based flood mapping described above. The factual simulation resulted in 111,668 buildings affected while 90,000 buildings were reported affected in official impact reporting[200] (Figure 82 below).

[200] CEPAL. (2021). Evaluación de los efectos e impactos de la tormenta tropical Eta y el huracán Iota en Honduras. https://www.cepal.org/es/publicaciones/46853-evaluacion-efectos-impactos-causados-la-tormenta-tropical-eta-huracan-iota

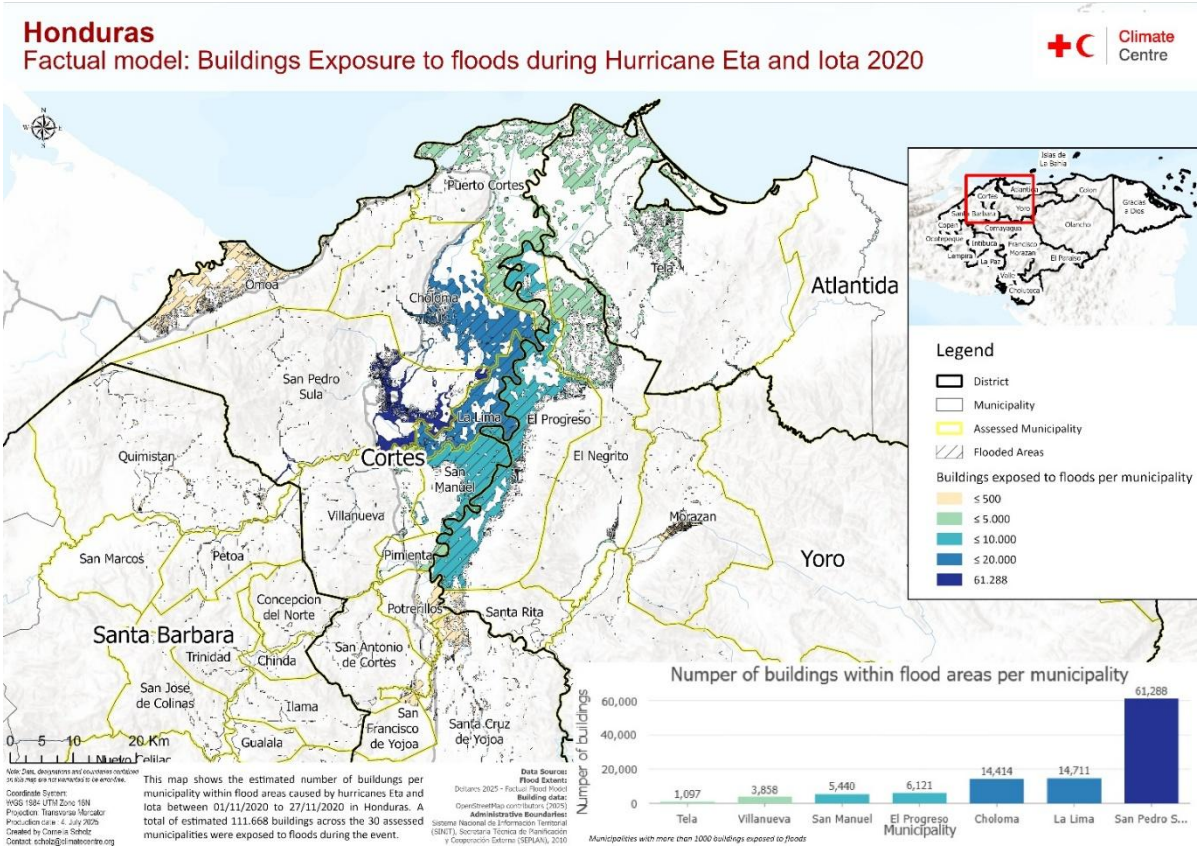

Figure 82 Factual model simulation of flood extent and building exposure during Hurricanes Eta and Iota, 2020.

Counterfactual model simulations resulted in 109,696 buildings affected which is slightly less than under the factual simulations (Figure 83 below). Again, this result is unexpected and results from the limited change in flooding extent under the counterfactual simulation.

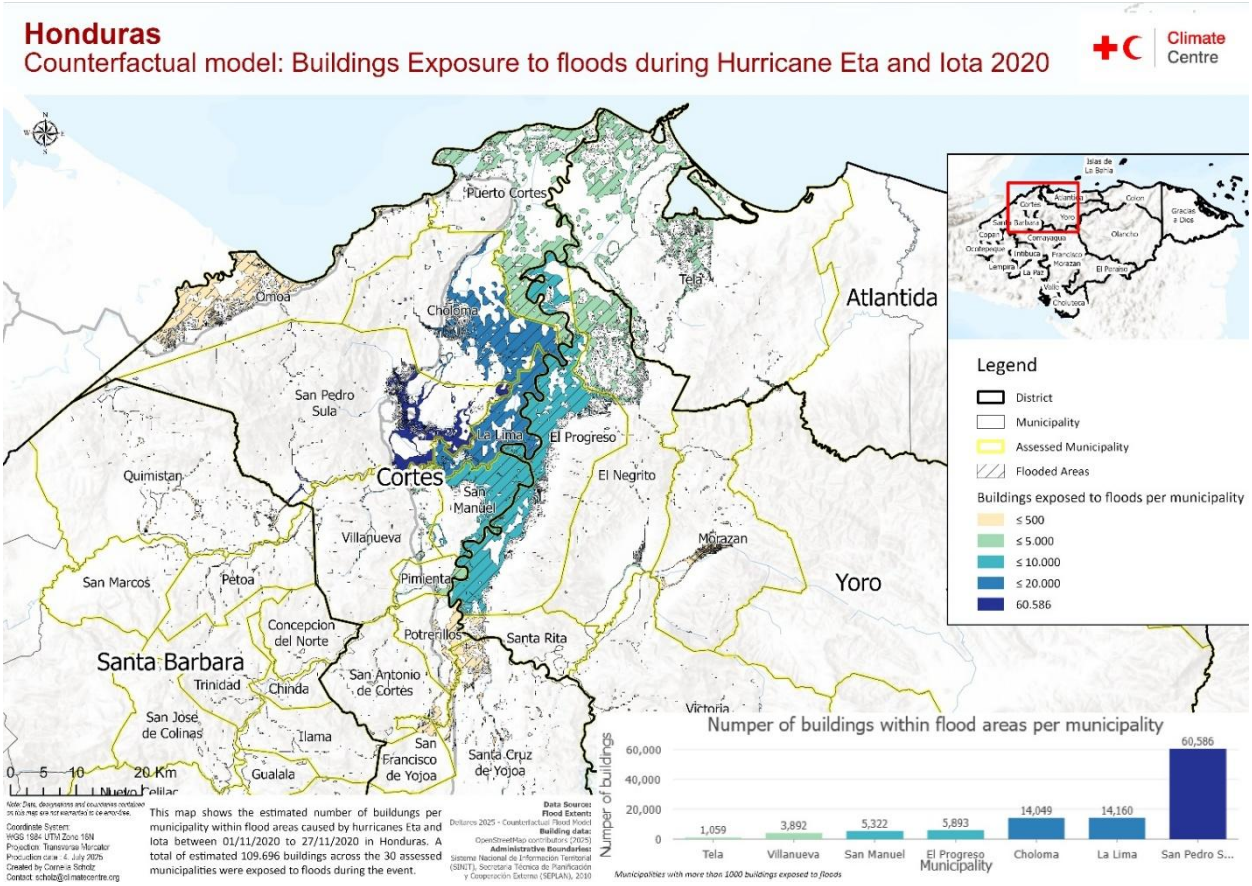

Figure 83 Counterfactual model simulation of flood extent and building exposure during Hurricanes Eta and Iota, 2020

7.7.2. Non-climate counterfactual

Alongside the climate-related counterfactuals described above, the impacts from Eta and Iota could also have unfolded differently due to non-climate factors. As described in the introduction, a range of risk drivers aggravated exposure, deepened vulnerability and/or complicated response to the tropical storms. For a full overview, see: https://storymaps.arcgis.com/stories/8fd49dccaf0f4b719a7aa6b5a2e0201a. This section will primarily focus on internal displacement, violence and COVID19 impacts.

No internal-displacement

Figure 84 maps the estimated numbers of people displaced due to Hurricanes Eta and Iota by the end of November 2020. Most the displacement occurring within the San Pedro Sulla municipality with more than 15,000 people displaced. As noted above and in Figure 78, internal displacement plays a significant role in the eventual impact on lives and livelihoods and is a key component of cascading risk and impacts.

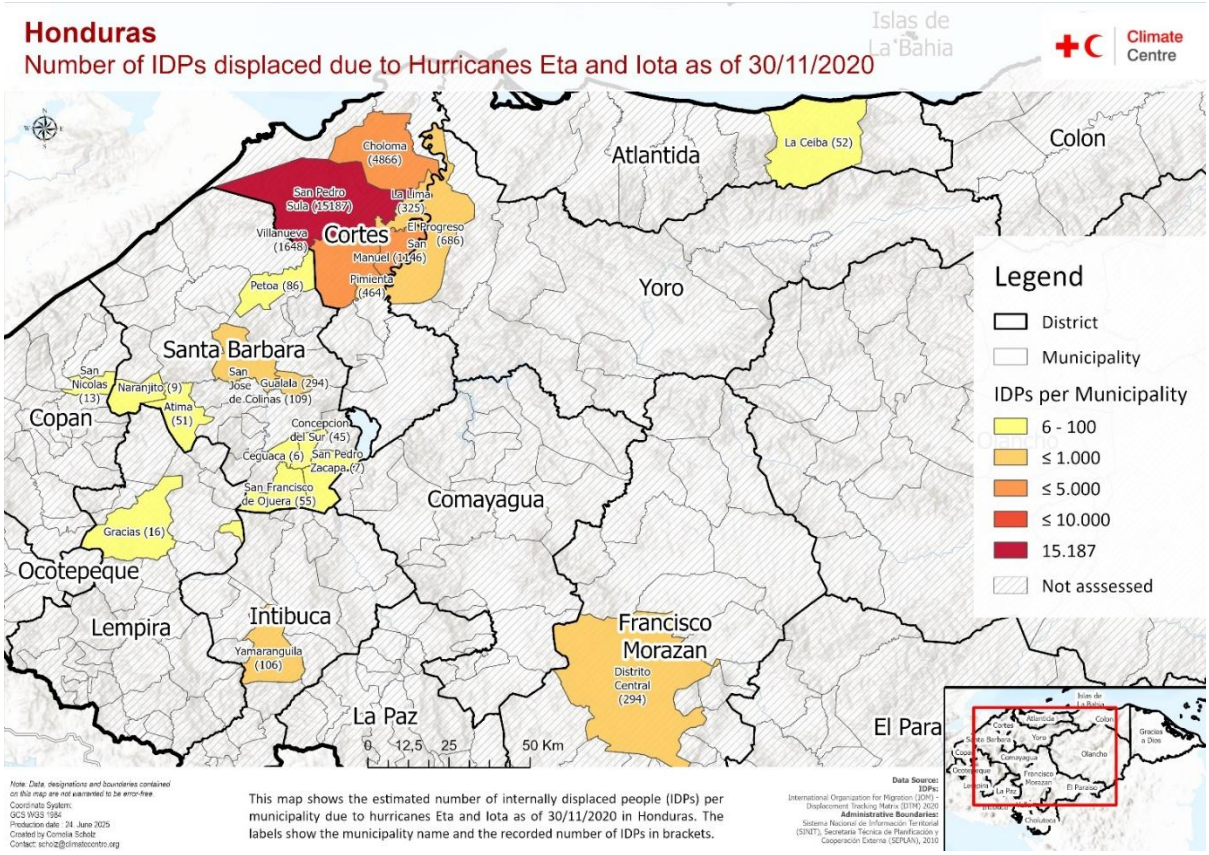

Figure 84 Numbers of people people displaced by Eta and Iota by the end of November 2020 (IOM displacement tracking matrix)

Counterfactual: No violence, insecurity or internal displacement during and after Eta/Iota in Honduras

This counterfactual scenario was the case on the Bay Islands (Islas de Bahía). The response, delivery of aid and trust in early warning messages in San Pedro Sula, an area highly affected by the storms, floods, landslides and historically a hotspot of gang-related violence, was very different in areas without violence.

Context

Honduras is deeply affected by fragility and violence. Analyses indicate that on an individual level, exposure to violence has a broad impact on vulnerability to disasters. For instance, violence drives displacement to flood and landslide-prone marginal areas, increases individual social and economic vulnerability and influences choices due to the risk of exposure to violence when faced with disasters such as the ones triggered by Eta and Iota. In the case of the Tropical Storms Eta and Iota, high levels of insecurity, especially in the suburbs of San Pedro Sula, severely limited the dissemination of storm warnings, reduced the willingness to evacuate due to security concerns and limited access for disaster response[201].

Gang violence is widespread in and around urban areas, and violence related to narcotics trafficking particularly affects rural areas[202]. Gangs exercise territorial control over neighborhoods. In Honduras, gangs or *maras* are small groups of young individuals who extort money from local businesses in exchange for protection. Getting caught in the crossfire of conflicts over territory, drug routes and forced recruitment are major risks for civilians. In particular the Mara Salvatrucha (MS-13) and the 18th Street gang (Barrio 18), are considered responsible for

[201] World Bank unpublished report (2022). Understanding Compound Events in Fragile Contexts: Retrospective compound risk analysis of Tropical Storms Eta and Iota in Honduras

[202] HRW. (2021). World Report 2021: Honduras . https://www.hrw.org/world-report/2021/country-chapters/honduras

Honduras' very high murder rate and are infamous for extortion and drug peddling[203]. These gangs have a highly concentrated presence in San Pedro Sula, one of the most impacted areas from Eta and Iota.

Violence is also a key driver of rural–urban migration and displacement within cities[204]. Poor migrants often end up in some of the most insecure neighborhoods around San Pedro Sula, where government assistance and social safety nets are scarce[205]. The departments of Cortés and Choloma, which were badly impacted by the Tropical Storms, are the main destinations for internally displaced people. Within San Pedro Sula itself, displacement linked to urban gang violence has been widely recognized as a major factor exacerbating economic and social vulnerability[206]. Being in conflict with the dominant gang, refusing to pay extortion fees, or behaving in ways perceived as disrespectful can be life-threatening and force residents to flee their neighborhoods.

Cortés, Choloma, and Yoro departments also receive large numbers of migrants returned from Mexico. In 2019, a record number of returnees was reported (109,185 people)[207]. With few options and often burdened by significant debt to smugglers, many people (at least temporarily) settle in low-cost neighborhoods of San Pedro Sula[208]. Although the number of returnees fell sharply during the COVID-19 pandemic, those who did return to Honduras were unable to leave the Sula Valley area due to disrupted public transportation[209]. This led to more people living in precarious conditions, lacking both economic resources and social networks to help them cope with shocks.

Compounding Impacts on Tropical Hurricanes Eta and Iota

The presence of violence has a clear impact on the successful delivery and action from early warning messages. There are different communication methods associated with early warnings. For example, driving around with loudspeakers, sharing information through social media, or sounding a siren. Several people interviewed for the World Bank study, highlighted the inconsistencies in the functioning of this system between different municipalities[210]. The differences could primarily be attributed to different capacities at the municipal level to organize and share warnings (trained staff, protocols, finances), as well as trust of government entities. Trust was closely connected to the presence of gangs and the ability of government entities to access gang-controlled areas[211].

In Sula Valley, flooding as a result of Eta and Iota impacted some of the poorest and most violent areas. Tragically, the threat of violence, including a fear of being robbed or inability to return, meant that many individuals did

---

[203] HRW. (2021). World Report 2021: Honduras . https://www.hrw.org/world-report/2021/country-chapters/honduras

[204] WFP. (2017). Food Security and Emigration: Why people flee and the impact on family members left behind in El Salvador, Guatemala and Honduras. https://docs.wfp.org/api/documents/WFP-0000019632/download/ ; key informant interviews for unpublished World Bank report

[205] ICRC. (2017). Displaced in Cities : Experiencing and Responding to Urban Internal Displacement Outside Camps. https://shop.icrc.org/displaced-in-cities-experiencing-and-responding-to-urban-internal-displacement-outside-camps-pdf-en.html

[206] ICRC. (2017). Displaced in Cities : Experiencing and Responding to Urban Internal Displacement Outside Camps. https://shop.icrc.org/displaced-in-cities-experiencing-and-responding-to-urban-internal-displacement-outside-camps-pdf-en.html

[207] CEPAL. (2021). Evaluación de los efectos e impactos de la tormenta tropical Eta y el huracán Iota en Honduras. https://www.cepal.org/es/publicaciones/46853-evaluacion-efectos-impactos-causados-la-tormenta-tropical-eta-huracan-iota

[208] WFP. (2017). Food Security and Emigration: Why people flee and the impact on family members left behind in El Salvador, Guatemala and Honduras. https://docs.wfp.org/api/documents/WFP-0000019632/download/ ; key informant interviews for unpublished World Bank report

[209] Key informant interviews for the unpublished World Bank report – Academic 1 and 4

[210] Key informant interviews for the unpublished World Bank report – Government 1, Civil society organization 1, Academic 1

[211] Key informant interviews for the unpublished World Bank report – Governent 1, Civil society organization 2

not leave their homes in advance[212]. In certain areas, (especially Baracoa, Celeo Gonzáles, Cortés, El Progreso, La Lima, La Planeta, Rivera Hernández and southern San Pedro Sula/Choloma), the ability of response teams to even enter was severely hampered[213]. To mitigate some of these challenges, it was essential to coordinate with heads of churches and community committees.

In contrast, early action in the highly exposed Islas de Bahía functioned well for a few key reasons according to interviews conducted as part of the World Bank study. Most relevantly, the absence of violence on the islands was said to be the most significant reason for the higher capacity to undertake early action and also translated into more willingness of communities to evacuate[214].

Counterfactual Differences

In the scenario of there being no violence or insecurity before or after Tropical Storms Eta and Iota, based on lessons learned from areas where there was violence (Sula Valley) and where there was not (Islas de Bahía), the following realities would likely have been different:

Humanitarian access

- Relief agencies and government responders would have reached remote and urban affected communities faster, without security constraints limiting their movements. In San Pedro Sula with severe floods, access issues hindered dissemination of warnings, evacuation and later response in some areas.
- Aid distribution points could have been set up in gang-controlled neighborhoods without fear of extortion, attacks, or roadblocks.

Storm related displacement and shelter

- Households would have been more likely to evacuate in advance without fear of violence, saving lives and livelihoods
- Many families who avoided official shelters for fear of violence, recruitment, or theft would have used them, reducing unsanitary improvised camps and secondary displacement.
- Women and children would have faced lower protection risks in shelters, improving uptake of services.

Livelihood recovery

- Small businesses and informal traders in violence-prone urban areas could have restarted economic activity sooner, reducing prolonged loss of income.
- Agricultural recovery efforts would have faced fewer thefts and extortion rackets affecting seed/fertilizer distribution.

Migration and displacement dynamics

- Households would not have been previously displaced, resulting in fewer households in highly exposed locations, resulting in lower physical damage to housing and infrastructure
- Households would not be facing previous insecurity due to displacement, resulting in a higher coping capacity to recover from shocks

[212] Key informant interviews for the unpublished World Bank report – Humanitarian worker 3 and 6, Government 1
[213] Spring, K., & Ceja, J. L. G. (2020). Episode 13: Hurricanes Iota and Eta: Not Just Natural Disasters. Honduras Now. https://www.hondurasnow.org/episode-13-hurricanes-iota-and-eta-not-just-natural-disasters/
[214] Key informant interviews for the unpublished World Bank report – Academic 1, Government 1

- The combined "push factor" of violence and disaster damage would have been less severe, possibly reducing the sharp spike in outward migration to the U.S. in the months after.
- Migrants would not have been exposed to additional layers of risk of violence and extortion from gangs.

Trust in authorities

- Communities would have been more willing to engage with government responders if not fearing collusion between criminal groups and officials, supporting better coordination.

Information flow

- Evacuation alerts and risk information could have circulated more freely without intimidation by armed groups controlling neighborhoods.

Resilience of services

- Critical infrastructure repairs (power, water, roads) in gang-affected urban areas could have been completed faster, shortening disruption periods.

Non-climate counterfactual: No COVID-19

Context

The health system in Honduras has faced historical funding challenges and COVID19, together with the dengue epidemic created severe shortages in capacity within the health system to respond to multiple health risks. With over 120,000 COVID19 cases and 3000 fatalities, the pressure COVID19 put on the system was extreme[215].

As a result of COVID19, the country experienced an economic downturn, exacerbating an already difficult economic context[216]. The impacts cut across almost all sectors, having a significant impact on livelihoods, food security, and physical security. Informal workers, small business owners, women working in the informal sector, and excluded populations were the most exposed to the economic shocks from COVID19[217]. Of relevance was the impact COVID19 had on food security given the pre-existing socio-economic context which contributed to deepening food access vulnerabilities[218]. With high levels of informal employment and a heavy reliance on remittances from family members abroad for household income, disruptions to both from COVID19 negatively impacted the purchasing power of many households. As a result, many households experienced a sharp increase in poverty, homelessness, and food insecurity[219]. Migration was one of the responses to the economic consequences of COVID19, acting as a significant driver for rural to urban migration flows[220].

---

[215] ASJ. (2020). Coronavirus in Honduras . https://www.asj-us.org/learn/coronavirus-in-honduras ; key informant interviews for unpublished World Bank report

[216] Díaz-Bonilla, E., Flores, L., Paz, F., Piñeiro, V., & Zandstra, T. (2021). Honduras: The impact of covid-19 and policy implications: Second report. https://doi.org/10.2499/P15738COLL2.134533

[217] UNDP. (2021). Análisis sobre la situación de la violencia y seguridad ciudadana en Honduras durante 2020. https://www.hn.undp.org/content/honduras/es/home/presscenter/articles/2021/analisis-multidimensional-de-la-seguridad-ciudadana-en-honduras-.html

[218] Jonathan Lara-Arévalo, Lucía Escobar-Burgos, E.R.H. Moore, Roni Neff, Marie L. Spiker, (2023), COVID-19, Climate Change, and Conflict in Honduras: A food system disruption analysis, Global Food Security (37). https://www.sciencedirect.com/science/article/pii/S2211912423000238

[219] Díaz-Bonilla, E., Flores, L., Paz, F., Piñeiro, V., & Zandstra, T. (2021). Honduras: The impact of covid-19 and policy implications: Second report. https://doi.org/10.2499/P15738COLL2.134533

[220] DTM. (2021). Honduras-Baseline assessment of migration flows and mobility tracking within the context of COVID-19 report #6 (June, 2021) | DTM. https://dtm.iom.int/reports/honduras-baseline-assessment-migration-flows-and-mobiity-tracking-within-context-covid-19-3

COVID19 also contributed to rising rates of violence. The dynamics of gang violence shifted due to lockdowns and economic pressure[221]. There were also some incidents of protests and violent public responses to movement restrictions, and alleged misappropriation of COVID19 medical funds, which eroded public trust in governmental authorities[222]. Gender-based violence and femicide also increased because of COVID19 lockdowns and economic desperation during 2020 and 2021[223].

Compounding Impacts on Hurricane Eta and Iota

In this context, where individuals and households were dealing with the health and economic consequences of COVID19, compounding impacts from Hurricane Eta and Iota further aggravated these vulnerabilities.

Those seeking health care from the impacts of the storms including water borne illnesses and dengue were doing so in health care structures which were already depleted and over capacity. Hurricane-related loss of income and livelihoods made the economic and food security situation worse for households and communities who were already struggling from the economic ramifications of COVID19. The ability to deliver early warning messages and respond in the immediate aftermath was hampered by increased mistrust for authorities due to COVID19 restrictions and negative perceptions of the government response, as well as heightened levels of violence.

Counterfactual Differences

In the scenario of there being no COVID19 before or after Tropical Storms Eta and Iota, household and community level coping capacity would have been much stronger with a greater ability to recover. In particular, the following realities would likely have been different:

Livelihood recovery

- The severe economic fallout from lockdowns and movement restrictions would not have drained household resources just before the storms.
- Without the strict lockdowns, non-essential businesses would have remained open, preserving incomes for millions working in the informal sector.
- People would have retained better access to markets, food supplies, and employment without COVID19 related poverty, homelessness and food insecurity

Migration dynamics

- Rural–urban migration flows would likely have been lower without COVID19 related economic distress as one of the drivers of migration

Food security

- Many households in services and industry sectors would not have lost their income, and food insecurity would not have expanded to groups previously unaffected

[221] World Bank unpublished report (2022). Understanding Compound Events in Fragile Contexts: Retrospective compound risk analysis of Tropical Storms Eta and Iota in Honduras.

[222] Human Rights Watch. (2021). World Report 2021: Events of 2020. https://www.hrw.org/sites/default/files/media_2021/01/2021_hrw_world_report.pdf

[223] CARE, & UN Women. (2020). Latin America and the Carribaen Rapid Gender Analysis for COVID-19. https://reliefweb.int/report/brazil/latin-america-and-carribean-rapid-gender-analysis-covid-19 ; UNSDG. (2021). Violence against women, the other pandemic impacting Honduras. https://unsdg.un.org/latest/stories/violence-against-women-other-pandemic-impacting-honduras

Capacity of health services

- Adequate capacity at health care centers to care for storm-affected patients[224].

Protection risks

- Gender-based violence rates, including domestic abuse, would likely have been lower.
- Precarious shelter conditions and protection risks would have been less severe, since the combined impact of the pandemic and the storms would not have compounded vulnerabilities to the same extent.

Trust in authorities

- Government emergency coordination and health services would have been more focused on the hurricane response, without competing demands from the COVID-19 crisis
- Protests and the misappropriation of COVID-19 medical funds would not have undermined public trust or diverted resources

7.7.3. Summary of attribution results

The quantitative simulated storyline results, driven by a counterfactual reduction in rainfall intensity of 9%, produced no clear change in flood extent or associated population and building exposure. This is unexpected but initial analysis suggests that the hydrology and topography of the region, including very narrow river valleys upstream of the main flooding area may have prevented the wflow model from realistically propagating the changing rainfall intensity into changing flooded areas. This points to an important learning related to operationalizing attribution modeling frameworks as there will be many cases where the model setup and selection of topography data or other parameters will influence the model behavior and require further testing and analysis to select the most realistic configuration. However, if a modeling framework is flexible enough and includes automated validation components then this model tuning could be streamlined into an operational system.

The qualitative attribution results in this use case were explored through stakeholder engagements and prior event retrospective analysis. While it is clear that operationalizing qualitative attribution assessments does not fit directly within the COMPASS attribution framework, it is useful to consider how an operational and

7.7.4. Stakeholder and policy relevance

A stakeholder workshop was held virtually with key stakeholders from Honduras including local government, Red Cross, and NGOs. Initial analysis of the impact of Eta and Iota were presented to the participants who were then asked a series of questions. When asked what the main knowledge gaps were related to Honduran resilience to tropical cyclones, the key gaps that emerged were:

- **Access to Information:** COPECO faces limitations in accessing critical information, which hinders effective planning and response.
- **Information Sharing:** There is a lack of data sharing between institutions, affecting coordination and decision-making.
- **Informational Independence:** The need for independence in the management and analysis of information is crucial to improving the response.
- **Early Warning Systems:** Current early warning and risk management systems are inadequate, reducing the capacity for proactive response.
- **Confidence in Predictions:** Low confidence in weather predictions limits preparedness and response to climate events.

[224] ASJ. (2020). Coronavirus in Honduras . https://www.asj-us.org/learn/coronavirus-in-honduras

- **Station Coverage:** Weather station coverage is very low, which prevents accurate and real-time monitoring of weather conditions.
- **Basin-level information coverage:** The need to integrate information at the basin level is key to decision-making in Honduras.
- **Regional Integration:** There is very good integration and coordination at the regional level with other countries through CEPREDENAC.

Furthermore, when asked if there is value in improved understanding of the complex and compounding risks of tropical cyclones in Honduras, the responses included:

- **Multicausality and Multifactoriality:** Recognizing that disaster responses are complex and influenced by multiple factors allows for more effective planning.
- **Multi-Hazard Analysis:** This approach helps identify and prioritize risks, improving preparedness and mitigation.
- **Documenting Experiences:** Learning from past experiences and documenting impacts is essential to improving future responses.
- **Comprehensive Intervention:** It is important to adopt a comprehensive approach that considers all aspects of the problem to develop more complete and effective solutions.

It seems clear that there is policy relevance to retrospective attribution studies as these would contribute to clear knowledge gaps. Additionally, the focus on compounding and complex events and approaches to improved understanding of these is essential given that such complexity is the norm rather than the exception.

8. Summary and synthesis

This report has detailed the first set of COMPASS compound event attribution studies implemented in order to test and refine the COMPASS operational compound event attribution framework and associated datasets. For each use case the report has detailed the nature of the driving hazards and how they compounded. In some cases, the compounding was multivariate, for example, compounding coastal storm surge and fluvial flooding (e.g UC3a). In other cases, the compounding was temporal, for example tropical cyclone Iota following within 10 days of tropical cyclone Eta in the Caribbean (e.g UC4). The recorded or reported intensity of the hazards and associated socio-economic impact was also provided as a reference for the later hazard and impact modeling assessment. In some cases, economic impact was a primary focus, enabled by newly developed datasets of sub-national GDP distribution (UC1). In other cases, impacts were derived from multiple sources and included both quantitative indicators of people affected, displaced, etc. and quantitative descriptions of socio-economic impacts (e.g. UC3 and UC4).

While a key objective of COMPASS is to develop a uniform modeling framework, for this first round of UCs different modeling configurations and component models were explored. Different attribution methods were also implemented including probabilistic/risk based (UC2) and storyline (UC1, UC3, UC4). While UC3 and UC4 utilized a very similar modeling framework, UC1 and UC2 implemented different frameworks. This has allowed more learning about the advantages and challenges of different frameworks and their particular dataset needs across different contexts.

Below we summarize the key attributions results emerging from this round of UCs noting that there are far more details about the results and associated considerations in the main document.

High level summary of attribution results

Use Case 1: France – storm Xynthia 2010: Climate change increased the impacts of coastal flooding by 11%, 10% and 12% across fatalities, persons affected, and economic loss respectively. This finding has very high confidence (90% confidence interval is +10% to +14%) due to the well-quantified influence of sea level rise since 1950. Attribution for windstorm losses indicates a 7% contribution from climate change, but with considerable uncertainty (90% confidence interval spans –71% to +44%). Importantly, the choice of attribution method and baseline (1950 vs. preindustrial) influenced the estimated impact. Using a 1950 baseline, climate change contributes 22% but still with high uncertainty.

Use Case 2a: UK Winter Storms, Somerset 2013/2014: A small attributable climate signal was found for flood extent in the selected Somerset region. The event was estimated to be 1.21 times more likely (with a wide 95% confidence interval of 0.33-4.45) due to climate change. This impact was not statistically significant, though the return period was estimated to have shortened from 249 years to 206 years due to anthropogenic warming.

Use Case 2b: UK Drought Heatwave, Luton Airport 2022: Climate change was determined to have made the runway melting event 12 times more likely (95% CI: 6-32 times more likely). The event's return period in a factual climate was 15 years, compared to 175 years in a counterfactual pre-industrial climate. The intensity of an equivalent return period event in the counterfactual climate was 2.1°C cooler (95% CI: 1.8-2.3), indicating that without climate change, the impact threshold would not have been reached. Low soil moisture was identified as a preconditioning factor exacerbating extreme temperatures during the heatwave.

Use Case 3a: Tropical Cyclones Idai, East Africa 2019: An assumed 8% increase in precipitation rate based on the Clausius-Clapeyron assumption, combined with an 10% increase in maximum wind speed and a 0.14m increase in regional mean sea-level resulted in a 2% increase in flood extent and a 29% increase in damages and 18% more exposed population.

Use Case 3a: Tropical Cyclone Kenneth, East Africa 2019: An assumed 8% increase in precipitation rate based on the Clausius-Clapeyron assumption, combined with an 10% increase in maximum wind speed and a 0.14m increase in regional mean sea-level resulted in a 3% increase in flood extent and a 14% increase in damages and 10% more exposed population.

Use Case 3b: Tropical Cyclone Freddy, East Africa 2023: An assumed 8% increase in precipitation rate based on the Clausius-Clapeyron assumption, combined with an 10% increase in maximum wind speed and a 0.14m increase in regional mean sea-level resulted in a 3% increase in flood extent and a 19% increase in damages and 13% more exposed population.

A significant theme across these TCs is that "the impact of climate change on flood damage is more profound than on flood hazard." This highlights how societal consequences can be amplified even by relatively small increases in individual flood drivers.

Use Case 4: Tropical Cyclones Eta and Iota, Honduras 2020: Quantitative storyline results, based on an assumed 9% increase in rainfall intensity, using the Clausius-Clapeyron assumption, showed "no clear change in flood extent or associated population and building exposure." This unexpected outcome points to modeling challenges related to river hydrology and topography, and the need for rigorous model tuning and validation in operational attribution systems. Qualitative counterfactuals were also explored and provided a rich perspective of compounding impacts resulting from the antecedent drought conditions, covid-19 epidemic responses, and chronic insecurity and violence. This exploration emphasises that the physical hazard and impacts are often strongly mediated and/or exacerbated by complex socio-economic and socio-political drivers and dynamics. Understanding this complex is critical to developing effective responses ranging from early warning systems that serve the most vulnerable through to adaptation and resilience measures that reduce risk rather than just move risk from one population group to another. This is further emphasized in the following summary of non-physical contributing factors identified in the use cases

Socio-Economic Drivers

In some use cases, the counter-factual scenarios included estimated changes in population and economic exposure over the same time period as the period over which the climate has changed. In these cases, it was found that, non-climate factors, particularly economic and population growth, were found to contribute significantly to the difference in impact between the factual and counterfactual scenarios.

Use Case 1: France – storm Xynthia 2010: economic losses were substantially increased by economic growth (633%) while population growth contributed (45-48%) since the reference date of 1950. The coastal zone experienced rapid growth in housing, especially seasonal housing which contributed significantly to the economic impact compared to.

*Use Case 2a: UK Winter Storms, Somerset 2013/2014***: Most** of the increase in population exposure to flooding resulted from increasing population and population density, rather than from a change in magnitude of impact due to climate change.

Use Case 2b: UK Drought Heatwave, Luton Airport 2022: Increased exposure, driven by higher airport usage, was found to have amplified the impacts of a runway melting event. Disrupted flights increased by 93% and affected passengers by 531% compared to a hypothetical 1980 event. Planned expansion will further exacerbate this, potentially disrupting "275 flights and over 32,000 passengers" by 2043.

Vulnerability drivers

Use Case 1: France – storm Xynthia 2010: Decreasing vulnerability was estimated to have compensated substantially for increases due to climate change and exposure growth (56-66% decrease). However, confidence in this finding is low due to high uncertainty in estimating past vulnerability and the model's underestimation of factual flood impacts.

Use Case 4: Tropical Cyclones Eta and Iota, Honduras 2020: the qualitative vulnerability assessment approach using stakeholder engagement, document analysis, and causal mapping highlighted how violence, insecurity, and the COVID-19 pandemic significantly compounded impacts. Violence limited early warning dissemination, reduced willingness to evacuate due to security concerns, and hampered access for disaster response teams, especially in gang-controlled areas. In contrast, the absence of violence on the islands was said to be the most significant reason for the higher capacity to undertake early action.

At the same time, the COVID-19 pandemic was found to have exacerbated pre-existing vulnerabilities by straining the health system, causing economic downturn, and eroding public trust in authorities due to movement restrictions and accusations of fund misappropriation.

Modeling framework challenges and limitations

A central goal of the use cases was to explore the challenges of developing an operational attribution modeling framework. The first round of use cases has identified several challenges that will inform ongoing development of the modeling framework as well as approaches to communicating the limitations with stakeholders.

Model accuracy and uncertainty

It is clear that model accuracy or realism is an important challenge with many use cases finding that modeled flood extents were larger than observed flood extents. In some cases, this was attributed to the climate models producing too much rainfall (e.g. UC2a) which could be corrected through appropriate bias adjustment. In other cases, such as UC4, flood extents were larger than observed, however it was not clear if the observed flood extents were themselves accurate as impacts modeled with the simulated flood extent were closer to reported impacts than when modeled with observed flood extents. This highlights the challenge of validating different types of models, which is especially challenging in data scarce regions with a strong reliance on remote sensing products that may have their own limitations.

We also note that extremes are by definition rare events and are often poorly represented in climate models. In particular, tropical cyclones are often not well simulated by climate models, creating challenges for attribution studies. Simultaneously, observations of key parameters such as rainfall intensity, for events like tropical cyclones in data scarce regions, involves significant uncertainties limiting the ability to validate climate models or reanalysis data.

Methodological choices

Clearly the choice of attribution method, whether probabilistic or storyline, plays a significant role in both the quantity and nature of the outcome which has implications for communication with stakeholders. This should be a stronger focus for the second round of use cases.

Other methodological choices also have significant implications including reference baselines (e.g. pre-industrial or 1950 in UC1), or flood level thresholds used to classify areas as flooded, which can significantly alter modeled impacts.

Further emphasis should be placed on characterizing these assumptions and associated uncertainties and translating them into clear communications for stakeholders.

Stakeholder and Policy Relevance

Several of the UCs considered the question of stakeholder and policy relevance of attribution studies. UC1 identified the value of the attribution results around windstorm loses to inform reevaluation of minimum building standards, seawall and dike renovations and development in existing identified flood zones.

UC2a noted that the Somerset Rivers Authority had been formed after the flooding event and a 10-year strategy developed to reduce flood impacts. In UC2b it was noted that construction materials with higher heat tolerance should be explored and that the attribution results could inform the Adverse Weather and Health Plan (AWHP) and associated Weather-Health Alerting System

For UC3a and UC3b in Mozambique it was clear from the results that climate change may increase the severity of TCs, putting additional pressure on the governments to invest in early warning systems, resilient infrastructure and better protect vulnerable communities

Stakeholder involved UC4 engagements in Honduras particularly noted the value of improved understanding of the complex and compounding risks of tropical cyclones, and highlighted knowledge gaps in information access, sharing, and early warning systems. Stakeholders reflected that the analysis confirmed that such complexity is the norm rather than the exception

Finally, it was noted for tropical cyclones in Mozambique and Honduras, impacts were not solely due to climate hazards but amplified by complex, deeply rooted socio-economic processes. These create reinforcing cycles of vulnerability and exposure such as poverty, food insecurity, weak infrastructure, political fragility, and social inequality. This emphasizes the need for socially inclusive climate resilience and disaster preparedness.

Conclusion and avenues for the second phase of Use Cases

The first phase of COMPASS UCs successfully demonstrated the application of both probabilistic and storyline attribution frameworks across diverse extreme events and geographical contexts. Key findings indicate a detectable, though sometimes uncertain, climate change signal in many extreme events, often amplifying their impacts. The UCs consistently underscore the important influence of socio-economic factors and existing vulnerabilities in shaping the ultimate impact of these events. Exposure growth, inadequate infrastructure, spatial planning, and pre-existing societal challenges (like violence and pandemics) frequently compounded the direct climate signal.

The UCS demonstrated clear potential and value in the COMPASS modeling framework and datasets that enabled significant streamlining and efficiencies across the UCs. The sharing of code, modeling components, and datasets, has enabled the generation of high-quality policy relevant results in a relatively short time suggesting that the transition towards operational modeling is indeed possible.

Challenges remain in modeling accuracy, particularly in data-scarce regions, and in the adequate representation of vulnerability within quantitative frameworks. The qualitative insights gained from stakeholder engagement in cases like Honduras proved invaluable in capturing the nuanced interplay of non-climate factors.

Opportunities for advancement in phase 2 of the UCs include:

Refinement of Modeling Frameworks: Improving the representation of defenses (e.g. coastal and riverine), increasing model resolution, and developing more sophisticated bias correction and spatial downscaling methods for climate model outputs, especially for rainfall.

Enhanced Vulnerability Modeling: Developing and integrating more robust counterfactual vulnerability assessments into quantitative attribution studies, moving beyond generic damage functions to account for local specificities.

Integration of Qualitative and Quantitative Attribution: Exploring harmonized approaches to combine the strengths of quantitative climate attribution with rich qualitative insights into socio-economic and non-climate compounding factors, particularly for stakeholder communication.

Systematic evaluation of methodological choices and assumptions: Approaches to include assessment of the sensitivity of attribution results to different methods (probabilistic vs. storyline) and baselines (e.g., preindustrial vs. 1950) to provide clearer guidance for practitioners and clear communication of results to stakeholders

Policy-Relevant Outputs: Continuously striving to translate attribution science into actionable insights for policymakers and stakeholders